NUMERICAL STUDY OF PERFORMANCE CHARACTERISTICS OF CENTRIFUGAL SLURRY PUMP

Thesis submitted in partial fulfillment of the requirements for the award of degree of

Master of Engineering
in
CAD/CAM and Robotics

By:
Phull Gurlovleen Singh
(80781018)

Under the supervision of:

Dr. S.K. Mohapatra
Professor & Head
MED

Mr. Satish Kumar
Lecturer
MED

MECHANICAL ENGINEERING DEPARTMENT
THAPAR UNIVERSITY
PATIALA – 147004

JULY 2009

Declaration

I hereby declare that the work, which is being presented in the dissertation work entitled **"Numerical study of performance characteristics of centrifugal slurry pump"**, submitted in partial fulfillment of the requirements for award of the Master's Degree in **CAD/CAM and Robotics** submitted in **Mechanical Engineering Department**, Thapar University, Patiala is an authentic record of my own work carried out under the supervision of **Dr. S.K. Mohapatra, Professor** and **Mr. Satish Kumar** Lecturer, Mechanical Engineering Department, Thapar university Patiala.

Date: July, 2009

Place: Patiala

(Phull Gurlovleen Singh)

.....

This is to certify that the above statement made by the candidate is correct to the best of our knowledge and belief.

Supervisor:

Dr. S.K. Mohapatra
Professor & Head
Mechanical Engineering Department
Thapar University, Patiala

Mr. Satish Kumar
Lecturer
Mechanical Engineering Department
Thapar University, Patiala

Dr. S.K. Mohapatra
Professor & Head
Mechanical Engineering Department
Thapar University, Patiala

Dr. R.K. Sharma
Dean of Academic Affairs
Thapar University, Patiala

ACKNOWLEDGEMENT

I would like to express my most sincere appreciation and deep sense of gratitude and indebtedness to my guides **Dr. S.K. Mohapatra** Professor and **Mr. Satish Kumar** lecturer Mechanical Engineering Department, Thapar University, Patiala for their continuous indefatigable guidance, which paved me on to the path to carry this project. I am highly indebted to them for their painstaking efforts and invaluable suggestions during the period of work.

Date: July'09

Place: Patiala

(Phull Gurlovleen Singh)

ABSTRACT

The choice of pumps or pumping systems for slurry transport will depend not only on the flow, head required, suction conditions, type of installation and location, as for any other pump application, but also on the slurry flow regime and properties. Centrifugal pump radial-flow type is the most common in slurry service. A conventional centrifugal pump is designed to handle clear liquids. However when slurries are to be transported the conventional centrifugal pump has to be modified to handle solid liquid mixtures. The modifications incorporated in the pump include enlargement of flow passages to accommodate bigger solid particles, robust impeller with smaller number of vanes, special seals and proper material of construction to ensure longer life. Conventional design method of centrifugal pump are largely based on the application of empirical and semi-empirical rules along with the use of available information in the form of different types of charts and graphs as proposed by successful designers. As the design of centrifugal pump involve a large number of interdependent variables, several other alternative design are possible for same duty. Computational fluid dynamics (CFD) is being increasingly applied in the design of the centrifugal pumps. 3-D numerical computational fluid dynamics tool can be used for simulation of the flow field characteristics inside the turbo machinery. Numerical simulation makes it possible to visualize the flow condition inside a centrifugal pump, and provides the valuable hydraulic design information of the centrifugal pumps. Present work is aimed to analyze the pressure and velocity distribution inside the pump passage and evaluate the pump performance using the Fluent, a computational fluid dynamics simulation tool. A numerical model of an impeller and casing has been generated and the complex internal pressure and velocity distribution are investigated by using the fluent computational code. . Pressure and velocity distribution inside impeller of the centrifugal pump has direct influence due to change of stream wise location.

CONTENTS

List of figures and tables

Nomenclature

D	Diameter, m
Q	Mass flow rate, m^3/sec
H	Head, m
BHP	Brake horse power, hp
N	Speed, RPM
ρ	Density of liquid, kg/m^3
$\vec{v}$	Velocity vector
$\bar{\bar{\tau}}$	Stress tensor
g	Acceleration due to gravity, m^2/sec
h_0	Enthalpy
μ_t	eddy viscosity
$\vec{F}$	Force vector, N
E	Total energy, J
$\dot{m}$	Flow rate
Q	flow rate of enthalpy, W
h	Species enthalpy
k	kinetic energy per unit mass, J/kg
U	Free stream velocity, m/s
$\in$	Turbulence dissipation rate, m^2/s^3
σ_k and σ_ε	Turbulent Prandtl numbers for k and ε, respectively

Suffix:

i	x coordinate
j	y coordinate
z	z coordinate
1	inner diameter
2	outer diameter

CHAPTER 1
INTRODUCTION

1.1 SLURRY

Slurry is a mixture of solids and liquids. The most commonly used liquid is water. Its physical characteristics are dependent on many factors such as size and distribution of solid particles, size of the conduit, level of turbulence, temperature, and absolute (or dynamic) viscosity of the carrier fluid. Single-phase liquids are allowed to flow at slow speeds from a laminar flow to a turbulent flow but in slurry flows, the flow must overcome a deposition critical velocity or a viscous transition critical velocity. If the speed of flow is not sufficiently high, the particles will not be maintained in suspension.

1.1.1 Types Slurry Flows

Based on the solid fluid interaction slurry flows are divided into two different types:

Homogeneous flows or non-settling slurries

In homogeneous flows solids are uniformly distributed throughout the liquid carrier. For example copper concentrate slurry after undergoing a process of grinding and thickening, drilling mud, sewage sludge, and fine limestone behave as homogeneous flows. Figure 1.1 (a) shows the distribution of solid particles in homogeneous flows.

Heterogeneous flows or settling slurries

In heterogeneous flows, solids are not uniformly mixed in the horizontal plane. Heavier particles tend to settle down and lighter particles tend to float. Sliding bed may form in the pipe, with the heavier particles at the bottom and the lighter ones in suspension. Heterogeneous slurries are encountered in many places mining, phosphate rock mining, and dredging applications. Heterogeneous flows require a minimum carrier velocity. Figure 1.1 (b) shows the distribution of solid particles in heterogeneous flows.

Homogeneous mixture

Heterogeneous mixture, partly stratified

Figure 1.1(a) Homogeneous slurry flow **Figure 1.1(b) Heterogeneous slurry flow**

Saltation

Saltation is a condition which exists in a moving stream of slurry when solids settle in the bottom of the stream in random agglomerations which build up and wash away with irregular frequency

1.1.2 Operating parameters of slurries

- **Apparent viscosity:** It is defined as the property of the fluid resistance offered to the flow.
- **Critical carrying velocity:** It is defined as the mean velocity of the specific slurry in a particular conduit, above which the solids phase remains in suspension, and below which solid-liquid separation occurs.
- **Effective particle diameter:** Effective particle diameter is the single or average particle size used to represent the behavior of a mixture of various sizes of particles in slurry. This designation is used to calculate system requirements and pump performance.
- **Concentration of solids by volume:** The actual volume of the solid material in a given volume of slurry, divided by the given volume of slurry, multiplied by 100.
- **Concentration of solids by weight:** The weight of dry solids in a given volume of slurry, divided by the total weight of the slurry, multiplied by 100.
- **Settling slurry:** A slurry in which the solids will move to the bottom of the containing vessel or conduit at a discernible rate, but which will remain in suspension if the slurry is agitated constantly.
- **Settling velocity:** It is the rate at which the solids in slurry will move to the bottom of stationary container.
- **Square root law:** This law is used to calculate the approximate increase in critical carrying velocity for given slurry when pipe size is increased. It states:

$$V_L = V_S = \left(\frac{D_L}{D_S}\right)^{\frac{1}{2}}$$

Where:

V_L = Critical carrying velocity in larger pipe

V_s = Critical carrying velocity in samller pipe

V_L = Diameter of larger pipe

V_s = Diameter of smaller pipe

- **Yield value (Stress):** It is the value of stress at which slurries will start to deform and under this value there will be no relative motion between adjacent particles in the slurry.

1.2 TRANSPORTATION OF SLURRY

Over the last few decades there has been a phenomenal growth in the demand of raw materials. This rise in demand has led to drastic changes the existing techniques of mining, food processing, power generation and other sectors where transportation of suspended solids play a major role. Due to this change, there has been an increase in requirements in slurry transportation. A typical slurry transport

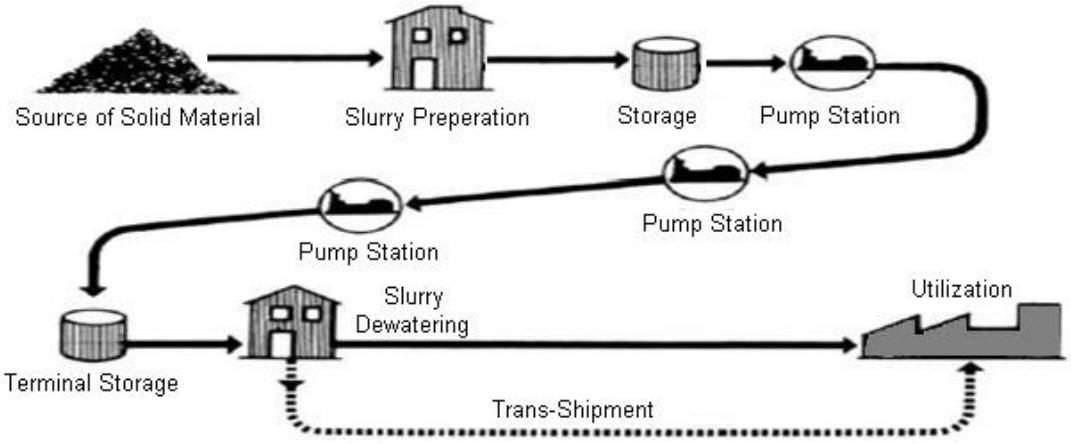

Figure 1.2 Transportation of slurry

system is shown in the figure 1.2. Pump plays a vital role in transportation of slurry; different types of pumps are available for slurry transportation, but centrifugal pumps are most widely used in slurry transportation applications due to the following reasons:

- Higher flow rates can be obtained.
- Pulse free flow can be obtained.
- Higher initial and maintenance cost of positive displacement pumps.
- Solid particle of any size can be transported.

For small distances one centrifugal pump is enough, but for transportation through long distances or for greater pressures two or more centrifugal pumps are connected in series.

1.3 MOTIVATION OF THE PRESENT WORK

Computational fluid dynamics (CFD) analysis is being increasingly applied in the design and simulation flow in centrifugal pumps. Numerical simulation makes it possible to visualize the flow condition inside a centrifugal pump, and provides valuable information about the centrifugal pump's hydraulic design. By using simulation result to calculate or predict the performance of a centrifugal pump, to replace or reduce the performance experiments in the process of pump design, a great deal of labor and facility will be saved, as well as its shortening design cycle. Therefore, great improvement on centrifugal pump design must be achieved by CFD analysis of inner flow inside a centrifugal pump and following application of its results in pump design processes.

The objective of the work is to model and numerically investigate the flow field inside the centrifugal slurry pump of pilot plant at IIT Roorkee using commercial CFD code FLUENT .

CHAPTER 2
LITERATURE REVIEW

Major problems associated with centrifugal pumps handling slurries are the estimation of hydraulic performance of the pump components. Several investigators attempted to correlate their experimental data of pump performance with some of affecting parameters and presented correlations for estimating the pump performance with slurries based on its performance with water. A review of literature available in this area has been presented in the following paragraphs to discuss the present state of knowledge

Rayan and Shawky[1] [1989] have evaluated erosion wear in the centrifugal slurry pump at different rotational speeds with different solid-liquid concentration by weighing method. They have reported that erosion wear rate increases with flow velocity as well as solid-liquid concentrations.

Dong et al.[2] [1992] used PDV technique to visualize the flow inside the volute of a centrifugal pump. Neutrally buoyant particles of 30μm mean diameter were used as seed and it was observed that although most of the blade effects occur near the impeller tip, they are not limited to this region.

V.K Gahlot et al.[3] (1992) studied the two different types of slurries namely zinc tailing & coal on the performance characteristics of centrifugal slurry pump. They observed that the head and the efficiency of the pump decrease with increase in solid concentration, particle size and specific gravity of solids where they are independent of the pump flow rate.

T.Cader et al.[4] (1992) have investigated water and solid water mixture flow at the impeller outlet of a centrifugal slurry pump using LDV (Laser Doppler Velocitimetry) system. Solid particle were taken as 0.8 mm diameter glass beads. They observed that solid particles have larger radial velocity than the carrier fluid at the impeller outlet, but they lag the water in the circumferential direction.

Cader et al.[5] [1994] have studied phase velocity distribution and overall performance of a centrifugal slurry pump by using LDA (Laser Doppler anemometer).Experiments conducted with a dilute suspension of concentration of 1% micron size tracers and 0.8 mm glass beads at the impeller casing flow interface. They evaluated the liquid and solid velocity distribution in the pump and observed that fluctuations of the pump flow rate, head and loss in efficiency due to particle slip, as the function of impeller position.

W.Huang et al.[6] [1995] investigated that two phase flow structure at the impeller-volute interface by using laser doper velocitimetry (LDV). They observed that in the impeller casing slip velocity, solid liquid velocity fluctuations are the function of radial distance and impeller angle. In the impeller rotation region flow is approximately forced vortex type and in casing region free vortex type.

S.Yedidiah[7] [1996] u**sed** a novel approach for calculating the head developed by a centrifugal impeller. The approach was based on the fact that the head developed by an impeller depends on the shape of the total blade and not just upon the magnitude of its outlet angle.

Ni et al.[8] (1996) have experimentally evaluated the effect of high delivered volumetric concentration (c_{vd}) on characteristics of a slurry pump. They performed extensive experiments by using three sorts of narrowly graded sands for the observation of pump and pipeline characteristics. They conclude that high solid concentration has a strong influence on the pump head, efficiency and power consumption and this influence behaves differently with different sand size. The pump efficiency in coarse sand slurry service may drop almost 60% compared to that of water service, when c_{vd} = 42%. Within the measured range of concentrations in each passages may experience similar stratification process occurred in pipelines. The mechanical friction regime in the impeller passages could be similar to that in pipelines. Therefore the delivered volumetric concentration and the size affect the head loss in the same way both in pumps and pipelines.

Miner, S. M.[9] **[1997]** has calculated numerically the flow field and pressure field within the rotor of an axial flow pump. Velocity and pressure profiles were developed on both sides of the impeller. It is observed that the value of tangential velocity increases from the centre line to the outer radius. The axial velocity profile shifts towards the outer radius because of the presence of nose on the hub. The use of coarse and fine mesh does not show significant difference in the values, thus even coarser mesh can be used

Chung[10] **[1999]** has developed optimum design code of the pump. They determined the geometric and fluid dynamic variables under the appropriate design constraints. Optimization problem has formulated with a non-linear objective function to minimize losses, net positive suction head required and product price of a pump stage depending on the weighting factor selected as the design compromise. Optimal solution obtained, efficiency $NPSH_R$ depends design variable of centrifugal pump. Selected in the range of weighting factor 0 to 1.designer can easily find the optimum value of design variable to meet their particular requirement of pump design.

Ogut, A. et al.[11] **[2000]** have provided an insight into the effectiveness of fluid injection as a boundary layer control method in suppressing or eliminating flow separation in the vaned diffuser at off-design flow conditions. The reverse flow was observed along the hub and shroud walls. The phenomenon of flow separation along the walls was also reduced by injecting the fluid. The pressure recovery will be maximum if injection rate was 3% to the 60% of design flow rate.

Majidi, K. et al.[12] **[2000]** have observed the secondary flow in volute and circular casings of centrifugal pumps. The static pressure was not distributed uniformly at the outlet of the impeller which results in the radial thrust. Also the maximum value of relative velocity occurs at the periphery of the impeller. The analysis shows that the curvature of the casing creates pressure gradients that cause vortices at cross-sectional planes of the casings.

Gandhi et al.[13] **[2001]** have studied erosion wear at various locations inside the volute casing of a centrifugal slurry pump for the flow of solid-liquid mixtures. They reported that the wear

increases all along the volute periphery with increase in the amount of solid suspended in the mixture and wear smaller when the pump operates near the (BHP).

Gandhi et al.[14] (2001) have studied the performance of two centrifugal slurry pumps for three solids materials having different particle size distribution (PSD) in terms of head, capacity and power characteristics. The results have shown that values of head and efficiency ratios are not only depended on solid concentration but are also affected by PSD of the solids and properties of slurry. They conclude that the head and efficiency of the pump decrease with increase in solid concentration, particle size and slurry viscosity, the decrease in the head being 2-10% higher than that of the efficiency. The presence of finer particles (<18 μm) in coarse slurries substantially attenuate the loss of the performance of the pump in terms of head and efficiency

Oh and Kim[15] [2001] developed a design optimization code for mixed flow pump to determine the geometric and fluid dynamic variables under appropriate design constraints. Optimization problem has been formulated with a nonlinear objective function to minimize the fluid dynamics losses.

Chung M K et al.[16] [2001] developed a simple and accurate correlation for the slip factor of centrifugal impeller. He investigated the radius of relative eddy inscribed by two adjacent vanes and the exit circle of a flow channel in the impeller to obtain the correlation.

Engin, T. et al.[17] [2001] have conducted the experimental study on the effects of solids in an unshrouded centrifugal pump impeller by varying the tip clearance when both handling water and solid-water mixtures. The tip clearance loss mechanisms seem to be similar to those in single phase pumping and a steady deterioration in pump performance was observed by increasing the tip clearances. The tip leakage losses increase as the tip clearance increases. The head reduction factor appears to be almost independent of the variation in the tip clearance, and which allows correlating the solids effects on the pump performance regardless of changes in the tip clearance. A slight decreasing trend was also observed in efficiency ratio when the tip clearance was increased.

Gandhi et al.[18] [2002] have evaluated performance characteristics of a centrifugal slurry pump at different rotational speeds with water as well as solid-liquid mixture. They found that the affinity relations applicable to conventional pumps for head and capacity can be applied to slurry pumps handling water and slurries at low concentrations (<20% by weight). For higher solids concentrations, these relationships needed to be corrected by taking into account the effect of solids

Kato, C. et al.[19] [2003] have observed boundary interface between impeller and volute casing by using overset grids from dual frames of reference. The overall grid was composed of several grid sets, and appropriate transactions take place at the interface regions. Large-eddy simulation was applied to the prediction of internal flows in a high–specific-speed, mixed-flow pump stage that possesses weak instability in its head-flow characteristics at low flow-rate ratios. The head-flow characteristics were also developed, although the large eddy simulation predicted the stall point at a lower flow-rate ratio than the measurements flow rate. The phase-averaged distributions of the meridional- and tangential-velocity components were also compared with those measured by an LDV.

Nursen, E. C. et al.[20] [2003] have developed an incompressible flow solver for the pump volute. The developed flow solver provides detailed pressure and velocity distribution information inside the volute, and the calculated results were verified by means of the experimental results.

Kadambi et al.[21] [2004]) have used Particle Image Velocitimetry to investigate the velocities of the slurry in the impeller of a centrifugal slurry pump for sodium-iodide solution (NaI) and 500micron glass beads slurry. The experiments conducted at 725 rpm, 1000rpm speed, and1%, 2%, 3% volumetric concentration. They observed that the in clear fluid flow conditions for both the pump rpm, flow separation takes place on the suction side of the blade in the region below the blade tip. For the same flow conditions, the flow moves smoothly along the suction side of the blade depicting a recirculation zone. The intensity of this recirculation zone decreases at the higher concentration of 3% due to particle inertia effects. On the pressure side of the blade the particles are pushed along the blade surface and can result in the frictional wear.

Hergt, P. et al.[22] [2004] have observed the unsteady velocity, pressure and flow angle at the impeller outlet of a centrifugal pump with and without volute casing at five operating points using the hotwire technology and a fast response single hole cylindrical probe. The test fluid was air. While the velocities and pressures depend only on the axial coordinate and were rotationally symmetrical. If there was no casing around the impeller, the influence of the volute on the circumferential distribution of these quantities increases with the deviation of the operating point from the design point.

Xu, C. et al.[23] [2005] have calculated the detailed flow structures in the volute and the compressor performance was calculated for different tongues. It was observed that the flow in the volute sections has a single vortex structure, as opposed to two counter-rotating vortices. The round tongue creates significant blockage near the tongue. This blockage forces secondary flow center away from the tongue area. It was shown that the round tongue produces better performance than the sharp tongue. The flow simulation was observed to better understand the volute flow mechanisms and provide design guidance in volute design to meet performance goals.

Addie et al.[24] [2007] have developed ANSI/HI standard of centrifugal slurry pump. They studied the effect of slurry on pump performance; net positive suction head required and wear by using the ANSI/HI standard.

Pullum et al.[25] [2007] have calculated the performance reduction of the centrifugal slurry pump by using Hydraulic Institute method for handling non-Newtonian coarse particle suspensions. Suspensions up to 38% v/v of coarse particles with mean diameters in the range of $1.1 < d50 < 3.4$ mm suspended in carrier fluids with dynamic yield stresses of $0 < \tau_\gamma < 17.2$ Pa and shear thinning indices in the range $0.35 < n < 0.79$ were examined. They found that the reduction in the head is the function of coarse solid concentration.

Min-Guan, Y. et al.[26] [2007] have observed the phenomena of two-phase flow with salt crystallizing in the chemical pump, the 3-D turbulent flow in the impeller of chemical pump was simulated at the condition of rinsing. The internal flow between the impellers of chemical pump

was investigated. Based on the Reynolds-averaging N-S equations and the standard *k*-ε two equations turbulent model, the simulations of turbulent flow between the impellers were performed using the flow computing software Fluent under different operating conditions. Based on the analysis of the calculated results of velocity and pressure profiles in the chemical pump and experimentally observed phenomenon of flow impact, secondary flow and recirculation, some design improvements were proposed, which give suggestions on the optimal design and internal two-phase flow study of the chemical pump.

CHAPTER 3

CENTRIFUGAL SLURRY PUMPS

3.1 PUMP

A pump is a mechanical device used to increase the pressure of fluids, such as gases, liquids or slurries. Pumps are used whenever any quantity of fluid is to be moved from one place to another. A pump displaces a volume by physical or mechanical action. Pumps are found in such services as steam power plants, water supply plants, sewage, drainage or irrigation, oil refineries, chemical plant, sand steel mills. While these pumps have much in common, they are varied to meet special requirements and particular needs of each service.

3.1.1 Classification of pump

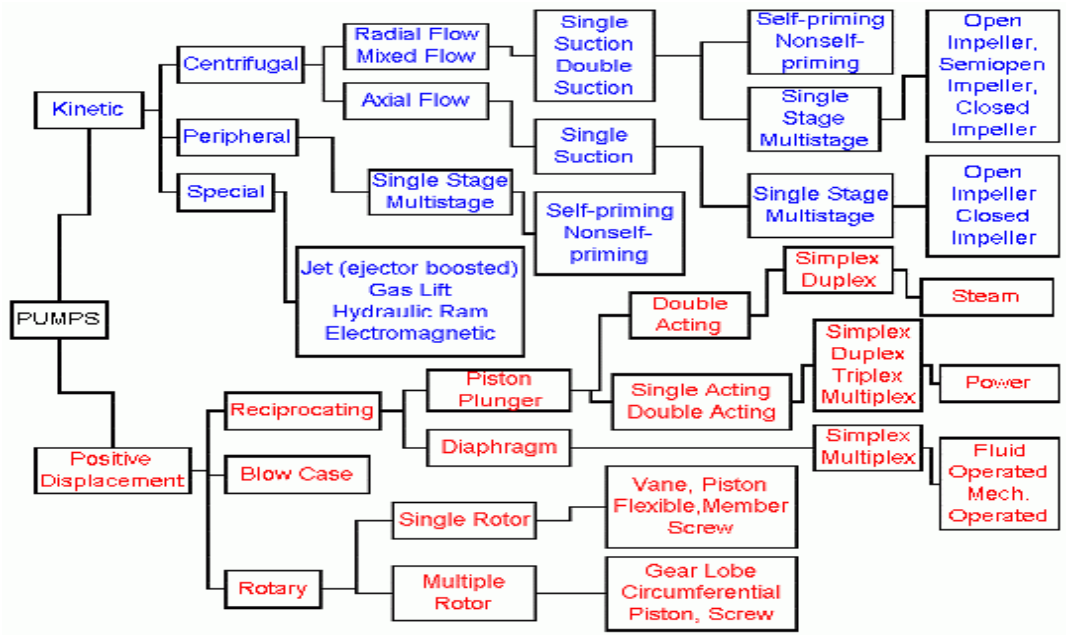

Figure 3.1 Classification of Pump

3.1.2 Pumps used for transportation of slurries

The choice of pumps or pumping systems for slurry transport will depend not only on the flow, head required, suction conditions, type of installation and location, as for any other pump

application, but also on the slurry flow regime and properties. Rotodynamic pumps, of which the centrifugal or radial-flow type is the most common in slurry service, are usually considered for the higher flow, lower head duties, whereas conversely, positive-displacement reciprocating types tend to be used for the lower flow, high pressure applications, e.g. long-distance pipelines. However, relatively high pressures may also be achieved with centrifugal pumps, depending on casing pressure limitations, by arranging them in series. For a given duty, centrifugal pumps are usually cheaper, occupy less space and have lower maintenance costs than positive displacement types, and can handle much larger solids. Figure 3.2 gives a pictorial idea of pump application depending upon discharge and particle size required.

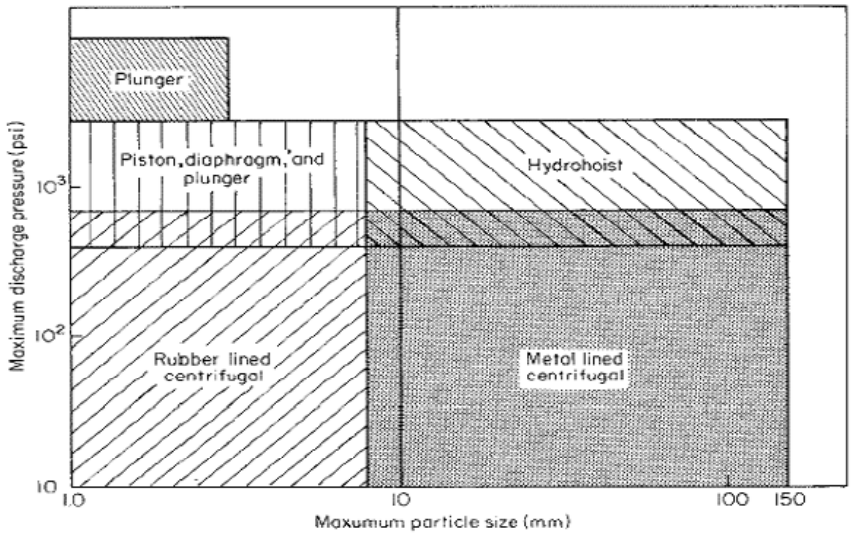

Figure 3.2 Pumps used for transportation of slurries

3.2 CENTRIFUGAL SLURRY PUMP

A conventional centrifugal pump is designed to handle clear liquids. However when slurries are to be transported the conventional centrifugal pump has to be modified to handle solid liquid mixtures. The modifications incorporated in the pump include enlargement of flow passages to accommodate bigger solid particles, robust impeller with smaller number of vanes, special seals and proper material of construction to ensure longer life. Slurry pumps are available in variety of materials of construction to best handle the abrasion, corrosion and impact requirements of nearly any solids handling application, replaceable liners are used in critical areas of wear to reduce the costs of parts replacement. The materials used have different properties to prevent

wear and erosion to ensure longer working life as compared to conventional pumps used for clear liquids. These modifications increase the hydraulic losses in the pump and deteriorate the pump performance. The efficiency of a centrifugal slurry pump is considerably low as compared to a conventional pump. The performance characteristics of slurry pumps are also poor as compared to the conventional pumps. The deterioration in the performance could be attributed to the modifications incorporated to allow free flow of solid particles along with the liquid to be transported. The designers of slurry pumps have to take the following parameters into account while designing the slurry pumps:

- Abrasive hardness
- Particle shape
- Particle size
- Particle velocity and direction
- Particle density
- Particle sharpness

During the design of such pumps, the requirements of longer life and reliability is to be balanced by the constrained of high initial costs and efficiency. Nearly all slurry pumps have larger diameter impellers than units for pumping clear liquids, to enable heads and capacities to be met at reduced rotational speed. Low speed operation is one of the most important wear reducing features of a slurry pump A centrifugal slurry pump is designed to handle solid-liquid mixture and is normally a single stage, end suction type having radial or mixed flow configurations to facilitate the motions of solid particles Some compromises are made in order to provide an acceptable pump life. Table 3.1 shows the design features, benefits, and compromises of the slurry pump

SLURRY PUMP DESIGN		
Design Feature	**Benefit**	**Compromise**
Thick Wear Sections	Longer component life	Heavier, more expensive parts
Larger Impellers	Slower pump speeds longer component life	Heavier, more expensive parts
Specialty Materials	Longer component life	Expensive parts
Semi Volute or Concentric Casing	Improved pump life	Loss in efficiency
Extra Rigid Power Ends	Improved bearing lives	More expensive shafts and bearings

Table 3.1 Slurry pump design features

3.2.1 Working principle of centrifugal pump

A centrifugal pump works by the conversion of the rotational kinetic energy, typically from an electric motor or turbine, to an increased static fluid pressure. The rotation of the pump impeller imparts kinetic energy to the fluid as it is drawn in from the impeller eye (centre) and is forced outward through the impeller vanes to the periphery. As the fluid exits the impeller, the fluid kinetic energy (velocity) is then converted to (static) pressure due to the change in area the fluid experiences in the volute section. Typically the volute shape of the pump casing (increasing in volume), or the diffuser vanes (which serve to slow the fluid, converting to kinetic energy in to

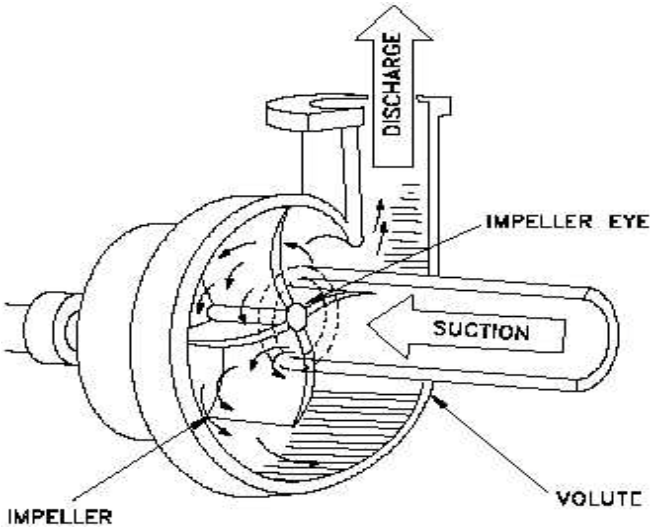

Figure 3.3 Working principle of Centrifugal pump

flow work) are responsible for the energy conversion. The energy conversion results in an increased pressure on the downstream side of the pump, causing flow. Centrifugal pumps are used in a variety of applications, such as, water supply and irrigation, power-generating utilities, flood control, sewage handling and treatment, food industries, chemical and petrochemical industries, domestic appliances, mining and ore processing, transporting liquid-solid mixtures, environmental control, spaceships, airplanes, and motor vehicles. Since they are used in a wide spectrum of application, the centrifugal pumps are manufactured in different shapes to meet the application requirements.

3.2.2 Components of a centrifugal slurry pump

The components of a slurry pump are same as the ones used in a conventional centrifugal pump.

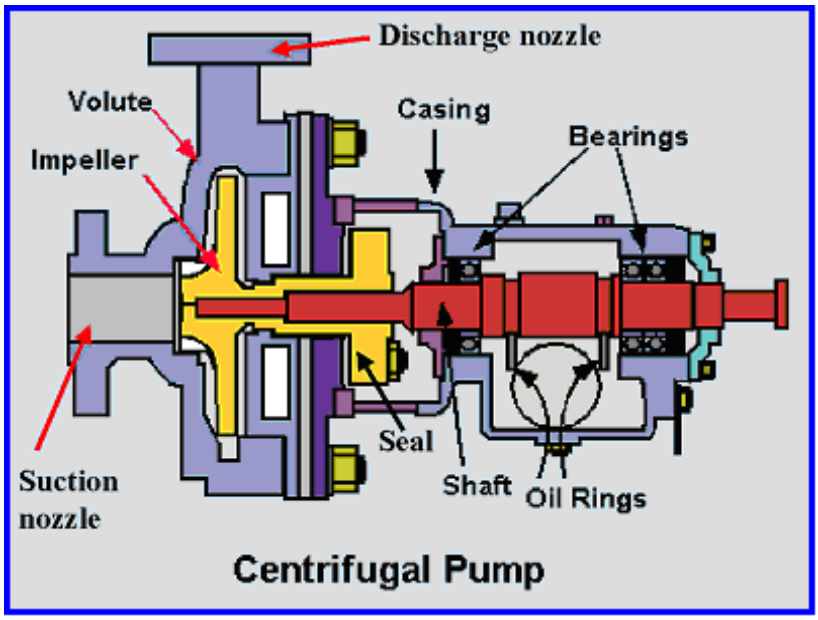

Figure 3.4 Components of centrifugal pump

3.2.2.1 Impeller

The rotating part of centrifugal pump is called impeller. It consists of a series of backward curved vanes. The impeller is mounted on a shaft, which is connected to the shaft of an electric motor. An impeller is usually made of iron, steel, aluminium or plastic, which transfers energy from the motor that drives the pump to the fluid being pumped by forcing the fluid outwards from the centre of rotation. Figure 1.6a shows the axial, radial and tangential component of flow.

Components of impeller

Vanes: The vanes in the pump impeller are series of backward or forward curved cavities which transfers the power from shaft to the fluid.

Hub and Shroud: The hub is the surface of the machine closest to the axis of rotation. It defines the inner fluid flow surface. The shroud is the surface of the machine farthest from the axis of rotation. It defines the outer fluid flow surface

Leading and trailing edges: The leading edge is the most upstream part of the blade. Any change to the leading edge changes the blade surfaces, which changes the periodic surfaces as well as the hub and shroud surfaces. The trailing edge is the most downstream part of the blade.

Impellers are also classified as to whether they are:

Open impellers: The open impellers are used pumps to perform a chopping, grinding action on the liquid. The totally open impeller imparts motion to a large volume flow, without creating greater head or pressure. With its open tolerances for moving and grinding solids, they are not high efficiency devices.

Semi-open impeller: A semi-open impeller has open blades, but with a support plate or shroud on one side. These types of impeller are generally used for liquids with a small percentage of solid particles from the bottom of a tank or river, or crystals mixed with the liquid. The efficiency of these impellers is governed by the limited free space or tolerance between the front leading edge of the blades and the internal pump housing wall.

Enclosed impeller: The enclosed impellers are designed with the blades between two support shrouds or plates. These impellers are generally used clean liquids because tolerances are tight at the eye and the housing, and there is no room for suspended solids, crystals or sediment, Figure 3.3c shows an enclosed impeller.

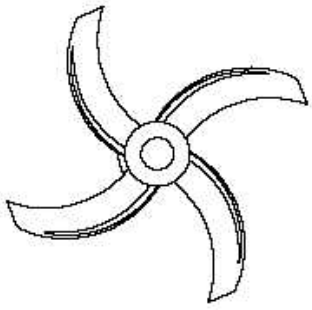

Figure 3.5(a) Open Impeller

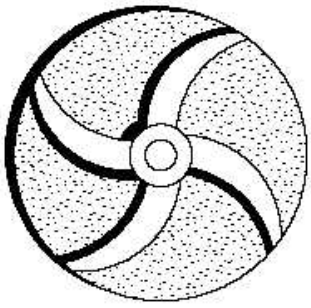

Figure 3.5(b) Semi-Open Impeller

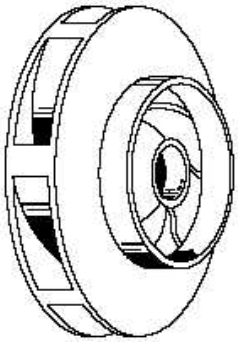

Figure3.5(c) Enclosed Impeller

3.2.2.2 Casing

Casing of a pump is an airtight passage surrounding the impeller and is designed in such a way that the kinetic energy of the water discharged at outlet of the impeller is converted into the pressure energy before the water leaves the casing and enters the delivery pipe.

Types of casing

Volute casing: Volute casing is of spiral type in which area of flow increase gradually. The increase in the area of flow decreases the velocity of flow. The decrease in velocity increases the pressure of the water flowing through the casing. In case of volute casing the efficiency of the pump increases slightly as a large amount of energy is lost due to formation of eddies in this type of casing.

Vortex casing: If a circular chamber is introduced between the casing and the impeller, the casing is known as vortex casing. By introducing the circular chamber, the loss of energy due to formation of eddies is reduced considerably. Thus, the efficiency of the pump is more than the pump with volute casing.

Casing with guide blades: In this type of casing, the impeller is surrounded by series of guide blades mounted on a ring, which is known as diffuser. The guide vanes are designed in such a way that water from the impeller enters the guide vanes without shock, the area of guide vanes increase reducing the velocity of flow through guide vanes and consequently increasing the pressure of pressure of water. The water from the guide vanes then passes through the surrounding casing, which is concentric with the impeller

3.2.2.3 Suction pipe with a foot valve and a strainer

A pipe whose one end is connected to the inlet of the pump and the other end dips into water in a sump is known as a suction pipe. A foot valve, which is non-return valve or one-way type of valve, is fitted at the lower end of suction pipe. The foot valve opens only in the upward direction. A strainer is also fitted at the lower end of suction pipe.

3.2.2.4 Delivery pipe

A pipe whose one end is connected to the outlet of the pump and the other delivers the water at the required height is known as delivery pipe.

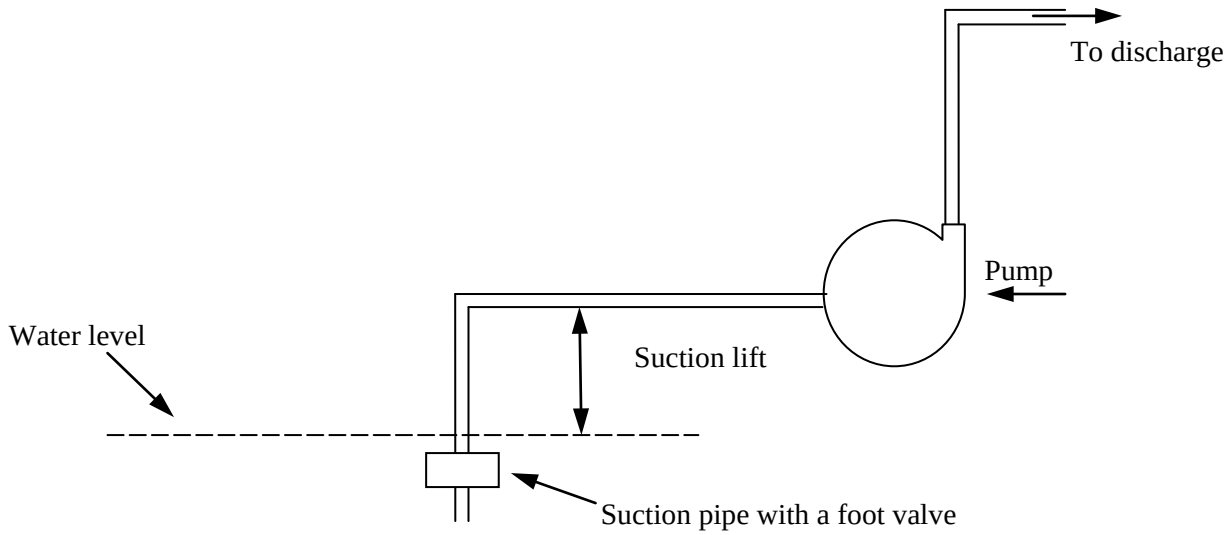

Figure 3.6 Centrifugal pump assembly unit

3.2.3 Centrifugal Pump Losses

The various losses occurring during the operation of a centrifugal pump may be classified as follows:

1. Hydraulic losses
2. Mechanical losses
3. Volumetric or Leakage losses

3.2.3.1 Hydraulic losses

The hydraulic losses that may occur within the pump consist of the following:

1. Shock or eddy losses at the entrance to and the exit from the impeller.
2. Friction losses in the impeller.
3. Friction and eddy losses in the casing section.

For the given values of the blade angles β_2 and speed of rotation, there can be only one rate of discharge that will insure tangential entry to the impeller and tangential exit from the impeller. But in real case pump is required to operate under varying conditions which results in the variation in the rate of discharge as such at the entrance and the exit of the impeller the shock

losses. Generally occur and at the exit from the impeller there occurs a loss of energy due to more or less abrupt change in the direction of velocity of liquid as it enters the casing and other hydraulic losses consist of the following:

1. Friction and other minor losses in the suction pipe.
2. Friction and other minor losses in the delivery pipe.

3.2.3.2 Mechanical losses

The mechanical losses occur in the centrifugal pump on the account of the following:

1. Disc friction between the impeller and the liquid which fills the clearance space between the impeller and the casing.
2. Mechanical friction of the main bearing and glands.

3.2.3.3 Volumetric or leakage loss

In centrifugal pumps as or ordinary built, it is not possible to provide a completely water tight seal between the delivery and suction spaces. As such there is always a certain amount of liquid which slips or leaks from the high pressure to the low pressure points in the pump and it never passes through the delivery pipe. The liquid which escapes or leaks from a high pressure zone to a low pressure zone carries with it energy which is subsequently wasted in eddies. This loss of energy is due to leakage of liquid.

3.2.4 Affinity Laws

The Pump Affinity laws predict the affects of changing the speed of a centrifugal or rotary pump on flow rate, head and power. These laws express the mathematical relationship between the several variables involved in pump performance. They apply to all types of centrifugal flow pumps. They are as follows:

With impeller diameter (D) held constant:

$$\frac{Q_1}{Q_2} = \frac{N_1}{N_2}$$

$$\frac{H_1}{H_2} = \left(\frac{N_1}{N_2}\right)^2$$

$$\frac{BHP_1}{BHP_2} = \left(\frac{N_1}{N_2}\right)^3$$

With speed N held constant:

$$\frac{Q_1}{Q_2} = \frac{D_1}{D_2}$$

$$\frac{H_1}{H_2} = \left(\frac{D_1}{D_2}\right)^2$$

$$\frac{BHP_1}{BHP_2} = \left(\frac{D_1}{D_2}\right)^3$$

Where:

Q = Capacity, m^3/sec

H = Total Head, m

BHP = Brake Horsepower

N = Pump Speed, RPM

When the performance (Q_1, H_1, & BHP_1) is known at some particular speed (N_1) or diameter (D_1), the formulas can be used to estimate the performance (Q_2, H_2, & BHP_2) at some other speed (N_2) or diameter (D_2). The efficiency remains nearly constant for speed changes and for small changes in impeller diameter.

3.2.5 Performance characteristics of centrifugal pumps

A pump is usually designed for a particular speed, flow rate and head, but in actual practice the operation may be at some other condition of head, and for the changed condition the behavior of the pump is less efficient than the quantity the value of velocity of flow of liquid through impeller will be changed. As a result, the value of relative velocity will be changed, and at the same time the loss will be increased so the efficiency of pump will lowered, therefore, in order to predict the behavior and performance of a pump under varying condition, tests are performed, and the result of test are plotted, the curve thus obtained are known as characteristic curve of a pump. Characteristic curve are usually prepared for the centrifugal pump

1) Main and operating characteristic curve

2) Constant efficiency curves

3) Constant head & Constant Discharge curve

3. 2.5.1 Main characteristics

These are obtained by fixing the speed at some arbitrary value of and plotting separately H, HP, & η against Q. The rate of flow Q is varied by means of the quantity H, HP, η are calculated. A number of different values of N are chosen and one such set of curves is drawn for each speed.

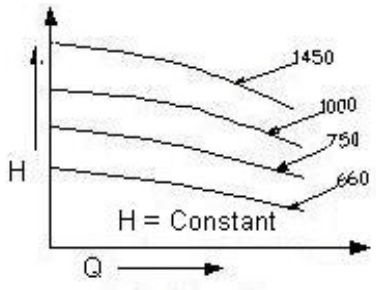

Figure 3.7(a) H v/s Q

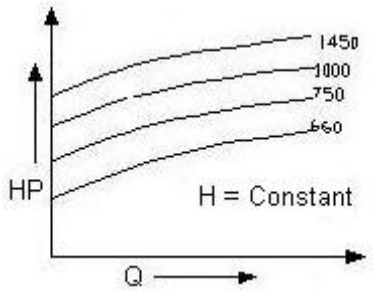

Figure 3.7 (b) HP v/s Q

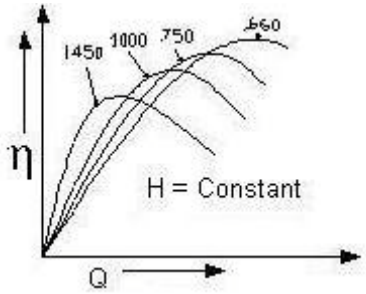

Figure 3.7(c) η v/s Q

3. 2.5.2 Operating characteristics

During operation the pump must run at a constant speed. Normally, this is the designed speed. The particular set of main characteristics which correspond to the designed speed is mostly used in operation and is therefore known as operating characteristics.

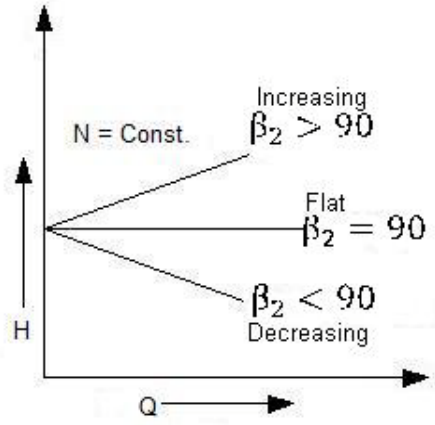

Figure 3.8(a) H v/s Q

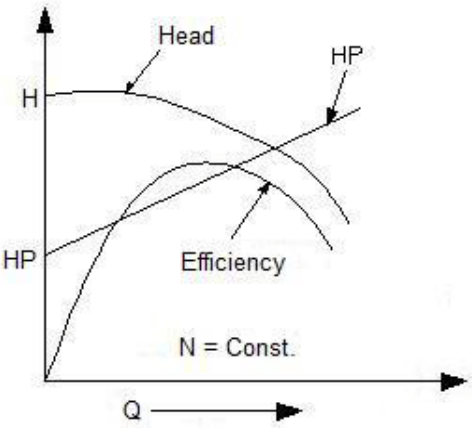

Figure 3.8(b) HP v/s Q

3. 2.5.3 Constant Head and Constant Discharge Curve

It is quite possible that a pump may be required to deliver water at a certain height, in which case it is fixed. If for some reason the speed varies, discharge will also be affected. The performance of the pump under such condition, it is necessary to drawn a constant H curve by plotting Q V N.

Similarly to determine the speed required to discharge a certain quantity at diff. pressure it is convenient to draw constant Q curves showing H against N.

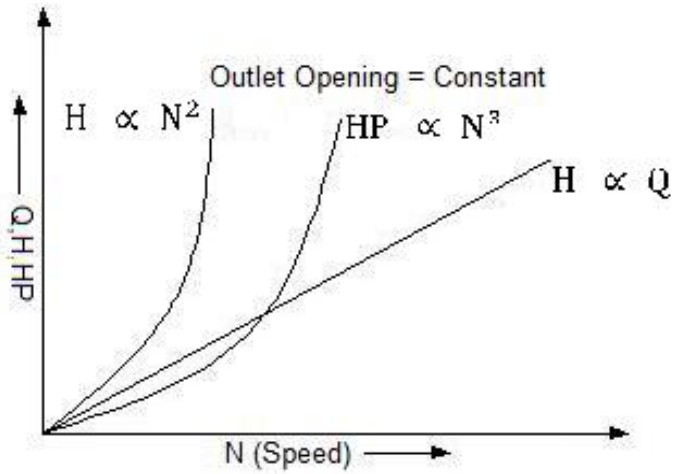

Figure 3.9 Q, H, HP v/s Speed

CHAPTER 4
COMPUTATIONAL FLUID DYNAMICS

4.1 INTRODUCTION

In the recent years, Computational Fluid Dynamics (CFD) has been increasingly used for a wide variety of engineering applications. In the beginning, the use of these techniques was customary only in the areas of aerospace and nuclear technology. Subsequently, the use has spread to a variety of products, physical situations, and manufacturing processes. Some examples of interesting applications of computational modeling are cooling of electronics systems, rotating and reciprocating machinery, furnaces and combustion chambers. The basis of computational fluid dynamics is the reduction of continuum deferential equation describing the dynamics of the fluid (Navier stokes, Mass & energy conservation equation) into a system of algebraic equation of finite number of "grid" points, and the solving of the equation at these limited number of points only. Computational Fluid Dynamics (CFD) provides a qualitative or quantitative prediction of fluid flows by means of

• Mathematical modeling (partial differential equations)
• Numerical methods (discretization and solution techniques)
• Software tools (solvers, pre- and post processing utilities)

Fluid flows and related phenomena can be described by partial differential (or integro differential) equations, which cannot be solved analytically except in few special cases. To obtain an approximate solution numerically, we have to use a discretization method which approximates the differential equations by a system of algebraic equations, which can then be solved on a computer. The approximations are applied to small domains in space and/or time so the numerical solution provides results at discrete locations in space and time. Much as the accuracy of experimental data depends on the quality of the tools used, the accuracy of numerical solutions is dependent on the quality of discretization used.CFD is finding its way into process, chemical, civil, and environmental engineering. Optimization in these areas can produce large savings in equipment and energy costs and in reduction of environmental pollution.

4.1.1 CFD procedure

In order to obtain better design in CFD, following procedure (Figure 4.1) is applied so that fluid flow can easily be modeled in the centrifugal pump impeller.

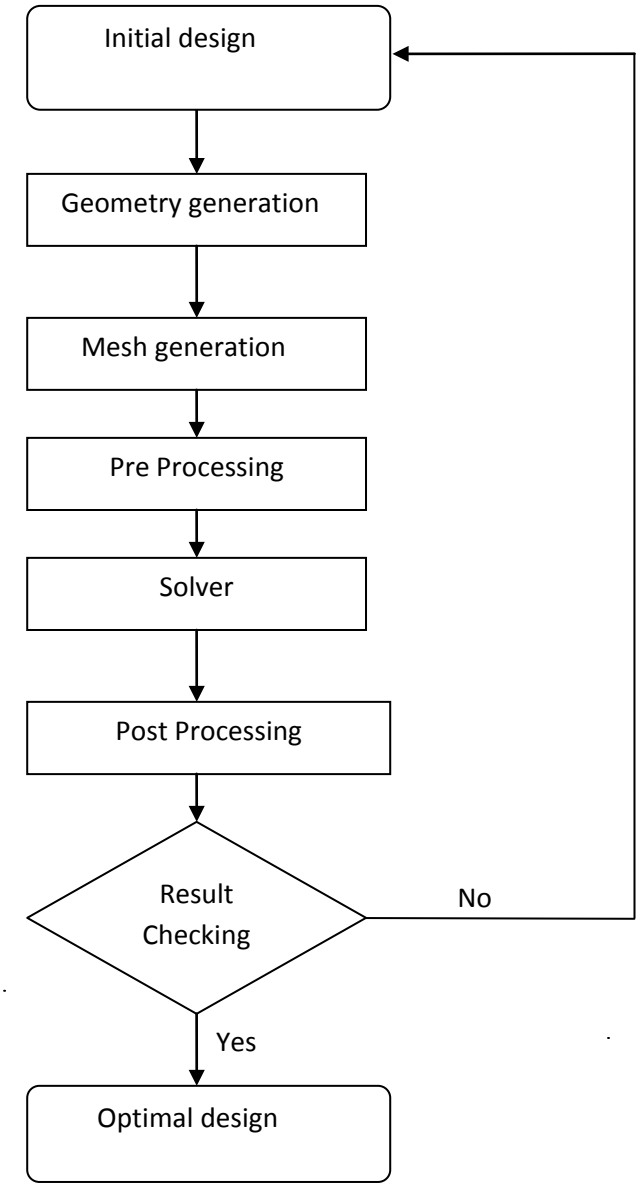

Figure 4.1 Flow chart of CFD procedure

All CFD codes contain three main elements:

1. A **pre-processor**, which is used to input the problem geometry, generates the grid; define the flow parameter and the boundary conditions to the code.
2. A **flow solver**, which is used to solve the governing equations of the flow subject to the conditions provided. There are four different methods used as a flow solver:

i. **Finite difference method**: Finite difference method utilizes the Taylor series expansion to write the derivatives of a variable as the differences between values of the variable at various points in space or time.

ii. **Finite element method**: In the finite element method, the fluid domain under consideration is divided into finite number of sub-domains, known as elements. A simple function is assumed for the variation of each variable inside each element. The summation of variation of the variable in each element is used to describe the whole flow field.

iii. **Finite volume method**: The finite volume method is currently the most popular method in CFD. The main reason is that it can resolve some of the difficulties that the other two methods have. Generally, the finite volume method is a special case of finite element.

3. A **post-processor**, which is used to massage the data and show the results in graphical and easy to read format

4.1.2 Difference between experiments and simulations

CFD gives an insight into flow patterns that are difficult, expensive or impossible to study using traditional (experimental) techniques.

Experiments	Simulations
i. Quantitative description of flow phenomena using measurements	i. Quantitative prediction of flow phenomena using CFD software
ii. For one quantity at a time	ii. For all desired quantities
iii. At a limited number of point and time instants	iii. With high resolution in space and time
iv. For a laboratory-scale method v. For a limited number of problems and operating conditions	iv. For all actual domain v. For virtually any problem and realistic operating condition
vi. Error sources: measurement errors, flow disturbance by the probes	vi. Error sources: modelling, iteration.

4.1.2 Governing equations of CFD

The physical aspects of any fluid flow are governed by the following three fundamental principles:

a) Conservation of mass
b) Conservation of momentum (Newton's second law)
c) Conservation of energy (first law of thermodynamics)

These fundamental principles can be expressed in terms of mathematical equations which in their most general form are usually partial differential equations. CFD is the art of replacing the governing partial differential equations of fluid flow with numbers and advancing these numbers in space and / or time domain to obtain a final description of complete flow field of interest. With the development of high-speed digital computers, CFD has become a powerful tool to predict flow characteristics in varied problem, in an economical way.

4.1.2.1 The mass conservation equation

The law of mass conservation is a general statement of kinematic nature, i.e. independent of the nature of the fluid or of the forces acting on it. It expresses the empirical fact that in a fluid system, mass cannot disappear from the system, nor be created. The quantity U is, in this case, the specific mass, $U = \rho$ in kg/m3.As noted , no diffusive flux exists for the mass transport, which means that mass can only be transported through convection. With the convective flux defined by $F\mathrm{C} = \rho v$ and in absence of external mass sources, the general integral mass conservation equation then becomes in differential form

This equation is also called the continuity equation

$$\frac{\partial \rho}{\partial t} + \nabla.(\rho \vec{v}) = S_m \qquad 4.1$$

The source S_m is the mass added to the continuous phase from the dispersed second phase (e.g. due to vaporization of liquid droplets) and any user-defined sources. For Steady state compressible fluid flow the continuity equation is given by;

$$\rho(\nabla.\vec{v}) = 0$$

Where,

$$\nabla = \frac{\partial}{\partial x_i}\hat{\imath} + \frac{\partial}{\partial x_j}\hat{\jmath} + \frac{\partial}{\partial x_k}\hat{k}$$

And

$$\vec{v} = u_i \hat{\imath} + u_j \hat{\jmath} + u_k \hat{k}$$

4.1.2.2 Conservation of momentum

Conservation of momentum in an inertial (non-accelerating) reference frame is described as

$$\frac{\partial}{\partial t}(\rho . \vec{v}) + \nabla . (\rho \vec{v} \vec{v}) = -\nabla \mathrm{p} + \nabla . (\bar{\bar{\tau}}) + \rho \vec{g} + \vec{F} \qquad 4.2$$

Where

$\rho \vec{g}$ =Gravitational body force

F=external body forces (e.g. that arise from interaction with the dispersed phase), respectively. F also contains other model-dependent source terms such as porous media and user-defined sources.

The stress tensor $\bar{\bar{\tau}}$ is given by

$$\bar{\bar{\tau}} = \mu \left[(\nabla \vec{v} + \nabla \vec{v}^{t}) - \frac{2}{3} \nabla . \vec{v} I \right] \qquad 4.3$$

Where, the second term on the right hand side is taken for considering the effect of volume dilation.

For steady state incompressible fluid flow, the momentum conservation equation is given by

$$\nabla . (\rho \vec{v} \vec{v}) = -\nabla \mathrm{p} + \nabla . (\bar{\bar{\tau}}) + \rho \vec{g} + \vec{F} \qquad 4.4$$

4.1.2.3 Conservation of energy

First law of thermodynamics applied to closed process, i.e. system taken through a complete cycle

$$\int (\mathrm{dQ} - \mathrm{dW}) = 0 \qquad 4.5$$

Change in internal energy during change in state from one point to another in the cycle

$$\mathrm{dE} = \mathrm{dQ} - \mathrm{dW} \qquad 4.7$$

For a steady flow process the conservation of energy per unit time is regarded, i.e. conservation of power.

$$\dot{dE} = \dot{m} \, . \, (\mathrm{dh_0} + \mathrm{g.dZ}) = \dot{Q} - \dot{W} \qquad 4.8$$

Where,

$\mathrm{dh_0}$ = the change in total enthalpy

g.dZ = change in specific potential energy.

Apart from hydraulic machines the latter can be neglected. Further more the process can be assumed as adiabatic leading to the conservation of energy for a steady turbo machine being written as

$$\dot{W} = \dot{m}.\ (h_{01} - h_{02}) \qquad 4.9$$

For work absorbing machines (compressors, pumps) $h_{01} < h_{02} \Rightarrow W < \mathbf{0}$ 4.10

4.2 TURBULENCE

Typical examples are flow around cars, aeroplanes and buildings. There is no definition on turbulent flow, but it has a number of characteristic features such as:

1. **Irregularity:** Turbulent flow is irregular, random and chaotic. The flow consists of a spectrum of different scales (eddy sizes) where largest eddies are of the order of the flow geometry (i.e. boundary layer thickness, jet width, etc). At the other end of the spectra we have the smallest eddies which are by viscous forces (stresses) dissipated into internal energy.
2. **Diffusivity**: In turbulent flow the diffusivity increases. This means that the spreading rate of boundary layers, jets, etc. increases as the flow becomes turbulent. The turbulence increases the exchange of momentum in e.g. boundary layers and reduces or delays thereby separation at bluff, bodies such as cylinders, airfoils and cars. The increased diffusivity also increases the resistance (wall friction) in internal flows such as in channels and pipes.
3. **Large Reynolds Number**: Turbulent flow occurs at high Reynolds number. For example, the transition to turbulent flow in pipes occurs that Re=2300, and in boundary layers at Re=100000
4. **Three Dimensional Flows**: Turbulent flow is always three-dimensional. However, when the equations are time averaged we can treat the flow as two-dimensional.
5. **Dissipation**: Turbulent flow is dissipative, which means that kinetic energy in the small (dissipative) eddies are transformed into internal energy. The small eddies receive the kinetic energy from slightly larger eddies. The slightly larger eddies receive their energy from even larger eddies and so on. The largest eddies extract their energy from the mean flow. This process of transferred energy from the largest turbulent scales (eddies) to the smallest is called *cascade process*.
6. **Continuum**: Even though we have small turbulent scales in the flow they are much larger than the molecular scale and we can treat the flow as a continuum.

4.2.1 Importance of turbulence modeling

Whenever turbulence is present in a certain flow it appears to be dominant over all other flow phenomenon. Turbulent flows are characterized by fluctuating velocity fields. These fluctuations mix transported quantities such as momentum, energy, and species concentration. Since these fluctuations can be of small scale and high frequency, they are too computationally expensive to simulate directly in practical engineering calculations. Instead, the instantaneous (exact) governing equations can be time-averaged, ensemble-averaged, or otherwise manipulated to remove the small scales, resulting in a modified set of equations that are computationally less expensive to solve. However, the modified equations contain additional unknown variables, and turbulence models are needed to determine these variables in terms of known quantities. Modeling turbulence increases the quality of numerical solutions considerably.

4.3 TURBULENCE MODELS

In turbulent flow we usually divide the variables in two components, one time-averaged part $\vec{U}$, which is independent of time (when the mean flow is steady), and other the fluctuating part u.

$$U = \vec{U} + u$$

The reason for decomposing the variables in two parts is:

- While measuring the flow quantities we are usually interested in the mean values rather that the time histories
- To solve the Navier-Stokes equation numerically it would require a very fine grid to resolve all turbulent scales and it would also require a fine resolution in time (turbulent flow is always unsteady).

Algebraic Models: An algebraic equation is used to compute a turbulent viscosity, often called *eddy* viscosity. The reynolds stress tensor is then computed using an assumption which relates the reynolds stress tensor to the velocity gradients and the turbulent viscosity. This assumption is

called the *Boussinesq assumption*. Models which are based on a turbulent (eddy) viscosity are called *eddy viscosity* models

One-Equation Models: In these models a transport equation is solved for a turbulent quantity (usually the turbulent kinetic energy) and a second turbulent quantity (usually a turbulent length scale) is obtained from an algebraic expression. The turbulent viscosity is calculated from Boussinesq assumption.

Two Equation Models: These models fall into the class of eddy viscosity models. Two transport equations are derived which describe transport of two scalars, for example the turbulent kinetic energy K and its dissipationϵ. The Reynolds stress tensor is then computed using an assumption which relates the Reynolds stress tensor to the velocity gradients and an eddy viscosity. The latter is obtained from the two transported scalars.

Reynolds stress models: Transport equation is derived for the Reynolds tensor $\overline{u_i u_j}$. One transport equation has to be added for determining the length scale of the turbulence. Usually an equation for the dissipation ε is used.

4.3.1 The K-ε Turbulence Model

The simplest complete models of turbulence are two-equation models in which the solution of two separate transport equations allows the turbulent velocity and length scales to be independently determined. The k-ε model falls within this class of turbulence model and has become the basic of practical engineering flow calculations in the time since it was proposed by Launder and Spalding. Robustness, economy, and reasonable accuracy for a wide range of turbulent flows explain its popularity in industrial flow and heat transfer simulations. It is a semi-empirical model, and the derivation of the model equations relies on phenomenological considerations and empiricism.

Transport Equations for the Standard k-ε Model

The turbulence kinetic energy k, and its rate of dissipation ε, is obtained from the following transport equations:

$$\frac{\partial}{\partial t}(\rho k) + \frac{\partial}{\partial x_i}(\rho k u_i) = \frac{\partial}{\partial x_j}\left[\left(\mu + \frac{\mu_t}{\sigma_k}\right)\frac{\partial k}{\partial x_j}\right] + G_k + G_b - \rho\varepsilon - Y_M + S_k \quad 4.11$$

And

$$\frac{\partial}{\partial t}(\rho \varepsilon) + \frac{\partial}{\partial x_i}(\rho \varepsilon u_i) = \frac{\partial}{\partial x_j}\left[\left(\mu + \frac{\mu_t}{\sigma_z}\right)\frac{\partial \varepsilon}{\partial x_j}\right] + C_k \frac{\varepsilon}{k}(G_k + C_{3\epsilon} G_b) - C_{2\varepsilon}\rho\frac{\varepsilon^2}{k} + S_k \quad 4.12$$

The turbulent (or eddy) viscosity, μ_t, is computed by combining k and ε as follows:

$$\mu_t = \rho C_\mu \frac{k^2}{\varepsilon} \quad 4.13$$

The values of the constants used are

$C_{1z} = 1.44$, $C_{2z} = 1.92$, $C_\varepsilon = 0.09$, $\sigma_k = 1.0$ and $\sigma_\varepsilon = 1.3$.

4.4 BOUNDARY CONDITIONS

Boundary conditions are the set of conditions specified for the behavior of the solution to a set of differential equations at the boundary of its domain. Boundary conditions are important in determining the mathematical solutions to many physical problems. These conditions specify the flow and thermal variables on the boundaries of a physical model. They are, therefore, a critical component of simulation and it is important that they are specified appropriately. The boundary conditions are defined on cell faces and they do not have a finite thickness and they provide a means of introducing a step change in flow properties.

4.4.1 Types of boundary conditions

The following boundary conditions at the walls are used with the equations of motion

- No slip conditions

  At fluid wall interface, there must be no slip

$$\vec{V}_{fluid} = \vec{V}_{wall}$$

- Temperature field

The principle different types of boundary conditions are as follows:

- Dirichlet boundary condition (first type)
- Neumann boundary condition (second type)
- Robbins boundary condition (third type)

4.5 ERRORS IN CFD

Error is a recognizable deficiency in a CFD model that is not caused by lack of knowledge. Causes of errors are:

(a) Numerical errors – round off errors, iterative convergence errors, discretization errors.

(b) Coding errors: mistakes or 'bugs' in the software

(c) User errors-human errors through incorrect use of software. Can be reduced / eliminated through adequate training and experience.

CHAPTER 5

MODELING OF PUMP COMPONENTS

5.1 INTRODUCTION

The pump under study is the part of a test loop used to study the slurries transportation physics at different speeds and concentrations. The purpose of the test loop is to conduct the slurry transportation under controlled conditions so that the effect of different parameters on slurry transport can be studied. The test loop consists of a closed circuit pipe test loop of 50 mm NB pipe having a length of 40m along with other necessary components. The main components of a pilot plant are shown in figure 5.1.

1. Centrifugal slurry pump
2. Observation chamber
3. Flow meters
4. Density meter
5. Slurry preparation tank
6. Measuring tank
7. Bypass line
8. Flow diverter
9. Stirrer

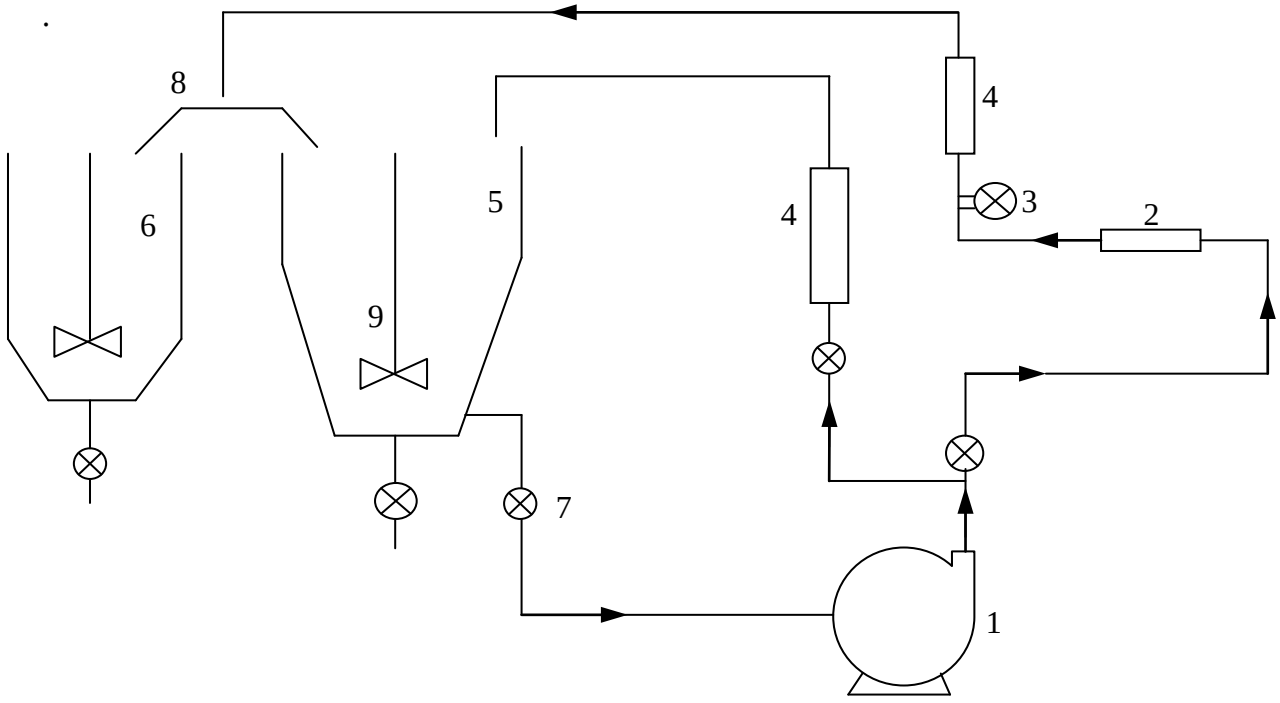

Figure 5.1 Schematic diagram of test loop

Slurry Preparation Tank-The slurry preparation tank is used to prepare slurries using different solids like limestone, zinc, nickel and other solids to be studied. This tank is in the shape of a hopper and consists of a stirrer which is rotated using a motor and a reduction gear unit.

Measuring Tank-The measuring tank in the loop is used to measure the rate of flow by taking reading if there is a change in the level of slurry in the tank over a certain time period.

Centrifugal Slurry Pump with VFD- The main function of VFD is to accurately change the operating speed of the pump with variable frequency drive.

Figure 5.2 Control panel of VFD

Electro-magnetic flow meter-The electro-magnetic flow meter is used to measure the flow rate of slurry through the circuit. The flow meter has an accuracy of ±5%.

Nucleonic density meter- A nucleonic density meter is used to measure the concentration of the slurry. It is installed in the vertical section of the pipe near discharge.

Figure 5.3 Pilot plant test loop

5.2 CENTRIFUGAL SLURRY PUMP

The slurry pump used in the test loop is as shown in the figure 5.4. The centrifugal pump used is designed for abrasive solids application such as those found in aggregate, cement, lime slurries and many other common industrial and mining applications. The pump can handle slurries with particle size ranging from 2x1 to 14x10 μm, and flow rates ranging from less than 2.2 m^3/hr to 910 m^3/hr.

Figure 5.4 Centrifugal slurry pump of the test loop

To prevent wear and erosion of the pump White iron, Ni-hard 4 and Max-alloy having 27% chromium were used to manufacture pump components.

5.3 MODELING OF THE PUMP COMPONENTS

To study the numerical analysis on the pump, the dimension data of the pump was required to generate a model in the software. For taking the dimensions of components reverse engineering techniques were used. The test loop was shut and all the valves were closed to prevent any leakage of water or slurry. The pump was first disconnected from the pipes of the test loop and the water in the pump assembly was drained. The pump assembly was disassembled and all the parts were separated. The assembly consisted of the casing, impeller and suction discs (frame

and follower plate). Since the pump was firmly placed on the foundation the suction passage extending from the flange to the frame was not removed.

5.3.1 Dimensioning

After the pump was disassembled, the task of taking dimensions of each component was divided into two phases.

1. The dimensions that could be taken directly like impeller outer diameter, casing outlet diameter, etc were taken using vernier calipers and steel rule.
2. For dimensions that could not be taken directly with instruments moulds of plaster of paris and clay were made.

Impeller

The impeller of pump is the enclosed type and has 5 vanes. The impeller tail extends from the center of the head through the discs till the suction passage where it rests on a disc connected to the shaft and embedded in the inlet passage. The tail section is circular in shape; this section has a constant diameter over a certain length and increases gradually over the end forming a bell mouth at the end. This bell mouth lies in the suction passage from where the flow enters the pump. The main purpose of the giving bell shape to the tail of the impeller is the smoothening of the flow to ensure uniform feed to the impeller. A fillet is given at the inlet in the impeller head where the flow enters the vanes. Due to this fillet the width of the vane increases at the inlet. Since the impeller is closed type and the vane at inlet is wider than the outlet, it was not possible to measure the dimensions at the impeller inlet. The profile of the vane at inlet was reconstructed by making a mould out of m-seal. The other parts of the impeller were modeled using plaster of paris moulds. The dimensions were then taken from these moulds by plotting them on the graph. Points were marked on the graph sheet with respect to a reference. These points were then plotted in the software following which a curve with a suitable radius was fitted through the points to get the smooth surface.

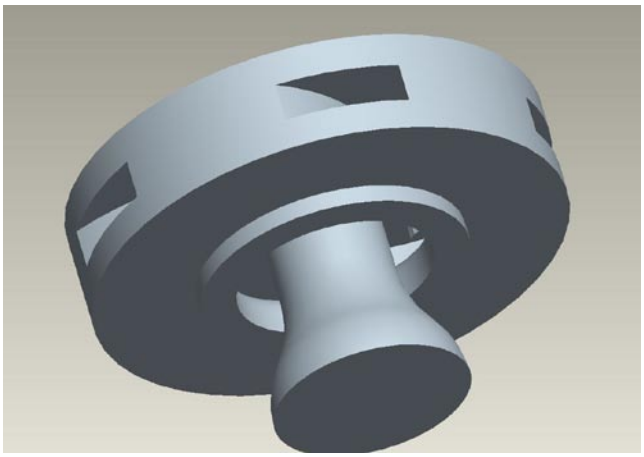

Figure 5.5(a) Impeller of the pump **figure 5.5 (b) Cad model of Impeller**

Casing

The casing is of semi-volute type having 275 mm base circle diameter and 11 degrees tongue angle. The casing was also modeled by making plaster of paris moulds. For the purpose, the casing was divided into 12 sectors each spanning over 30 degrees. Once divided moulds of each of these sectors were casted. The moulds were not casted for the entire sector but only for the area beyond the base circle, this was done to optimize the requirement of plaster of paris and also because only the area which is increasing was required. These 12 sectors were then put together to reconstruct the casing and check the conformation with the casing. These sectors were then grinded on the edges to get a clear cross-section on the graph. Each sector was then drawn over a base circle in the software. The cross-section was drawn by connecting the points with Nerbs. Once the cross-section of each sector was made, the casing was constructed with the bottom up approach by creating faces and volumes.

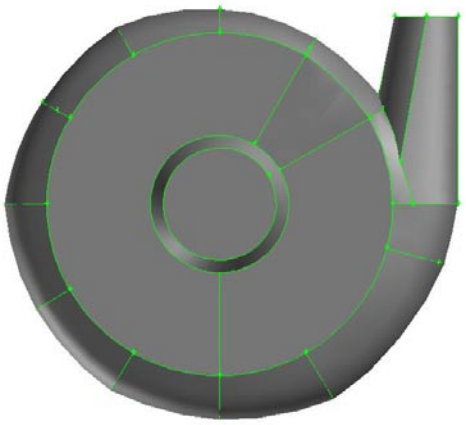

Figure 5.6(a) Casing of the pump **Figure 5.6(b) Cad model of fluid in casing**

Follower plate, Frame and Flange

The dimensions of the follower plate and frame were taken directly as the geometry was simple both to measure and construct in CAD software. The cross-section of the disc was modeled according to the dimensions and then rotated about an axis to model the discs. The flange was a made by joining the cross-section at pump inlet and the flange connected to the pipe. The cross-section at pipe end was circular while it had a different cross-section at the inlet. The two sections made and then joined.

Figure 5.7(a) frame of the pump

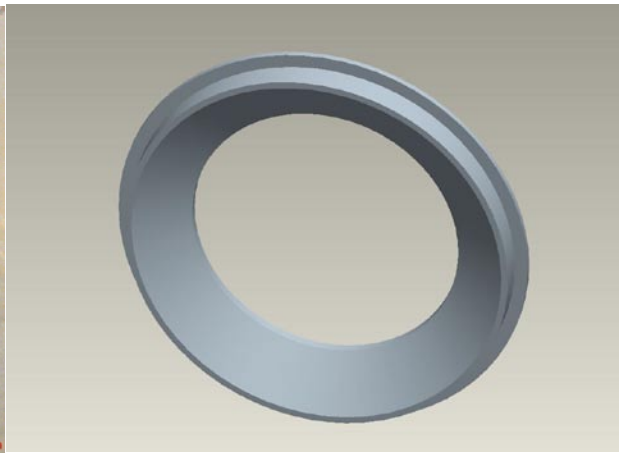

Figure 5.7(b) Cad model of frame

Figure 5.8(a) Follower plate of the pump

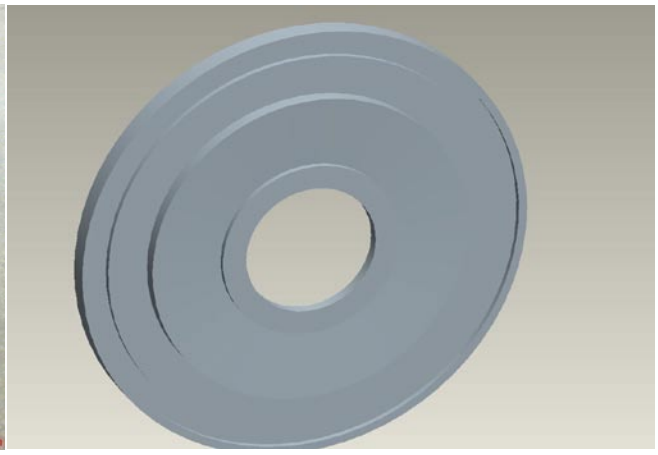

Figure 5.8(b) CAD model of follower plate

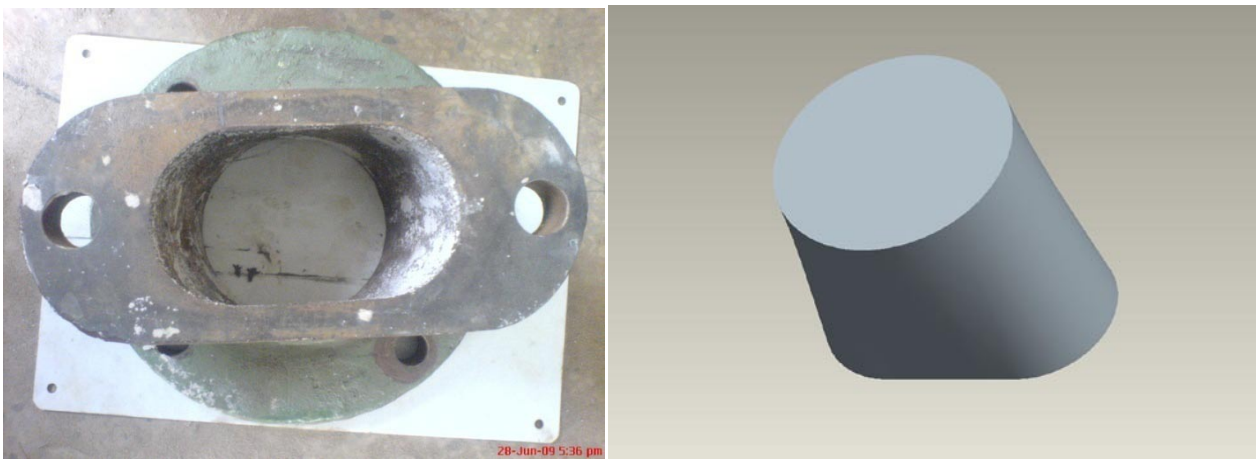

Figure 5.9 Flange of test loop and CAD model of fluid volume in flange

Inlet passage

The inlet passage of the centrifugal slurry pump had a complicated structure with several fillets and sections at different angles. For this reason several moulds of different areas were made; from these sections geometry of passage at different locations was obtained. These sections were extended and combined together to model the fluid portion in the inlet passage.

The modeling was done in two different software's Pro-engineer and Gambit. This was because Pro-Engineer is a modeling software and has sophisticated modeling tools that helped in modeling the complex geometries. Apart from the modeling tools the software has features that helped in creating cross-sections at different locations which helped in better visualization and

Figure 5.10 Inlet passage of pump in test loop

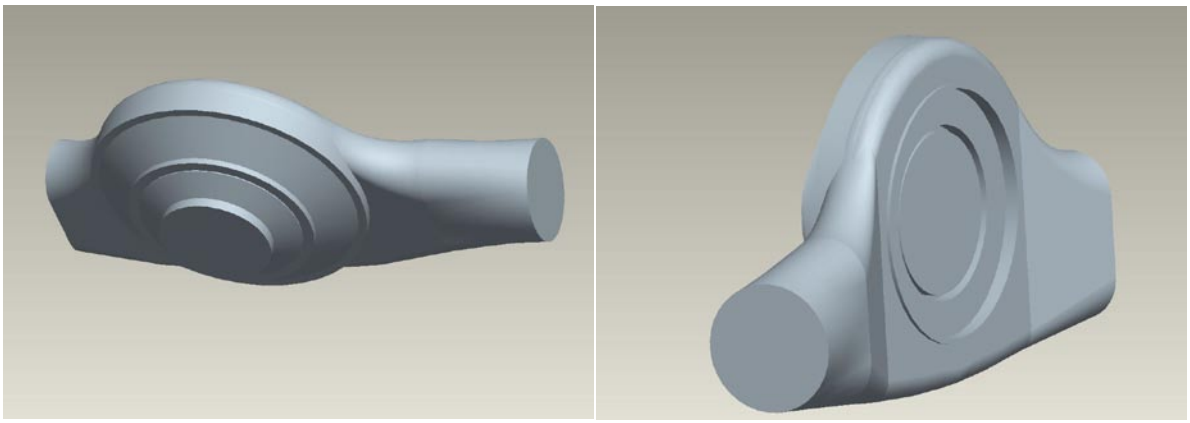

Figure 5.11 CAD model of fluid volume of inlet passage

understanding of the actual pump geometry. Gambit is a pre processor and has powerful tools for meshing and defining the problem for analysis. Since the problem was to be solved in Fluent gambit was preferred as it is specifically programmed for defining problems in Fluent. The meshing tools in Gambit help in controlling the mesh of the model. The modeling tools in gambit are more powerful when using bottom up approach in modeling the geometry as it is more flexible and any complicated geometry can be easily modeled if the required data is available.

5.4 MESH GENERATION

The first step after modeling the pump components is importing the model in pre-processor and descretize it into smaller elements. The model is descretized so that the affect of external or internal forces acting on a body can be captured at any point on the body. This process of discretization is called meshing. The larger the number of these elements, finer will be the mesh which will give accurate result. But a large number of elements or a fine mesh needs greater computational capabilities and time. To optimize the meshing, a finer mesh is used at points where the forces have maximum impact and a coarser mesh is used at other locations. For meshing, the model was taken to a commercially available pre-processor called GAMBIT. Gambit provides a large variety of tools for meshing. Every tool has various schemes that give flexibility in discretization of the model. The various meshing schemes are explained below.

5.4.1 Boundary layers

Boundary layers define the spacing of mesh nodes in regions immediately adjacent to edges and faces. They are used primarily to control mesh density and, thereby, to control the amount of information available from the model in specific regions of interest. For e.g. by attaching a boundary layer to the face that represents the pipe wall, you can increase the mesh density near the wall and decrease the density near the center of the cylinder, thereby obtaining sufficient information to characterize the gradients in both regions while minimizing the total number of mesh nodes in the model.

5.4.2 Edge meshing schemes

The various schemes for meshing the edges are:

- Successive Ratio
- First Length
- Last Length
- First Last Ratio
- Last First Ratio
- Exponent
- Bi-exponent
- Bell Shaped

The first six schemes listed above are **non-symmetric** schemes—that is, they can produce grading patterns that are not necessarily symmetric about the center of the edge. The last two schemes are **symmetric** schemes—that is, they are constrained to produce grading patterns that are symmetric about the center of the edge.

Non-symmetric grading scheme

For each of the non-symmetric grading schemes, the mesh nodes are created along the edge such that the ratio of any two succeeding interval lengths is constant and is governed by the following equation:

$$\frac{l_{i+1}}{l_i} = R$$

where,

l_i and l_{i+1} are the lengths of intervals i and i+1, respectively, and R is a fixed value

For any given number of intervals (*n*), the grading schemes differ from each other only with respect to the manner in which the pre-processor determines the value of the interval length ratio, *R*. When grading or meshing an edge using a non-symmetric scheme, it must be specified whether the grading scheme is *single-sided* or *double-sided*. Double-sided grading differs from single-sided grading in that the edge is divided into two separate segments for grading purposes, and each segment is graded according to its own grading parameter.

Center of grading

To specify double-sided grading, either a node or an interval is created at the center of grading for the edge. The form of the grading center (node or interval) depends on the total number of edge intervals (*n*) as follows. If *n* is even, a mesh *node* is created at the center of grading. If *n* is odd, a mesh *interval* is created at the center of grading. The location of the center node (*n* even) or the location and size of the center interval (*n* odd) is determined according to the following rules.

- If *n* is even, the edge is graded such that the lengths of the intervals on either side of the center node are equal.
- If *n* is odd, the edge is graded such that the length of the center interval conforms to the meshing parameters specified for both segments of the edge.

Symmetric grading schemes

In symmetric grading scheme, two symmetric grading schemes for edge meshing are available:

- Bi-exponent
- Bell Shaped

Both schemes grade a given edge such that mesh node placement is symmetric about the center of the edge. The schemes differ from each other in the manner in which pre-processor determines the mesh node spacing along the edge.

Bi-exponent scheme

The Bi-Exponent scheme divides the edge into two segments of equal length and applies the exponent grading scheme separately to each segment. The Exponent input parameter, *x* specified by means of the ratio field on the mesh edges form, produces the following grading characteristics for the Bi-exponent scheme.

x	Grading Characteristic
< 0.5	Mesh nodes are densest near the center of grading and least dense near the endpoints of the edge.
= 0.5	Mesh nodes are evenly spaced along the entire edge.
> 0.5	Mesh nodes are densest near the endpoints of the edge and least dense near the center of grading.

Table 5.1 Relation between input and grading characteristic

Bell shaped scheme

The Bell Shaped scheme grades the edge such that the mesh node density obeys a normal distribution centered at the geometric center of the edge. The user-specified input parameter for the Bell Shaped scheme—specified by means of the ratio field on the mesh edges form—produces grading characteristics identical to those shown above for the Bi-exponent scheme.

Element type

For meshing edges, two types of elements can be used depending upon the required discretization of the edge. The edge element type determines the number of edge mesh nodes corresponding to face and volume elements in the model

- A 2-node edge element creates mesh nodes only at the end points of the edge mesh intervals.
- A 3-node edge element creates an additional mesh node at the center of each mesh intervals.

The location of the center node (*n* even) or the location and size of the center interval (*n* odd) is determined according to the following rules.

- If *n* is even, the pre-processor grade the edge such that the lengths of the intervals on either side of the center node are equal.
- If *n* is odd, the pre-processor grades the edge such that the length of the center interval conforms to the meshing parameters specified for both segments of the edge.

A change in the edge element type specification, automatically changes all corresponding face and volume element types. Likewise, when you change the face or volume element types, pre-processor automatically changes the edge element type. Table 5.2 summarizes the general correspondence between edge, face, and volume element types.

Edge	Face		Volume	
nodes	shapes	nodes	shapes	nodes
2	Triangle	3	Tetrahedral	4
	Quadrilateral	4	Hexahedral	8
			Wedge	6
			Pyramid	5
3	Triangle	6	Hexahedral	27
	Quadrilateral	9	Tetrahedral	10
			Wedge	18
			Pyramid	13

Table 5.2 Correspondence between edge, face and volume element type

5.4.3 Face meshing schemes

The shape and topological characteristics of the face, as well as the vertex types associated with the face, determine the types of mesh schemes that can be applied to the face.

Specifying the meshing scheme

To specify the face-meshing scheme, the following parameters must be specified:

- The **Elements** parameter defines the shapes of the elements that are used to mesh the face.

- The **Type** parameter defines the pattern of mesh elements on the face.
- The **Smoother** specification determines the type of smoothing algorithm used to smooth a mapped mesh during the meshing operation.

Specifying scheme elements

- Quad Specifies that the mesh includes only quadrilateral mesh elements
- Tri Specifies that the mesh includes only triangular mesh elements
- Quad/Tri Specifies that the mesh is composed primarily of quadrilateral mesh elements but includes triangular corner elements at user-specified locations

Specifying scheme type

- **Map** creates a regular, structured grid of mesh elements
- **Submap** divides an un-mappable face into mappable regions and creates structured grids of mesh elements in each region
- **Pave** creates an unstructured grid of mesh elements
- **Tri Primitive** divides a three-sided face into three quadrilateral regions and creates a mapped mesh in each region
- **Wedge Primitive** creates triangular elements at the tip of a wedge shaped face and creates a radial mesh outward from the tip

Quad-Map meshing scheme

To apply the Quad-Map meshing scheme to a face, the pre-processor meshes the face using a regular grid of quadrilateral face mesh elements. The Quad-Map meshing scheme is applicable primarily to faces that are bounded by four or more edges, however not all such faces are suitable for mapping. To be “mappable,” a face must not violate restrictions related to the following parameters:

- Vertex types
- Edge mesh intervals

Quad/Tri-map meshing scheme

The Quad/Tri-Map meshing scheme is applicable only to geometry that constitutes a narrow, logical sliver. To apply the Quad/Tri-Map meshing scheme, the pre-processor creates triangular mesh elements at the two endpoints of the sides and creates quadrilateral elements across the rest

of the face. The vertex-type and edge mesh interval restrictions for the Quad/Tri-Map meshing scheme are as follows.

Vertex types

To employ the Quad/Tri-Map meshing scheme to a sliver-shaped face, vertices are specified as follows:

Tips of the sliver - Tri-element

All other vertices - Side

Edge mesh intervals

If you grade or mesh the edges that comprise the sides of a sliver-shaped face before applying the Quad/Tri-Map meshing scheme, the edge grading is specified such that the sides possess identical numbers of intervals.

Sub-map meshing scheme

To fit the Sub-map meshing scheme to a face, the pre-processor divides the face into one or more mappable regions and creates a mapped mesh in each region. Like the Map meshing scheme, the Sub-map meshing scheme is subject to restrictions related to vertex types and edge mesh intervals.

Quad-Pave meshing scheme

In the Quad-Pave meshing scheme, the pre-processor creates an unstructured face mesh consisting of quadrilateral mesh elements

Tri-Pave meshing scheme

In Tri-Pave meshing scheme, the pre-processor creates a face mesh consisting of irregular triangular mesh elements

Quad/Tri-Pave meshing scheme

To apply the Quad/Tri-Pave meshing scheme to a face, the pre-processor creates a paved mesh that consists primarily of quadrilateral elements but employs triangular mesh elements in any corners the edges of which form a very small angle with respect to each other. You can also

impose the creation of triangular mesh elements in corners of the face by setting the associated vertices as Tri-element vertices.

Tri Primitive meshing scheme

The Tri Primitive meshing scheme creates a sub mapped mesh on a three-sided face. It is to be noted that any side of the three-sided face may consist of more than one edge. When you apply the Tri Primitive meshing scheme to a three-sided face, the pre-processor locates a point internal to the face that serves as a common endpoint for three mappable sub regions. In this scheme the face is divided into three mappable regions, each of which shares a common endpoint.

Wedge Primitive meshing scheme

The Wedge Primitive meshing scheme creates a radial mesh on a three-sided face. When you apply the Wedge Primitive meshing scheme, the pre-processor creates a mapped mesh that includes a group of triangular mesh elements emanating from common endpoint. Face meshes are created by means of the Wedge Primitive mesh scheme consist of regular quadrilateral mesh elements and a group of triangular mesh elements that share a common endpoint.

Face element type

The Face Element Type specifies the mesh node configuration associated with either of two available face element shapes. To set the face element type the node pattern associated is specified with each of the face element shapes. There are two face element shapes available:

- Quadrilateral
- Triangle

Each face element shape is associated with three different node patterns, and each node pattern is characterized by the number of nodes in the pattern. Figure 5.11 and Figure 5.12 show the node patterns associated with the quadrilateral and triangular face element types, respectively.

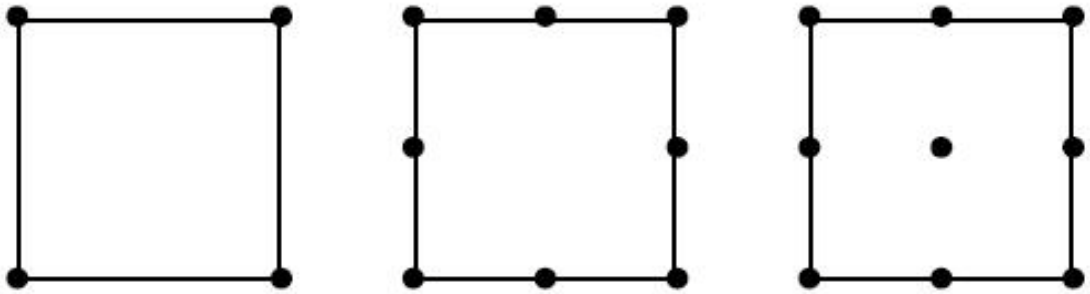

Figure 5.12 Quadrilateral face element types 4, 6 and 8 Node elements

Figure 5.13 Triangular face element types 3 Node and 6 Node elements

When setting a face element type, the pre-processor applies the type to all face elements of the specified shape. For example, to specify 8-node quadrilateral face elements, the pre-processor locates mesh nodes according to the 8-node pattern for all quadrilateral face elements produced in the subsequent face meshing operation.

5.4.4 Meshing the volumes

The Pre-processor specifies any volume for a meshing operation however, the shape and topological characteristics of the volume, as well as the vertex types associated with its faces; determine the types of mesh schemes that can be applied to the volume. The pre-processor provides option to select any of the following volume meshing elements options. Table 5.3 describes the basic shapes of each of the mesh elements.

Option	Description
Hex	Specifies that the mesh includes only hexahedral elements.
Hex/Wedge	Specifies that the mesh is composed primarily of hexahedral elements but includes wedge elements where appropriate.
Tet/Hybrid	Specifies that the mesh is composed primarily of tetrahedral elements but may include hexahedral, pyramidal, and wedge elements where appropriate.

Table 5.3 Shapes of mesh elements

Specifying scheme type

Each of the elements options listed above is associated with a specific set of type options

Option	Description
Map	Creates a regular, structured grid of hexahedral elements
Sub-map	Divides an un-mappable volume into mappable regions and creates a structured grid of hexahedral elements in each region
Tet Primitive	Divides a four-sided volume into four hexahedral regions and creates a mapped mesh in each region
Cooper	Sweeps the mesh node patterns of specified “source” faces through the volume
T-Grid	Creates a mesh that consists primarily of tetrahedral elements but which may also contain hexahedral, pyramidal, and wedge mesh elements
Stairstep	Creates a regular hexahedral mesh and a corresponding faceted volume that approximates the shape of the original volume
Hex Core	Creates a core of regular hexahedral elements surrounded by transition layers of tetrahedral, pyramidal, and wedge elements

Table 5.4 Volume meshing schemes

Map meshing scheme

To apply the Map meshing scheme to a volume, the pre-processor meshes the volume using an array of hexahedral mesh elements. Each mesh element includes at least eight nodes—located at the corners of the element. To specify an alternative volume element node pattern, pre-processor creates either 20 or 27 nodes per mesh element. The Map volume meshing scheme can only be applied to volumes that can be meshed such that the mesh represents a logical cube. To represent a logical cube, a volume mesh must satisfy the following general requirements.

1. There must exist exactly eight mesh nodes that are attached to only three mesh element faces. (These eight mesh nodes comprise the corners of the logical cube.)
2. Each of the eight corner mesh nodes must be connected to three other corner mesh nodes by means of a straight chain of mesh edges—that is, a chain of mesh edges all of which belong to a single logical row of mesh nodes.

According to the criteria described above, the most basic form of a mappable volume is a rectangular brick. For such a volume, the mesh nodes located at the corner vertices of the brick constitute the corners of the mesh cube. Although the strict definition of volume mappability is best expressed in terms of the mesh itself, it is possible to state mappability requirements in terms of the general geometrical configuration of a given volume. Specifically, volume mappability criteria may be stated as follows:

To be mappable, a volume should contain six sides, each of which can be rendered mappable by the correct specification of vertex types.

However, it is possible to transform the other volumes into mappable volumes by means of vertex-type assignments and virtual geometry operations. The following sections describe the operations required to render each volume mappable.

Sub-map meshing scheme

To apply the Sub-map meshing scheme to a volume, the pre-processor subdivides the volume into logical mesh cubes each of which can be mapped. According to a Map meshing scheme to be sub-mappable, a volume must be configured such that it satisfies the following criteria:

- Each face must be either mappable or sub-mappable.
- Opposing sub-mappable faces must be configured consistently with respect to their vertex types.

Face Mappability and Sub-mappability

In order for the pre-processor to apply a Sub-map meshing scheme to a volume, each face that bounds the volume must be either mappable or sub-mappable

Tet Primitive meshing scheme

The Tet Primitive volume meshing scheme applies only to volumes that constitute logical tetrahedra. To constitute a logical tetrahedron, a volume must include only four sides, each of which constitutes a logical triangle. On applying the Tet Primitive meshing scheme, the pre-processor creates Tri Primitive meshes on each of the faces of the tetrahedron, then subdivides the volume into four hexahedral quadrants and creates a Map-type volume mesh in each quadrant. the pre-processor creates Tri Primitive meshes on each face, then subdivides the volume into four quadrants and meshes each quadrant with hexahedral mesh elements.

Cooper meshing scheme

In Cooper meshing scheme the pre-processor treats the volume as consisting of one or more logical cylinders each of which is composed of two end caps and a barrel. Faces that comprise the caps of such cylinders are called “source” faces; faces that comprise the barrels of the cylinders are called “non-source” faces. In general, the Cooper meshing scheme applies to volumes that demonstrate either of the following characteristics.

- At least one face is neither mappable nor sub-mappable.
- All faces are mappable or sub-mappable, but the vertex types are specified such that the volume cannot be divided into mappable sub-volumes.

Faces that meet either of the criteria outlined above, as well as those that are logically parallel to such faces, constitute source faces for the volume and the end caps of the corresponding logical cylinder.

T-Grid meshing scheme

In the T-Grid meshing scheme the pre-processor creates a mesh that consists primarily of tetrahedral mesh elements but which may also contain elements that possess other shapes. To mesh one or more faces of the volume by means of a Quad or Quad/Tri scheme before applying the T-Grid volume meshing scheme, the pre-processor creates hexahedral, pyramidal, or wedge

elements where appropriate in proximity to the previously meshed faces. The T-Grid has the following features:

- The T-Grid meshing scheme imposes no restrictions on the types of edge or face meshes that can be previously applied to the volume.
- There is a control tool for the refinement of the tetrahedral mesh by means of the pre-processor program defaults. The program also allows controlling several aspects of prism boundary layer elements. For a description of the use of the pre-processor program defaults.
- In general, it is best to avoid creating quadrilateral face mesh elements with aspect ratios greater than 5 on the boundaries of any volume to be meshed by means of the T-Grid meshing scheme. Face mesh elements with high aspect ratios produce highly skewed transition pyramidal elements. As a result, the T-Grid volume meshing may fail or produce low-quality elements
- To employ a face boundary layer when meshing a volume by means of the T-Grid meshing scheme, it is best to attach the boundary layer to the face itself rather than to its bounding edges. Also to apply the boundary layers to the bounding edges rather than to the face, the T-Grid scheme will create pyramidal elements on the side faces but not on the face itself. As a result, the volume will not contain boundary layers of transition elements in the region adjacent to the face.

Stairstep meshing scheme

The Stairstep meshing scheme creates and meshes a faceted volume the shape of which approximates the volume to be meshed. The pre-processor does not mesh the original volume itself, and the created faceted volume is not connected to any existing geometry—including geometry to which the original volume is connected. For e.g. to mesh the elliptical cylinder by means of the Stairstep scheme using an overall interval size of 0.75, the pre-processor creates and meshes the faceted volume. Note that the shape of the faceted volume crudely approximates the shape of the original elliptical cylinder and that all mesh elements are cubic hexahedra of uniform size.

Hex Core meshing scheme

The Hex Core meshing scheme creates a mesh consisting of two regions:

- An inner region composed of regular hexahedral elements.
- An outer region consisting of pyramidal, tetrahedral, and wedge elements where appropriate.

It is to be noted that wedge elements are created only when boundary layers are attached on faces pre-meshed with triangular elements. The hex core mesh consists of a core of hexahedral elements surrounded by a transition region consisting of pyramidal elements adjacent to the core itself and a shell of tetrahedral elements filling the remainder of the volume. The existence of the hexahedral-element core significantly reduces the total number of elements for the mesh relative to a pure tetrahedral mesh.

Volume element type

Volume Element Type is used to specify the number of mesh nodes and the node pattern associated with any of four available volume element shapes. To set the volume element type, you must specify the numbers of nodes associated with each of the volume element shapes. There are four volume element shapes available.

- Hexahedron
- Wedge
- Tetrahedron
- Pyramid

Every volume element shape is associated with as many as five different node patterns. Each node pattern is characterized by the number of nodes in the pattern. The node patterns associated with each volume element shape are as follows:

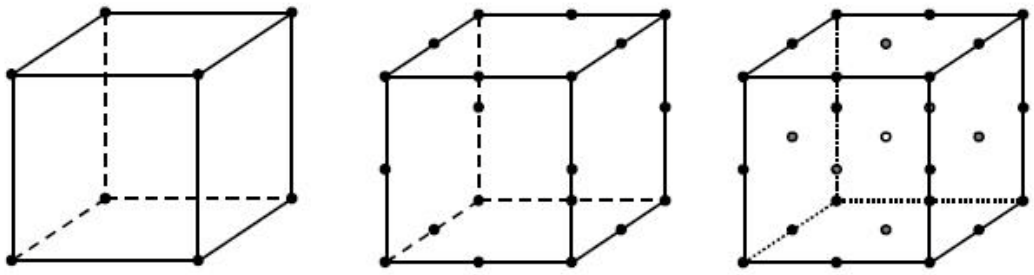

Figure 5.14 Hexahedron volume elements

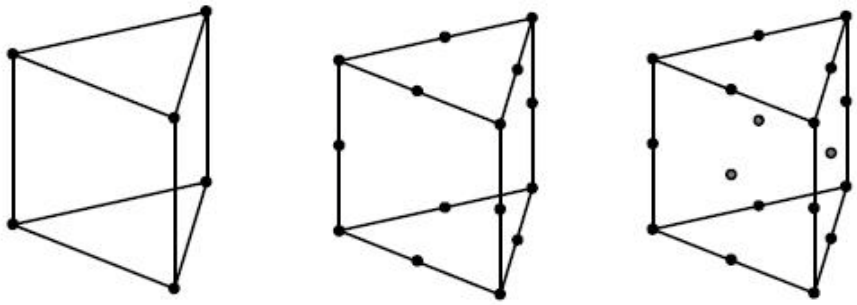

Figure 5.15 Wedge volume elements

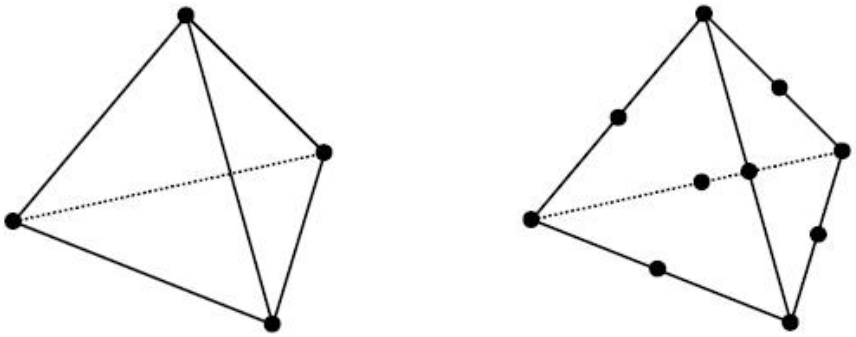

Figure 5.16 Tetrahedron volume elements

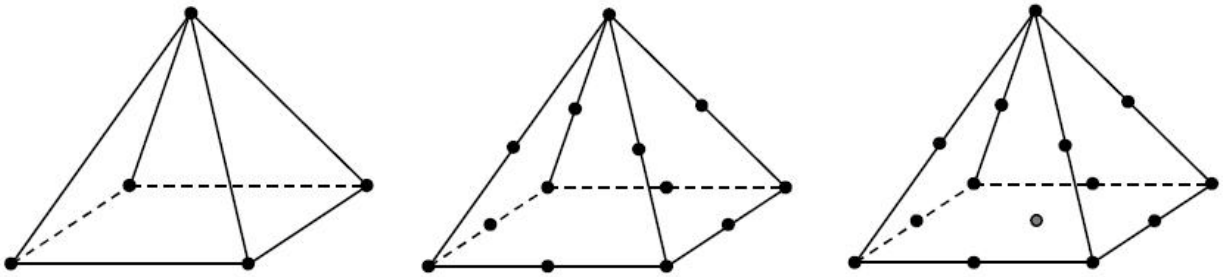

Figure 5.17 Pyramid volume elements

Shape	Numbers of Nodes
Hexahedron	8, 20, 27
Wedge	6, 15, 18
Tetrahedron	4, 10
Pyramid	5, 13, 14

Table 5.5 Element shape and number of nodes

to set a volume element type, the pre-processor applies the specified mesh node pattern to all volume elements of the specified shape. For example, if you specify 20-node wedge volume

elements, pre-processor locates mesh nodes according to the 20-node pattern for all wedge volume elements produced in the subsequent volume meshing operation.

5.5 MESHING THE MODEL

After modeling, the components were imported to Gambit. To reduce the total no of mesh elements, the impeller was not meshed but subtracted from all volumes and the surfaces adjacent to impeller were given wall conditions which were kept in rotating frame of reference. The impeller was subtracted from the casing to create a separate volume representing the fluid portion in impeller. The entire geometry was divided in three volumes:

- Inlet passage-Fluid continuum
- Fluid in impeller-Fluid continuum
- Fluid in casing-Fluid continuum

To get an initial solution T-Grid scheme was used to mesh the model. An interval count of 6 was taken to generate a coarse mesh. Table 5.6 shows the number of elements in each volume

No of elements	Volume
30760	Fluid in impeller
116026	Inlet passage(4 highly skewed elements)
110149	Casing

Table 5.6 No of elements in each volume

5.6 BOUNDARY CONDITIONS

The pump inlet was defined as mass flow rate boundary condition and pressure outlet was given at the pump outlet. The pressure outlet condition is appropriate when the flow exits at atmospheric pressure and back pressure is created in the flow and is best suited for pumps. The outer surfaces such as walls of casing and inlet passage were given wall boundary conditions.

CHAPTER 6

RESULTS AND DISCUSSIONS

6.1 SIMULATION

After meshing of the model of pump assembly commercial CFD code fluent is used for simulation of the pump performance. The boundary conditions of mass flow rate and pressure outlet are given at pump inlet and outlet respectively. The performance results are obtained at different mass flow rate conditions with constant operating speed. Numerical performance results compared with the experimental results at the same operating conditions.

6.1.1 Assumptions

The following assumptions were taken for simulation:

1. The walls of the casing were assumed to be smooth hence any disturbances in flow due to roughness of the surface were neglected.
2. The friction co-efficient for all surfaces were set to 0, hence friction between the walls and fluid was neglected.
3. Steady state conditions and incompressible fluid flow.
4. No leakage losses.

6.1.2 Solution parameters

1. 3-D double precision solver used to solve for simulation
2. Multiple reference frame technique used to simulate the pump performance
3. Clear water used is taken as working fluid
4. Standard K-Epsilon model is used for turbulence modeling.
5. Convergence criteria for continuity, velocity and turbulence parameters was set to 10^{-3}
6. First order scheme is used for pressure correction as well as for solving momentum, turbulent kinetic energy and turbulence dissipation rate.
7. A simple scheme is used for pressure velocity coupling

8. To achieve convergence is less time under relaxation factor applied are 0.3 for pressure, 0.7 for momentum equation, 0.8 for turbulence kinetic energy and 0.8 for turbulence dissipation rate.

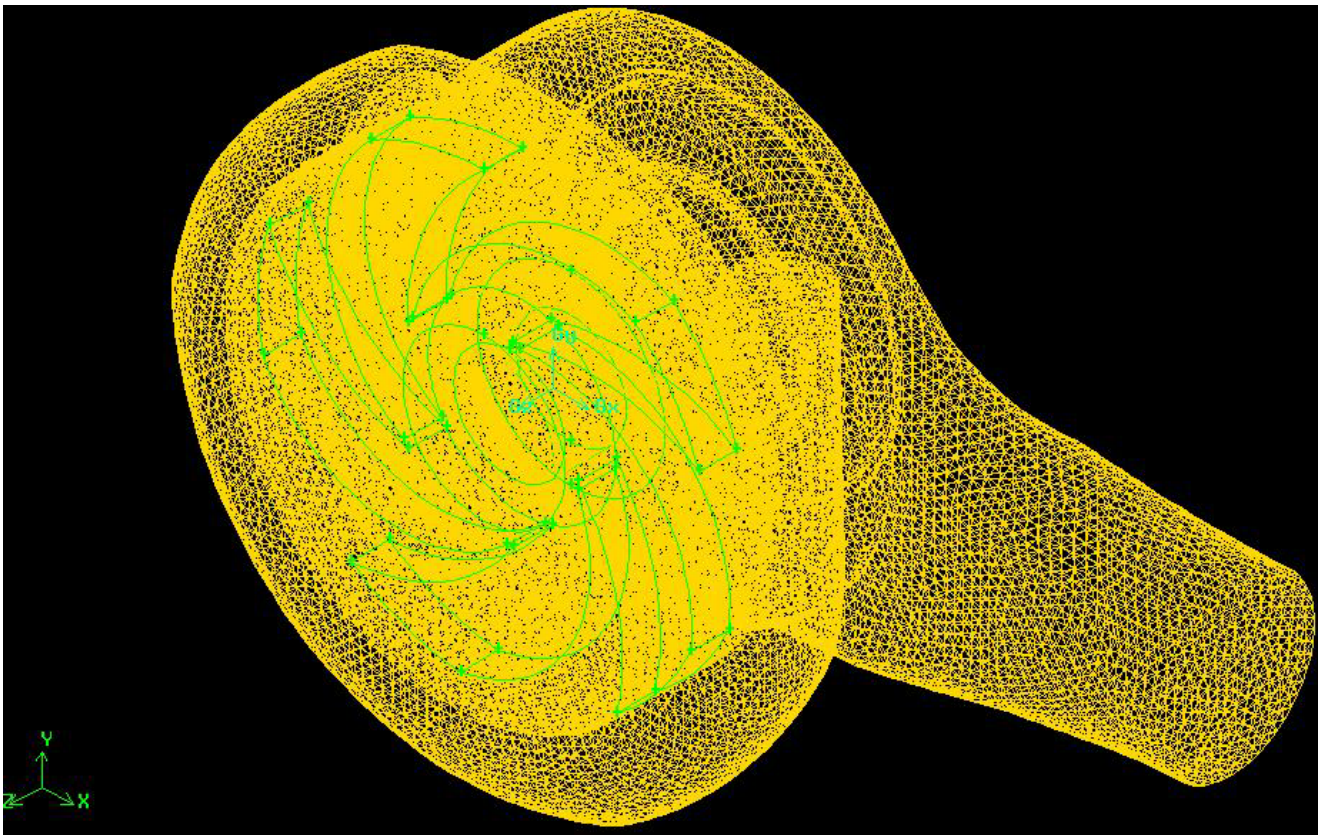

Figure 6.1 Coarse mesh (tetrahederal elements with interval count 6)

Table 6.1 Number of elements in different mesh volumes

Volume	No of elements
Fluid in impeller	30760
Inlet passage(4 highly skewed elements)	116026
Casing	110149

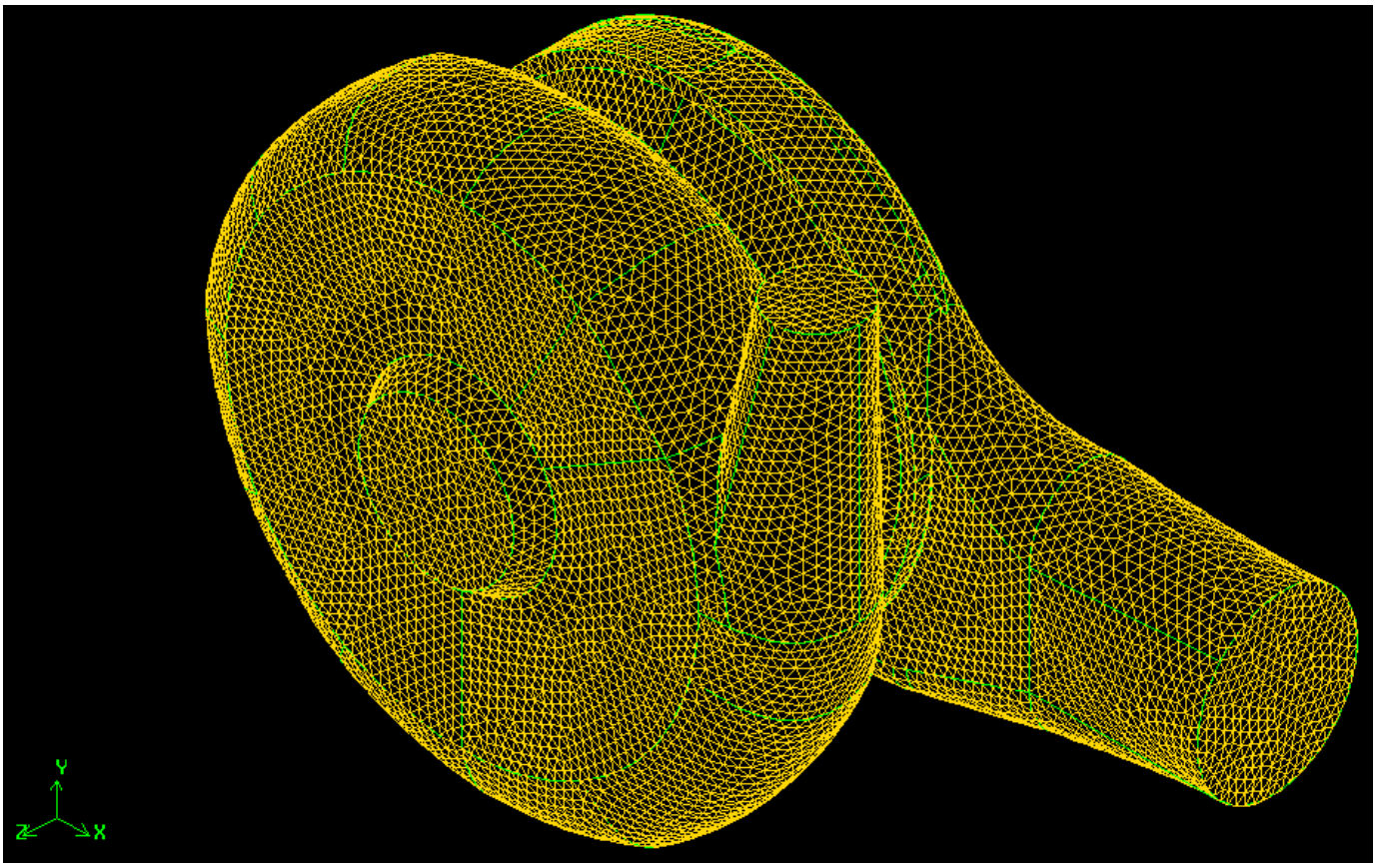

Figure 6.2 Mesh (tetrahederal elements with interval count 5)

Table 6.2 No of elements in different mesh volumes

Volume	No of elements
Fluid in impeller	91736
Inlet passage(2 highly skewed elements)	247462
Casing	334676

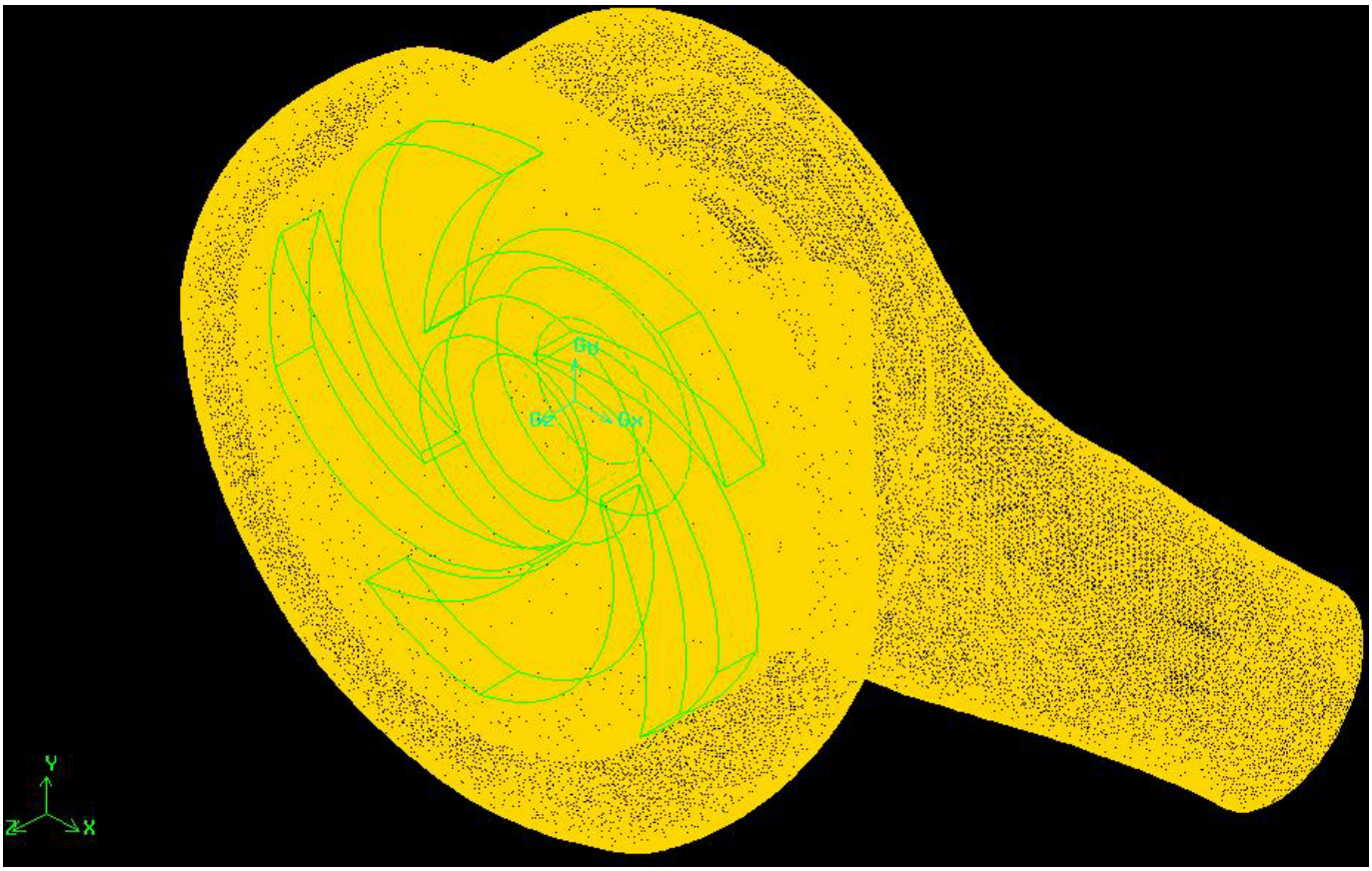

Figure 6.3 Fine mesh (tetrahederal elements with interval count 3)

Table 6.3 No of elements in different mesh volumes

Volume	No of elements
Fluid in impeller	153730
Inlet passage(2 highly skewed elements)	733536
Casing	739357

6.1.3 Pressure and velocity distribution in impeller

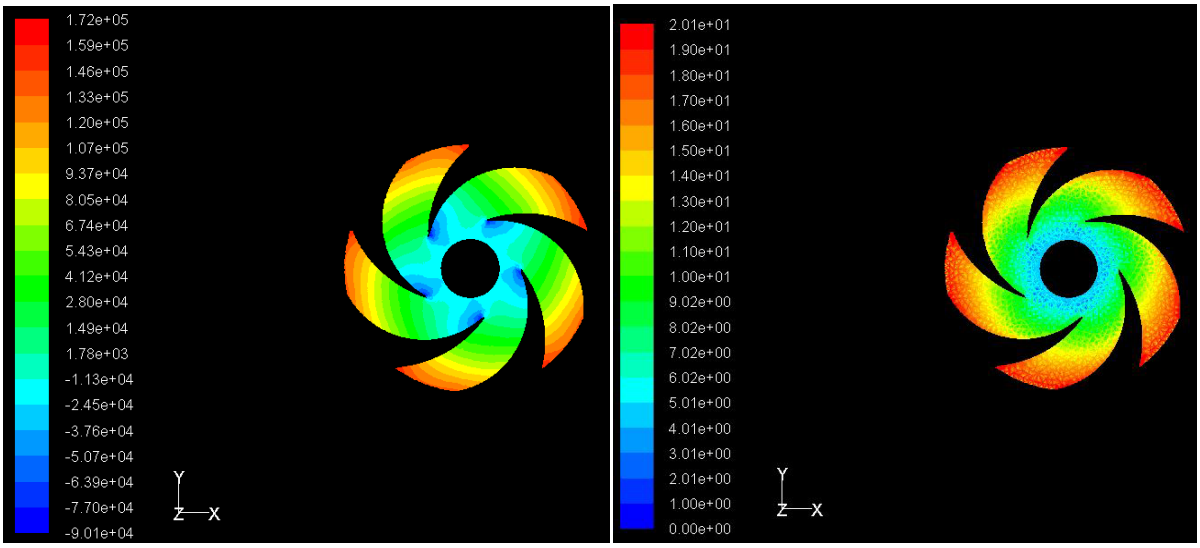

Figure 6.4 Pressure and velocity contours for impeller at 1450rpm and 16.22lps

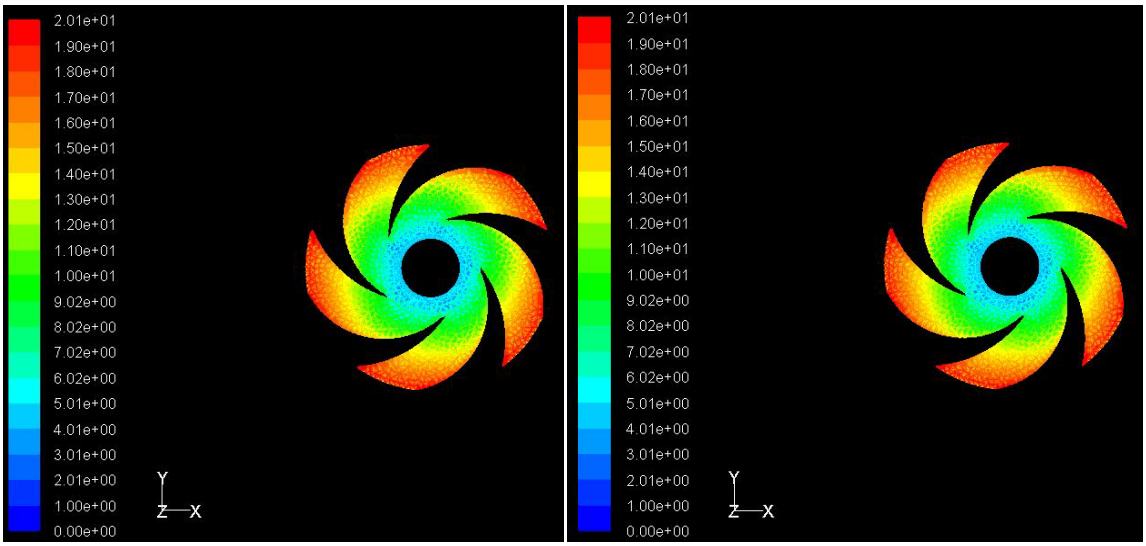

Figure 6.5 Pressure and velocity contours for impeller at 1450rpm and 16.07lps

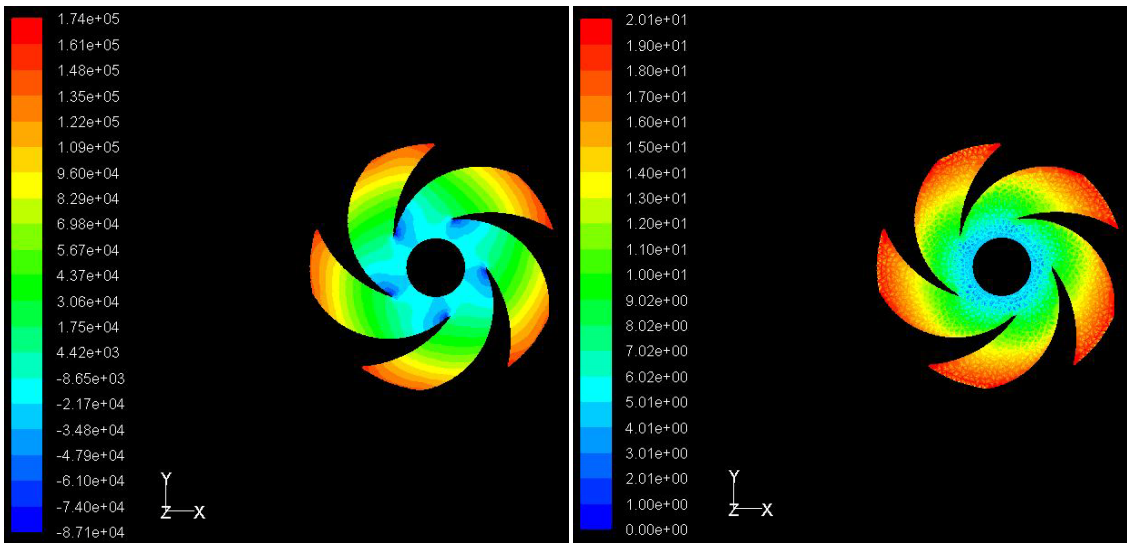

Figure 6.6 Pressure and velocity contours for impeller at 1450rpm and 15.14lps

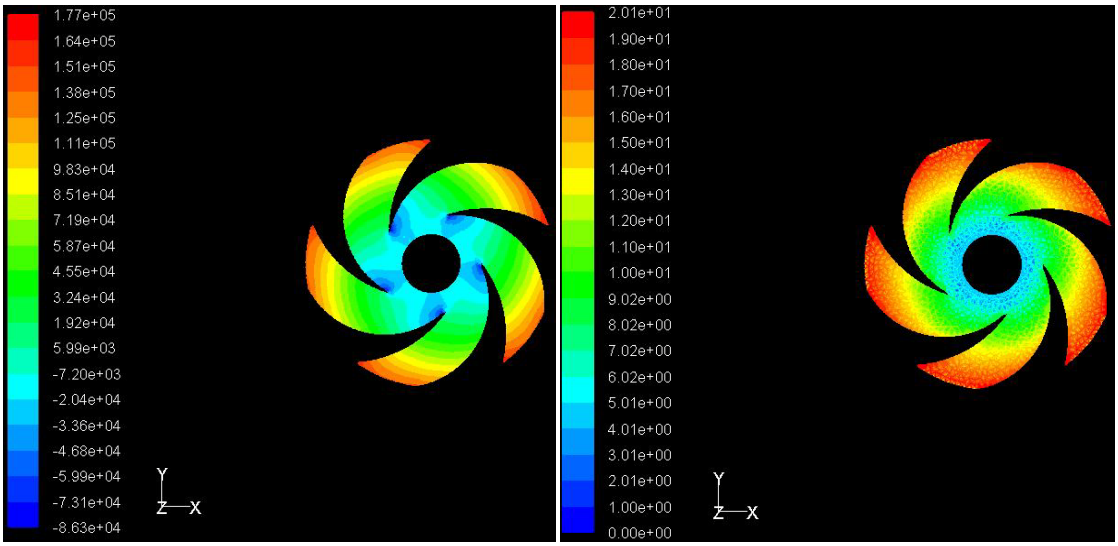

Figure 6.7 Pressure and velocity contours for impeller at 1450rpm and 14.07lps

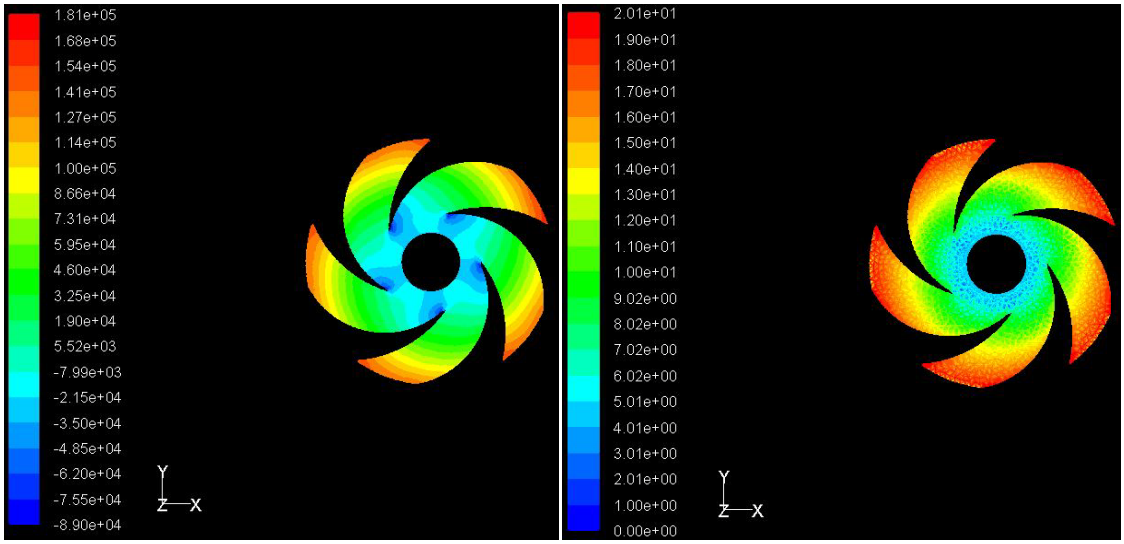

Figure 6.8 Pressure and velocity contours for impeller at 1450rpm and 12.98lps

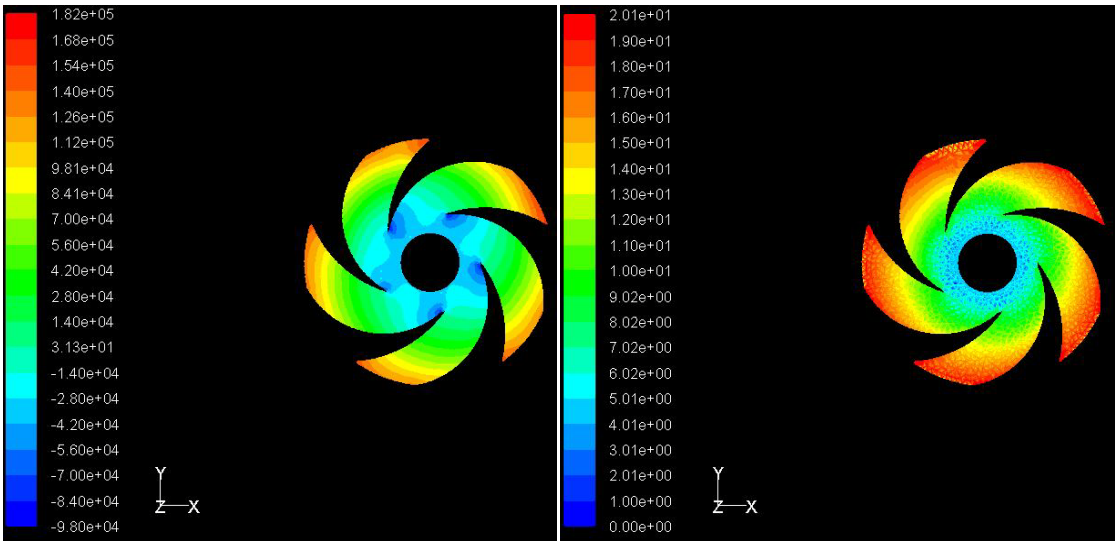

Figure 6.9 Pressure and velocity contours for impeller at 1450rpm and 10.74lps

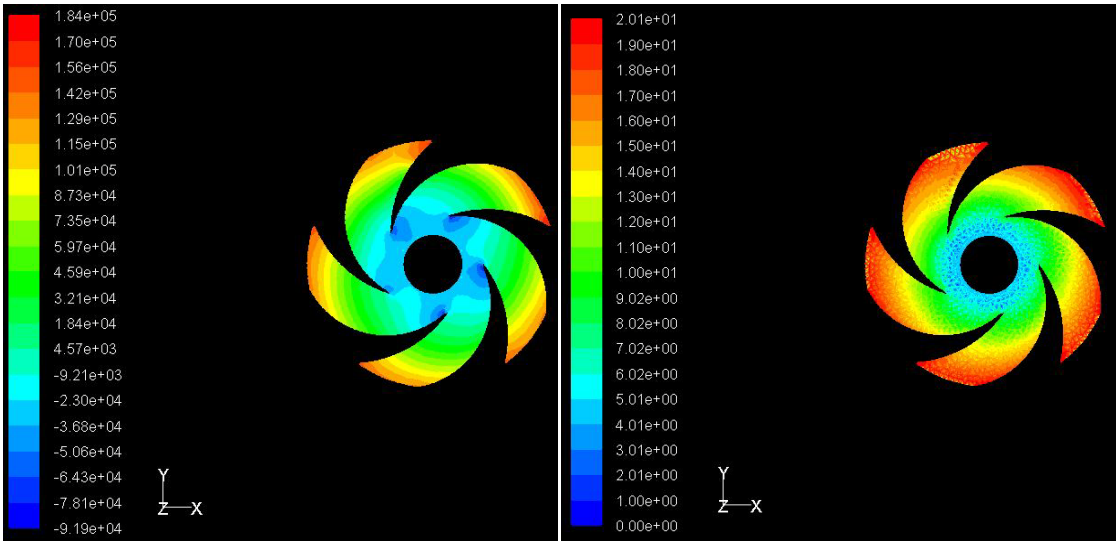

Figure 6.10 Pressure and velocity contours for impeller at 1450rpm and 8.3lps

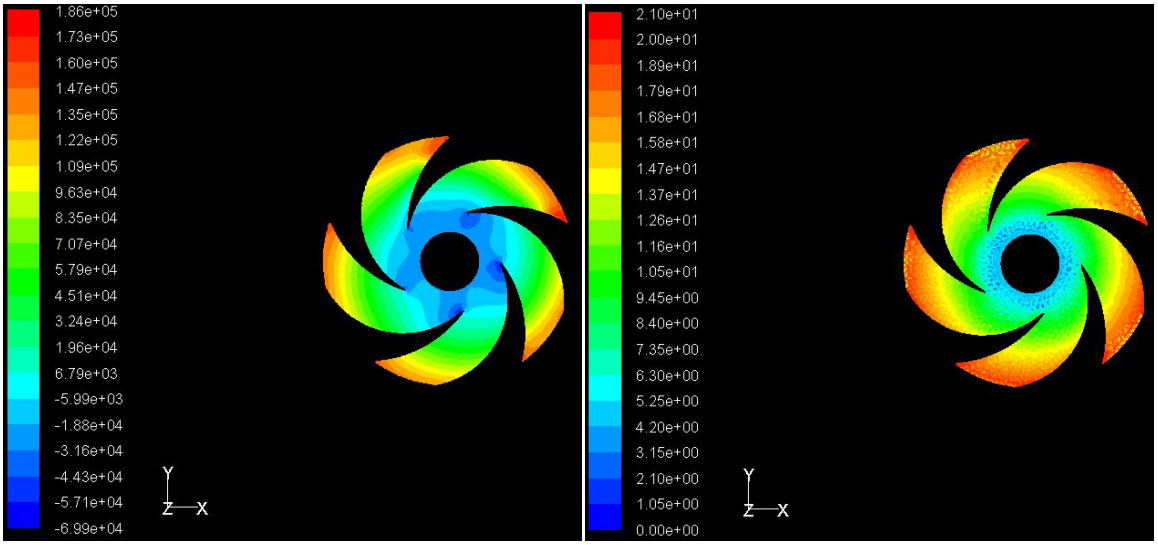

Figure 6.11 Pressure and velocity contours for impeller at 1450rpm and 5.26lps

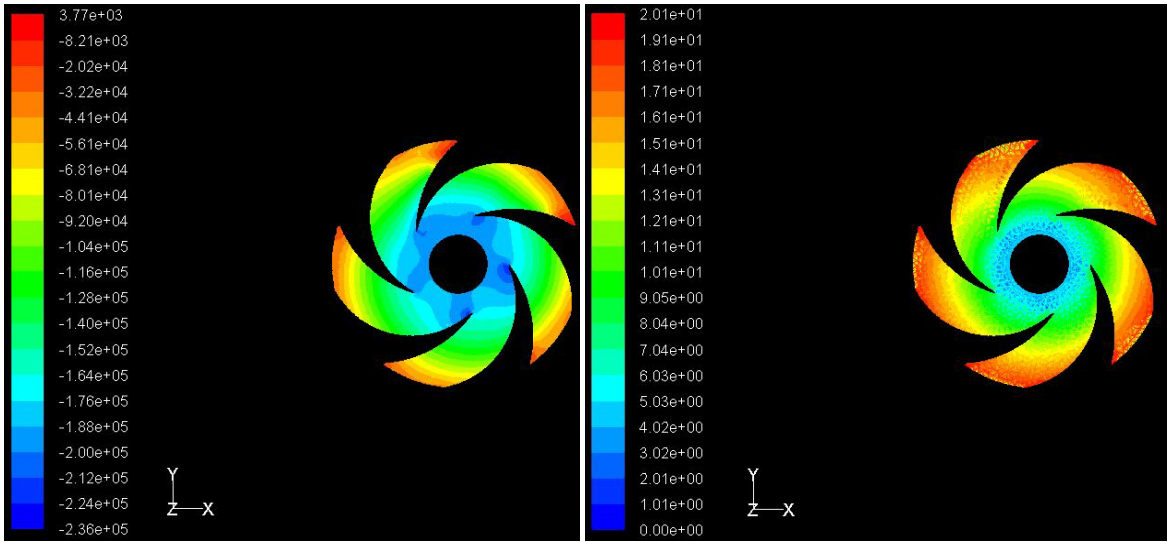

Figure 6.12 Pressure and velocity contours for impeller at 1450rpm and 4.5lps

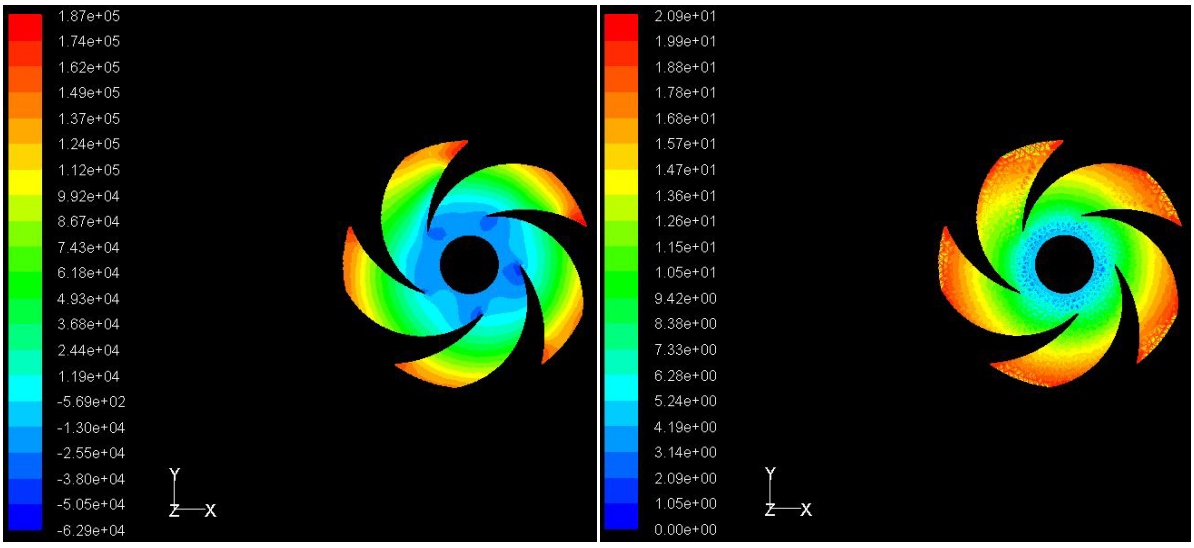

Figure 6.13 Pressure and velocity contours for impeller at 1450rpm and 3.71lps

Fig 6.4 to 6.13 shows the pressure and velocity contours in the impeller at the 1450 rpm with different mass flow rates. The result shows that the pressure increases from inlet to outlet. It has a minimum value at inlet and increases at the tip of the vane.

6.1.4 Pressure distribution and velocity vectors in casing

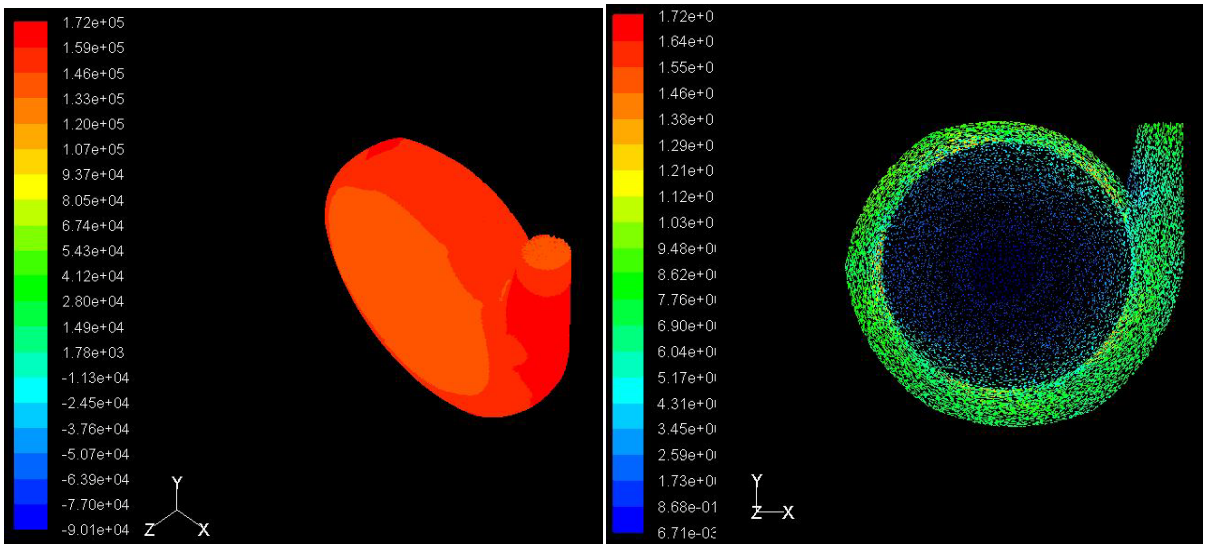

Figure 6.14 Pressure contour and velocity vectors for casing at 1450rpm and 16.22lps

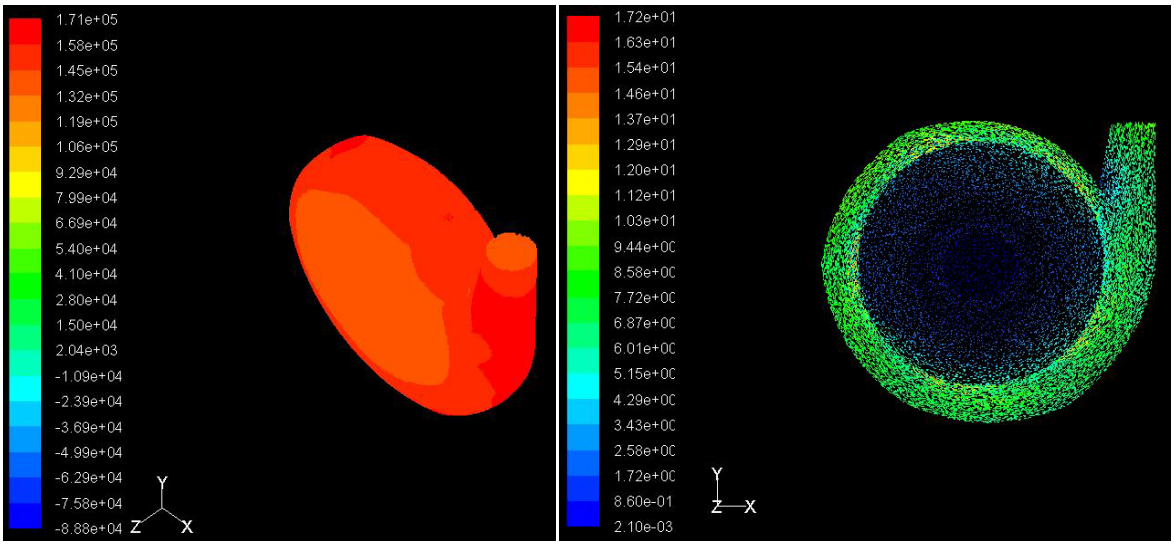

Figure 6.15 Pressure contour and velocity vectors for casing at 1450rpm and 16.07lps

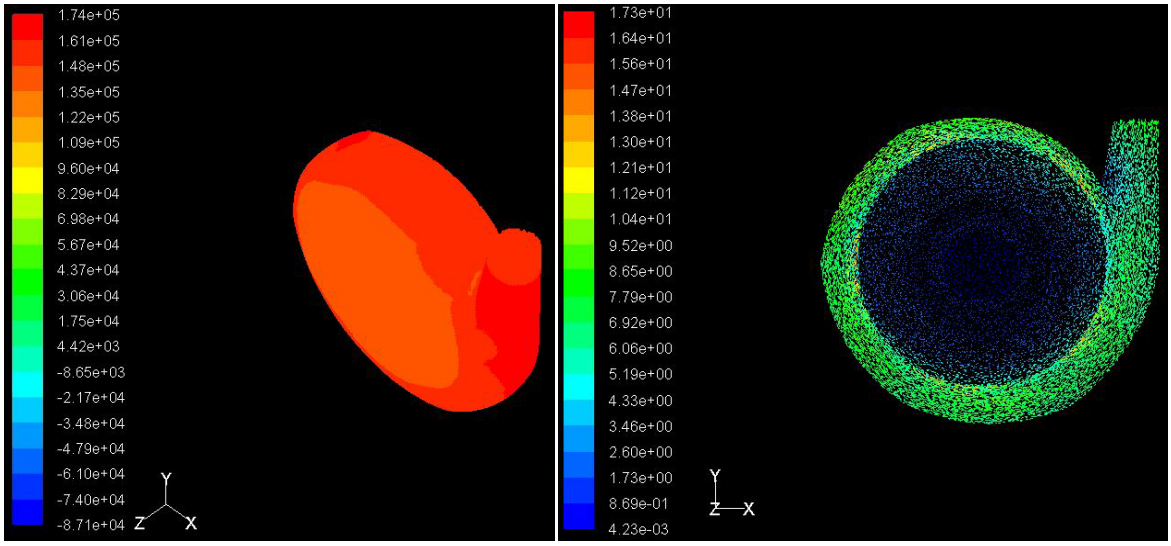

Figure 6.16 Pressure contour and velocity vectors for casing at 1450rpm and 15.14lps

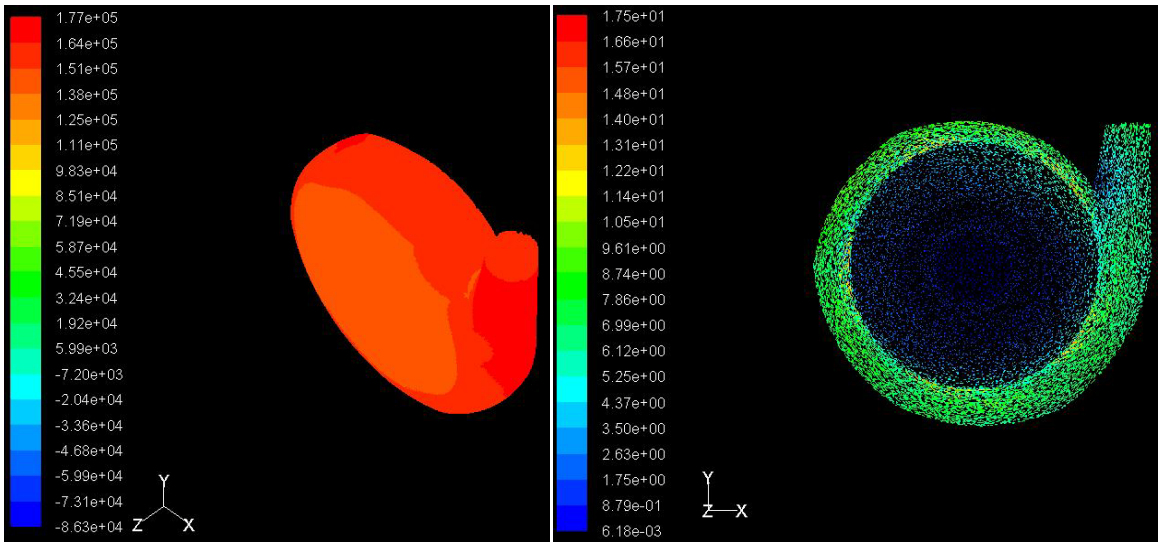

Figure 6.17 Pressure contour and velocity vectors for casing at 1450rpm and 14.07lps

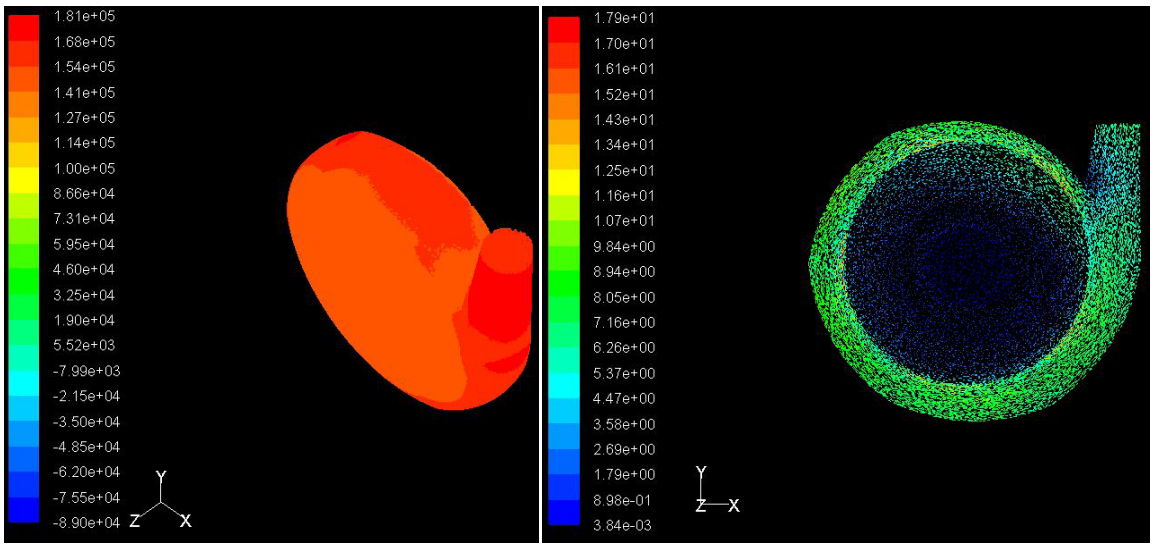

Figure 6.18Pressure contour and velocity vectors for casing at 1450rpm and 12.98lps

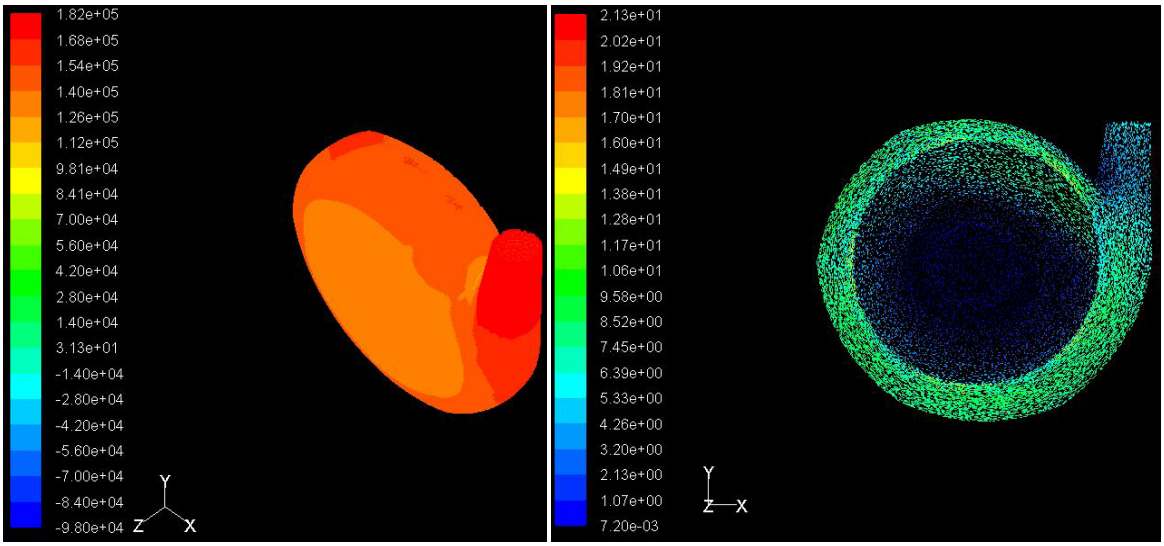

Figure 6.19 Pressure contours and velocity vectors for casing at 1450rpm and 10.74lps

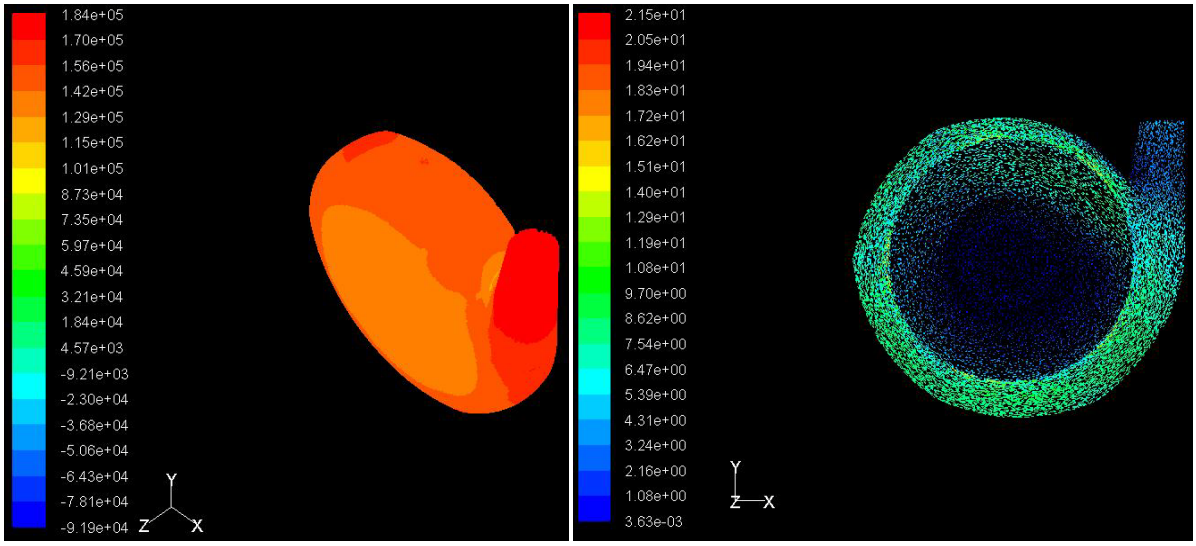

Figure 6.20 Pressure contours and velocity vectors for casing at 1450rpm and 8.3lps

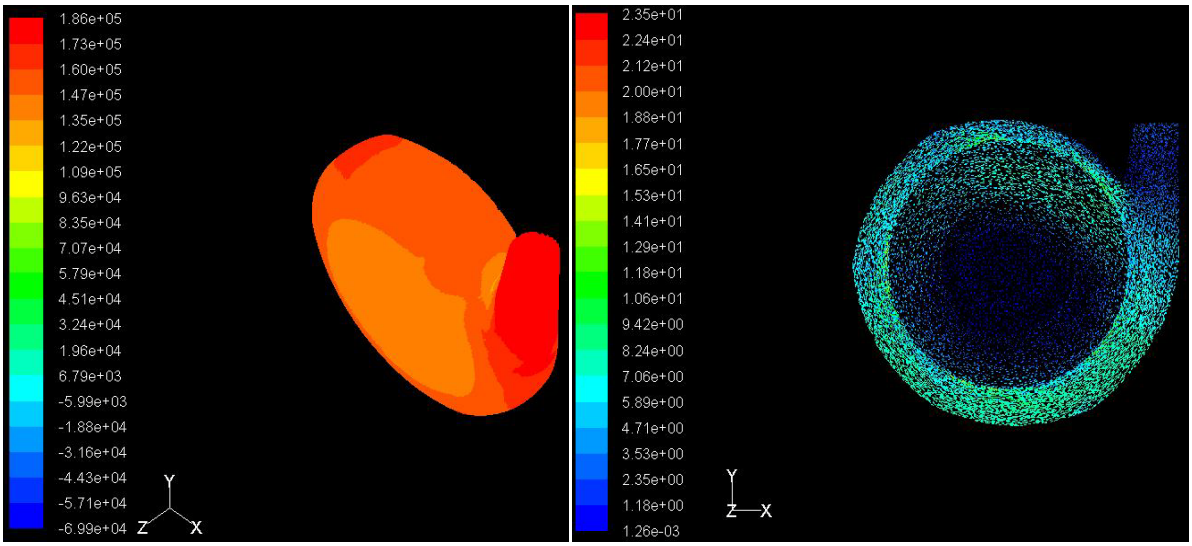

Figure 6.21 Pressure contours and velocity vectors for casing at 1450rpm and 5.26lps

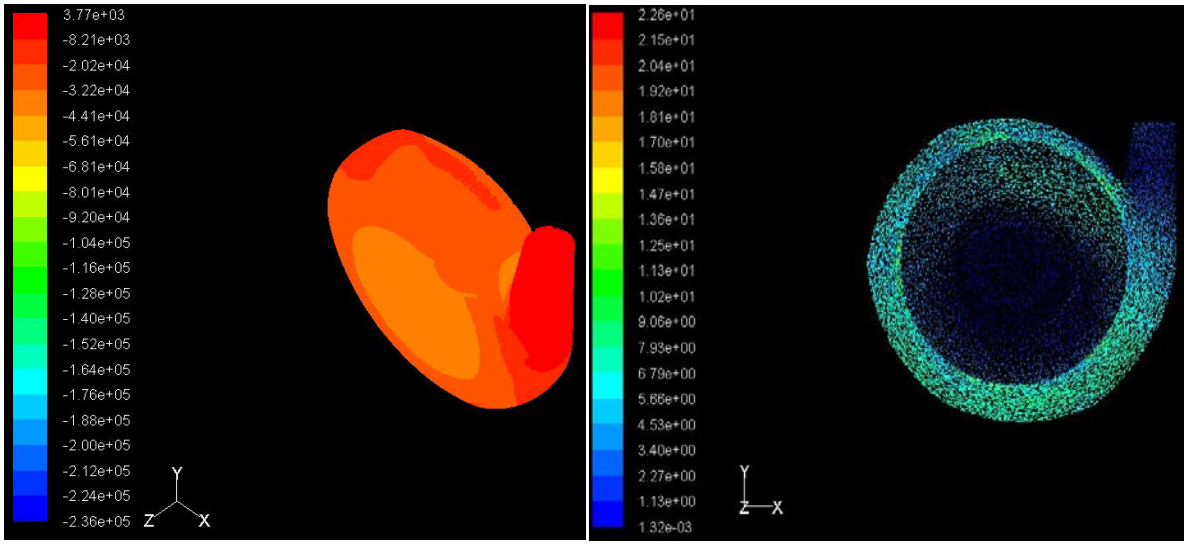

Figure 6.22 Pressure contours and velocity vectors for casing at 1450rpm and 4.5lps

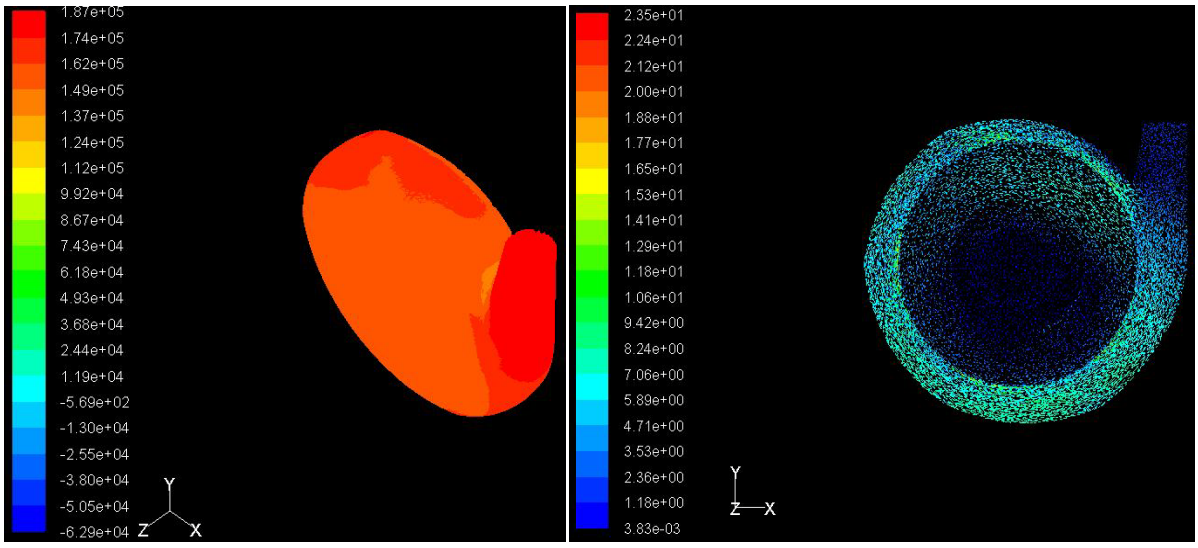

Figure 6.23 Pressure contours and velocity vectors for casing at 1450rpm and 3.71lps

Fig 6.14 to 6.23 shows Pressure contours and velocity vectors for casing at 1450rpm with different mass flow rates. The pressure contours show that the pressure increases from inlet to delivery and velocity is decreasing from inlet to outlet and maximum velocity is at the inlet of impeller.

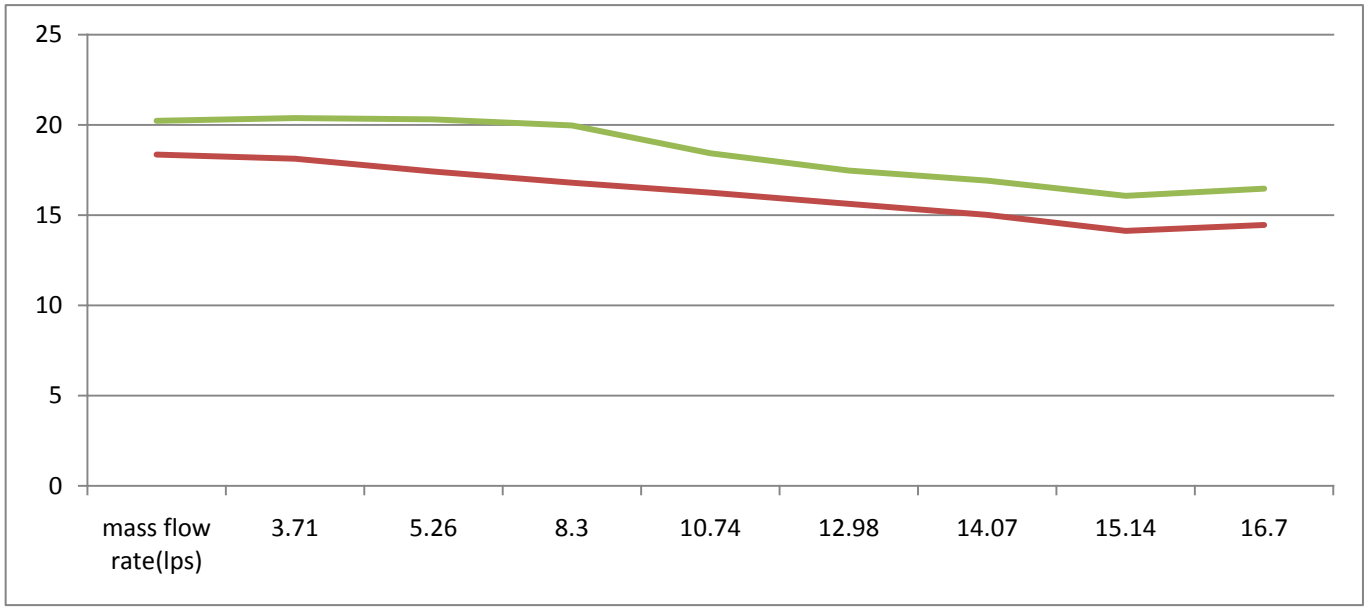

Figure 6.24 Head v/s Discharge

Figure 6.24 shows that the at a constant operating speed when the mass flow rate increases the total static head decreases.

CHAPTER 7

CONCLUSION AND FUTURE SCOPE

Conclusion

The geometry of pump components impeller, casing, inlet passage, frame and follower plate is modeled using Gambit and Pro-E. The mesh is generated successfully using Gambit. Complex internal flow field, pressure and velocity distribution investigated using fluent commercial computational code. The simulation results are obtained at the operating speed 1450rpm with different mass flow rates for transportation of clear liquid. The performance results show that total static head is the function of the mass flow rate with constant operating speed. Numerical performance results compared with the experimental results at the same operating conditions.

Future Scope

1. Pressure and velocity distribution for pump impeller and casing can be calculated for slurries.
2. Effect on performance of pump by changing inlet and outlet vane angle can be studied.
3. Similar computational simulation models can also be used for analyzing the pressure, velocity and stress distribution of the turbines, compressor, fan and blower.

REFERENCES

1. M A Rayan, M Shawky,‘‘ Evaluation Of Wear In a Centrifugal Slurry Pump’’ Proceedings Institution of Mechanical Engineers, 1989, Vol 203.
2. Dong, R., Chu, S., and Katz, J., ‘‘Quantitative Visualization of the Flow within the Volute of a Centrifugal Pump. Part A: Technique,’’ASME J. Fluids Eng., 1992, Vol.114**,** pp. 390–395.
3. Gahlot, V. K., Seshadri, V., and Malhotra, R. C., ‘‘Effect of Density, Size Distribution, and Concentration of Solid on the Characteristics of Centrifugal Pumps.’’ J. Fluids Eng., 1992, ASME Vol 114, 386–389.
4. Cader, T., Masbernat, O., and Roco, M.C., ‘‘LDV Measurements in a Centrifugal Slurry Pump: Water and Dilute Slurry Flow,’’ ASME J. Fluids Eng., 1992, Vol.114, pp. 606–615.
5. Cader, T., Masbernet, O., and Roco, M. C., ‘‘Two-Phase Velocity Distributions And Overall Performance of a Centrifugal Slurry Pump,’’ ASME J.Fluids Engineering Conf., Washington, DC, June 20–24,1994, Vol.116, pp. 176–186.
6. W.Huang,T Cader ,M C Roco, ‘‘Two Phase Flow Structure at The Impeller-Volute Interface ’’April 3-7, 1995, Proceedings Of The 2nd International Conference On Multiphase Flow,Kyoto Japan.
7. S.Yedidiah, ”A New Toll for Solving Problems Encountered with Centrifugal Pumps”April 1996 world Pumps Elsevier science.
8. Ni, F, Vlasblom, W. J., and Zwartbol, A., ‘‘Effect of High Solid Concentration on Characteristics of a Slurry Pump,’’ Hydrotransport 14, BHRA Fluid Engg. Maastricht, The Neatherland, 1996, pp. 141–149.
9. Miner, S. M., “3-D Viscous Flow Analysis of an Axial Flow Pump Impeller” International Journal of Rotating Machinery, 1997, Volume 3, No. 3, pp 153-161.
10. Oh and M.K. Chung (1999), “Optimum values of design variables versus specific speed for centrifugal pumps”. Proceedings Institution of Mechanical Engineers, 1999, Vol. 213 ,

11. Ogut, A. and Pastor, D. G., “Simulation of flow in turbopump vaneless and vaned diffusers with fluid section” International Journal of Rotating Machinery, 2000, Volume 6, No. 1, pp 57-65.
12. Majidi, K. and Siekmann H. E., “Numerical calculation of secondary flow in pump volute and circular casings using 3D viscous flow techniques” International Journal of Rotating Machinery, 2000, Volume 6, No. 4, pp 245-252
13. B.K Gandhi, S.N. Singh, V. Seshadri, “Variation of wear along the volute casing of a centrifugal slurry pump”. JSME International Journal, 2001, Vol.44, 2001.
14. Gandhi, B. K., Singh, S. N., and Seshadri, V., ‘‘Performance Characteristics of Centrifugal Slurry Pumps,’’ 2001, ASME J. Fluids Eng., **123**, pp. 271–28.
15. Oh and Kim, “Conceptual Design, Optimization of mixed-flow pump impellers using mean streamline analysis”. Proceedings of Institution of Mechanical Engineers, 2001, Vol. 215.
16. K S Paeng, M K Chung, ”A New Slip Factor For Centrifugal Impellers”, Proceedings of Institution of Mechanical Engineers, 2001, Vol 215 Part A.
17. Engin, T., and Gur, M., ‘‘Performance Characteristics of a Centrifugal Pump Impeller with Running Tip Clearance Pumping Liquid-Solid Mixtures,’’ ASME J. Fluids Eng., 2001, 123, pg. 532–538.
18. B.K Gandhi, S.N. Singh, V. Seshadri, “Effect of Speed on the Performance Characteristics of a Centrifugal Slurry Pump”, Journal of fluid Engineering, February, 2002.
19. Kato, C., Mukai, H., and Manabe, A., “Large-eddy simulation of unsteady flow in a mixed-flow pump” International Journal of Rotating Machinery, 2003, volume 9, pp 345–351.
20. Nursen, E. C., and Ayder, E., “Numerical calculation of the three- dimensional swirling flow inside the centrifugal pump volutes” International Journal of Rotating Machinery, 2003, volume 9, 247–253.
21. J R.Kadambi, Charoenngam P, Subramanian A, Mark P.Wernet, John M.Sankovic, Addie G, Courtwright R,”Investigation of Particle Velocities in a Slurry pump using PIV:Part 1,The Tongue and Adjacent Channel Flow” Journal Of Energy Resources Technology, ASME. December 2004, Vol-126/271.

22. Hergt, P., Meschkat, S. and Stoffel, B., “The flow and head distribution within the volute of a centrifugal pump in comparison with the characteristics of the impeller without casing” Journal of Computational and Applied Mechanics, 2004, Volume 5, pp 275-285.
23. Xu, C. and Muller, M., “Development and design of a centrifugal compressor volute” International Journal of Rotating Machinery, 2005, volume 3, pp 190–196.
24. A.Sellgren, ”The new ANSI/HI centrifugal slurry pump standard”, 17th International conference on the hydraulic transport of solids, The southern African Institute of Mining and Metallurgy and the BHR group, 2007.
25. L.Pullum,L.J.W Graham and M.Rudman, ”Centrifugal pump performance calculations for homogeneous and complex heterogeneous suspensions”,17th International conference on the hydraulic transport of solids,The southern African Institute of Mining and Metallurgy and the BHR group, 2007.
26. Min-Guan Yang,Dong Liu,Xiang Dong, ”Analysis of turbulent Flow in the Impeller of a Chemical Pump”, Journal of engineering science and technology,Vol-2,N0.- 3,2007,Pg-218-225.

BIBLIOGRAPHY

1. Stepanoff, A. J., (1958), "Centrifugal and axial flow pumps theory design and application", 2nd, John Wiley and sons, New York.
2. Vasandani, V. P., (1993), "Hydraulic machines theory and design", 10th edition, Khanna Publishing house, New Delhi.
3. Kumar Satish, (2006), "A text book of Fluid Machines", 1st edition, Dhanpat Rai Publications, New Delhi
4. ANSYS CFX-Manual, (2006), Published by, ANSYS CFX, Release 11.0, December, 2006, ANSYS, Inc.
5. Cherkassy V.M., (1985), "Pumps Fans Compressors", 2nd edition, Mir Publishers.
6. Addison H., (1990), "Centrifugal and other Rotodynamic Pumps", 2nd edition, Chapman and Hall London.
7. Ghoshdastidar, P. S., (1998), "Computer simulation of flow and heat transfer", Tata McGraw-Hill, New Delhi.
8. Fluent-Manual, (2003), published by, Fluent Inc., Release 6.3, January 2003.

ANNEXURE I

RESIDUALS OF SIMULATION

iter continuity x-velocity y-velocity z-velocity k epsilon time/iter
reversed flow in 144 faces on pressure-outlet 6.
1 1.0000e+00 8.1566e-04 9.1852e-03 3.9678e-04 5.1261e-02 1.9767e+00 0:58:13 499
reversed flow in 31 faces on pressure-outlet 6.
2 1.0000e+00 3.0058e-01 1.7017e-01 7.9816e-02 1.5155e+01 3.0674e+03 0:58:06 498
reversed flow in 24 faces on pressure-outlet 6.
turbulent viscosity limited to viscosity ratio of 1.000000e+005 in 10 cells
3 3.1742e-01 2.0716e-01 2.0392e-01 1.4102e-01 6.0423e-01 2.0589e+01 0:56:20 497
reversed flow in 19 faces on pressure-outlet 6.
4 2.3713e-01 1.0984e-01 1.1690e-01 9.3137e-02 2.1069e-01 5.9450e-01 0:54:53 496
reversed flow in 15 faces on pressure-outlet 6.
5 2.0114e-01 5.8649e-02 5.5163e-02 3.7955e-02 1.1096e-01 2.5274e-01 0:53:43 495
reversed flow in 9 faces on pressure-outlet 6.
6 1.7579e-01 3.9398e-02 3.4740e-02 2.4344e-02 9.5797e-02 1.8136e-01 0:52:46 494
7 1.2224e-01 2.9352e-02 3.0210e-02 2.2845e-02 9.1066e-02 1.6965e-01 0:52:00 493
8 9.3703e-02 2.5536e-02 2.4481e-02 1.8637e-02 8.3520e-02 1.5697e-01 0:51:21 492
9 6.6172e-02 1.6709e-02 1.5658e-02 1.0697e-02 7.9356e-02 1.5064e-01 0:50:49 491
10 5.2678e-02 1.3568e-02 1.3558e-02 9.4968e-03 7.1560e-02 1.3781e-01 0:50:22 490
11 4.4692e-02 1.0641e-02 1.0781e-02 6.9095e-03 6.2117e-02 1.2067e-01 0:48:22 489
iter continuity x-velocity y-velocity z-velocity k epsilon time/iter
12 3.8211e-02 8.9393e-03 9.0478e-03 5.2816e-03 5.2197e-02 1.0223e-01 0:46:45 488
13 3.3237e-02 8.2122e-03 8.1510e-03 4.6554e-03 4.3014e-02 8.4732e-02 0:45:26 487
14 2.9279e-02 7.7083e-03 7.5093e-03 4.2637e-03 3.5559e-02 6.9967e-02 0:44:22 486
15 2.6030e-02 7.2610e-03 7.1468e-03 3.9758e-03 2.9836e-02 5.8377e-02 0:43:31 485
16 2.3437e-02 6.7436e-03 6.6202e-03 3.5852e-03 2.5860e-02 5.0003e-02 0:42:48 484
17 2.1502e-02 6.4084e-03 6.3249e-03 3.3696e-03 2.3283e-02 4.4233e-02 0:42:13 483
18 1.9959e-02 6.1736e-03 6.0833e-03 3.2109e-03 2.1702e-02 4.0774e-02 0:41:44 482
19 1.8735e-02 5.9782e-03 5.8737e-03 3.0692e-03 2.0664e-02 3.7993e-02 0:41:20 481
20 1.7781e-02 5.7937e-03 5.6981e-03 2.9477e-03 1.9886e-02 3.5884e-02 0:41:00 480
21 1.7030e-02 5.6421e-03 5.5513e-03 2.8561e-03 1.9234e-02 3.4765e-02 0:40:43 479
22 1.6464e-02 5.5149e-03 5.4193e-03 2.7758e-03 1.8610e-02 3.3754e-02 0:40:28 478
iter continuity x-velocity y-velocity z-velocity k epsilon time/iter
23 1.6022e-02 5.3975e-03 5.3100e-03 2.6940e-03 1.8096e-02 3.3317e-02 0:40:16 477
24 1.5623e-02 5.2914e-03 5.2095e-03 2.6227e-03 1.7643e-02 3.2751e-02 0:41:40 476
25 1.5289e-02 5.2225e-03 5.1238e-03 2.6130e-03 1.7402e-02 3.2937e-02 0:41:11 475
26 1.4737e-02 5.1077e-03 4.9853e-03 2.4855e-03 1.7051e-02 3.2231e-02 0:40:46 474
27 1.4369e-02 5.0058e-03 4.8831e-03 2.4322e-03 1.6636e-02 3.1413e-02 0:42:00 473
28 1.4039e-02 4.8922e-03 4.7678e-03 2.3709e-03 1.6263e-02 3.0325e-02 0:41:24 472
29 1.3723e-02 4.7927e-03 4.6667e-03 2.3219e-03 1.5868e-02 2.9068e-02 0:40:54 471
30 1.3436e-02 4.6812e-03 4.5599e-03 2.2739e-03 1.5556e-02 2.7817e-02 0:42:03 470
31 1.3112e-02 4.5611e-03 4.4459e-03 2.2198e-03 1.5346e-02 2.7322e-02 0:41:23 469
32 1.2766e-02 4.4356e-03 4.3401e-03 2.1743e-03 1.5149e-02 2.7086e-02 0:40:50 468

33	1.2446e-02	4.3067e-03	4.2276e-03	2.1276e-03	1.4965e-02	2.7176e-02	0:41:56	467
iter	continuity	x-velocity	y-velocity	z-velocity	k	epsilon	time/iter	
34	1.2114e-02	4.1781e-03	4.1120e-03	2.0848e-03	1.4663e-02	2.6698e-02	0:41:15	466
35	1.1792e-02	4.0548e-03	3.9977e-03	2.0412e-03	1.4249e-02	2.5526e-02	0:42:14	465
36	1.1402e-02	3.9277e-03	3.8835e-03	1.9951e-03	1.3834e-02	2.4448e-02	0:41:27	464
37	1.1042e-02	3.8169e-03	3.7794e-03	1.9529e-03	1.3321e-02	2.3566e-02	0:42:21	463
38	1.0770e-02	3.7271e-03	3.6912e-03	1.9321e-03	1.2836e-02	2.2647e-02	0:41:30	462
39	1.0437e-02	3.6225e-03	3.5966e-03	1.8711e-03	1.2399e-02	2.2018e-02	0:42:21	461
40	1.0149e-02	3.5365e-03	3.5163e-03	1.8434e-03	1.1968e-02	2.1433e-02	0:43:00	460
41	9.8414e-03	3.4560e-03	3.4381e-03	1.8105e-03	1.1542e-02	2.0909e-02	0:43:31	459
42	9.5813e-03	3.3798e-03	3.3644e-03	1.7769e-03	1.1148e-02	2.0293e-02	0:42:22	458
43	9.3802e-03	3.3126e-03	3.2974e-03	1.7446e-03	1.0778e-02	1.9777e-02	0:42:57	457
44	9.1806e-03	3.2504e-03	3.2344e-03	1.7109e-03	1.0377e-02	1.8968e-02	0:43:25	456
iter	continuity	x-velocity	y-velocity	z-velocity	k	epsilon	time/iter	
45	9.0217e-03	3.1851e-03	3.1668e-03	1.6752e-03	1.0022e-02	1.8335e-02	0:42:14	455
46	8.8474e-03	3.1216e-03	3.1063e-03	1.6419e-03	9.6761e-03	1.7745e-02	0:42:48	454
47	8.6495e-03	3.0577e-03	3.0466e-03	1.6061e-03	9.3542e-03	1.7284e-02	0:43:13	453
48	8.4628e-03	2.9914e-03	2.9913e-03	1.5706e-03	9.0300e-03	1.6890e-02	0:42:02	452
49	8.2849e-03	2.9215e-03	2.9340e-03	1.5344e-03	8.7017e-03	1.6331e-02	0:42:34	451
50	8.1420e-03	2.8531e-03	2.8719e-03	1.4995e-03	8.4264e-03	1.5833e-02	0:42:59	450
51	8.0178e-03	2.7830e-03	2.8167e-03	1.4648e-03	8.0928e-03	1.5182e-02	0:43:17	449
52	7.8828e-03	2.7218e-03	2.7634e-03	1.4368e-03	7.8154e-03	1.4724e-02	0:43:31	448
53	7.7753e-03	2.6685e-03	2.6963e-03	1.4121e-03	7.5213e-03	1.4246e-02	0:42:11	447
54	7.6132e-03	2.6035e-03	2.6390e-03	1.3710e-03	7.2550e-03	1.3839e-02	0:42:35	446
55	7.4838e-03	2.5486e-03	2.5840e-03	1.3362e-03	7.0169e-03	1.3455e-02	0:42:54	445
iter	continuity	x-velocity	y-velocity	z-velocity	k	epsilon	time/iter	
56	7.3969e-03	2.5027e-03	2.5333e-03	1.3122e-03	6.8009e-03	1.3031e-02	0:41:38	444
57	7.2710e-03	2.4575e-03	2.4834e-03	1.2870e-03	6.6321e-03	1.2801e-02	0:42:06	443
58	7.0918e-03	2.4199e-03	2.4316e-03	1.2643e-03	6.5167e-03	1.2676e-02	0:42:27	442
59	6.8957e-03	2.3761e-03	2.3848e-03	1.2339e-03	6.3846e-03	1.2499e-02	0:42:42	441
60	6.7517e-03	2.3288e-03	2.3381e-03	1.2078e-03	6.2569e-03	1.2260e-02	0:41:25	440
61	6.5949e-03	2.2839e-03	2.2918e-03	1.1820e-03	6.0413e-03	1.1851e-02	0:41:50	439
62	6.4520e-03	2.2325e-03	2.2390e-03	1.1575e-03	5.7706e-03	1.1165e-02	0:42:09	438
63	6.2767e-03	2.1836e-03	2.1915e-03	1.1283e-03	5.4899e-03	1.0488e-02	0:40:56	437
64	6.1302e-03	2.1420e-03	2.1469e-03	1.1079e-03	5.2493e-03	9.9453e-03	0:41:23	436
65	5.9860e-03	2.1028e-03	2.1060e-03	1.0836e-03	5.0249e-03	9.5465e-03	0:41:44	435
66	5.8549e-03	2.0671e-03	2.0705e-03	1.0645e-03	4.8330e-03	9.1992e-03	0:41:59	434
iter	continuity	x-velocity	y-velocity	z-velocity	k	epsilon	time/iter	
67	5.7266e-03	2.0333e-03	2.0401e-03	1.0448e-03	4.6608e-03	8.8596e-03	0:42:10	433
68	5.6323e-03	2.0029e-03	2.0112e-03	1.0290e-03	4.5036e-03	8.5137e-03	0:42:18	432
69	5.5555e-03	1.9750e-03	1.9838e-03	1.0137e-03	4.3541e-03	8.1787e-03	0:42:23	431
70	5.4834e-03	1.9464e-03	1.9598e-03	1.0010e-03	4.2185e-03	7.8633e-03	0:42:26	430
71	5.4118e-03	1.9220e-03	1.9339e-03	9.8725e-04	4.0929e-03	7.5736e-03	0:42:27	429
72	5.3341e-03	1.8985e-03	1.9084e-03	9.7664e-04	3.9691e-03	7.2985e-03	0:42:26	428
73	5.2544e-03	1.8765e-03	1.8823e-03	9.6438e-04	3.8635e-03	7.0934e-03	0:42:25	427
74	5.1715e-03	1.8560e-03	1.8580e-03	9.5181e-04	3.7737e-03	6.9208e-03	0:43:47	426

75	5.1143e-03	1.8362e-03	1.8330e-03	9.4135e-04	3.6903e-03	6.7588e-03	0:42:02	425
76	5.0649e-03	1.8180e-03	1.8086e-03	9.2875e-04	3.6228e-03	6.6427e-03	0:42:02	424
77	5.0203e-03	1.8000e-03	1.7844e-03	9.2038e-04	3.5684e-03	6.5497e-03	0:42:00	423
iter	continuity	x-velocity	y-velocity	z-velocity	k	epsilon	time/iter	
78	4.9807e-03	1.7858e-03	1.7571e-03	9.1260e-04	3.5216e-03	6.4809e-03	0:41:58	422
79	4.9109e-03	1.7665e-03	1.7344e-03	8.9929e-04	3.4800e-03	6.4110e-03	0:41:55	421
80	4.8700e-03	1.7518e-03	1.7133e-03	8.9436e-04	3.4547e-03	6.3693e-03	0:41:51	420
81	4.8100e-03	1.7337e-03	1.6948e-03	8.8326e-04	3.4203e-03	6.3102e-03	0:41:47	419
82	4.7574e-03	1.7181e-03	1.6778e-03	8.7825e-04	3.3906e-03	6.2523e-03	0:41:42	418
83	4.7012e-03	1.7015e-03	1.6592e-03	8.7004e-04	3.3646e-03	6.1897e-03	0:41:37	417
84	4.6652e-03	1.6864e-03	1.6429e-03	8.6542e-04	3.3430e-03	6.1301e-03	0:41:32	416
85	4.6399e-03	1.6713e-03	1.6274e-03	8.5915e-04	3.3205e-03	6.0780e-03	0:41:27	415
86	4.5784e-03	1.6557e-03	1.6110e-03	8.4978e-04	3.2912e-03	6.0240e-03	0:41:22	414
87	4.5335e-03	1.6393e-03	1.5944e-03	8.4550e-04	3.2630e-03	5.9686e-03	0:42:39	413
88	4.4986e-03	1.6248e-03	1.5792e-03	8.3781e-04	3.2374e-03	5.9288e-03	0:42:16	412
iter	continuity	x-velocity	y-velocity	z-velocity	k	epsilon	time/iter	
89	4.4448e-03	1.6088e-03	1.5648e-03	8.2761e-04	3.2111e-03	5.8938e-03	0:41:57	411
90	4.4004e-03	1.5936e-03	1.5490e-03	8.1985e-04	3.1815e-03	5.8519e-03	0:41:41	410
91	4.3778e-03	1.5820e-03	1.5365e-03	8.1362e-04	3.1389e-03	5.7869e-03	0:41:27	409
92	4.3179e-03	1.5675e-03	1.5214e-03	8.0053e-04	3.0953e-03	5.7161e-03	0:42:36	408
93	4.2847e-03	1.5559e-03	1.5064e-03	7.9593e-04	3.0547e-03	5.6510e-03	0:42:08	407
94	4.2326e-03	1.5410e-03	1.4924e-03	7.8504e-04	3.0034e-03	5.5657e-03	0:41:45	406
95	4.1887e-03	1.5262e-03	1.4794e-03	7.7712e-04	2.9515e-03	5.4808e-03	0:41:25	405
96	4.1607e-03	1.5142e-03	1.4666e-03	7.7100e-04	2.9000e-03	5.3991e-03	0:41:08	404
97	4.1087e-03	1.4978e-03	1.4525e-03	7.5929e-04	2.8487e-03	5.3133e-03	0:42:13	403
98	4.0870e-03	1.4850e-03	1.4372e-03	7.5137e-04	2.7975e-03	5.2250e-03	0:41:44	402
99	4.0376e-03	1.4679e-03	1.4231e-03	7.3984e-04	2.7444e-03	5.1330e-03	0:41:20	401
iter	continuity	x-velocity	y-velocity	z-velocity	k	epsilon	time/iter	
100	3.9897e-03	1.4531e-03	1.4112e-03	7.3242e-04	2.6908e-03	5.0423e-03	0:40:59	400
101	3.9480e-03	1.4413e-03	1.3978e-03	7.2673e-04	2.6414e-03	4.9569e-03	0:40:41	399
102	3.8819e-03	1.4262e-03	1.3864e-03	7.1430e-04	2.5914e-03	4.8758e-03	0:39:06	398
103	3.8216e-03	1.4095e-03	1.3742e-03	7.0517e-04	2.5422e-03	4.8004e-03	0:39:08	397
104	3.7839e-03	1.3932e-03	1.3626e-03	6.9684e-04	2.4928e-03	4.7336e-03	0:39:09	396
105	3.7189e-03	1.3780e-03	1.3480e-03	6.8495e-04	2.4421e-03	4.6682e-03	0:39:09	395
106	3.6406e-03	1.3604e-03	1.3363e-03	6.7296e-04	2.3975e-03	4.6090e-03	0:39:07	394
107	3.5968e-03	1.3445e-03	1.3232e-03	6.6699e-04	2.3580e-03	4.5618e-03	0:39:04	393
108	3.5303e-03	1.3271e-03	1.3106e-03	6.5325e-04	2.3186e-03	4.5177e-03	0:39:01	392
109	3.4899e-03	1.3101e-03	1.3001e-03	6.4666e-04	2.2807e-03	4.4738e-03	0:38:57	391
110	3.4329e-03	1.2912e-03	1.2897e-03	6.3522e-04	2.2445e-03	4.4304e-03	0:37:35	390
iter	continuity	x-velocity	y-velocity	z-velocity	k	epsilon	time/iter	
111	3.3992e-03	1.2721e-03	1.2773e-03	6.2641e-04	2.2136e-03	4.3906e-03	0:37:46	389
112	3.3697e-03	1.2557e-03	1.2650e-03	6.1970e-04	2.1837e-03	4.3446e-03	0:37:54	388
113	3.3288e-03	1.2396e-03	1.2527e-03	6.1353e-04	2.1545e-03	4.2942e-03	0:37:59	387
114	3.2663e-03	1.2218e-03	1.2374e-03	6.0317e-04	2.1267e-03	4.2405e-03	0:39:19	386
115	3.2089e-03	1.2064e-03	1.2228e-03	5.9738e-04	2.0990e-03	4.1838e-03	0:40:21	385
116	3.1602e-03	1.1891e-03	1.2078e-03	5.8771e-04	2.0722e-03	4.1219e-03	0:39:53	384

117	3.1208e-03	1.1721e-03	1.1939e-03	5.8218e-04	2.0463e-03	4.0593e-03	0:39:29	383
118	3.0782e-03	1.1576e-03	1.1802e-03	5.7695e-04	2.0199e-03	3.9991e-03	0:39:08	382
119	3.0354e-03	1.1419e-03	1.1683e-03	5.6990e-04	1.9920e-03	3.9377e-03	0:38:51	381
120	3.0185e-03	1.1298e-03	1.1548e-03	5.6506e-04	1.9616e-03	3.8587e-03	0:38:36	380
121	2.9786e-03	1.1143e-03	1.1418e-03	5.5512e-04	1.9266e-03	3.7713e-03	0:38:23	379
iter	continuity	x-velocity	y-velocity	z-velocity	k	epsilon	time/iter	
122	2.9441e-03	1.1013e-03	1.1286e-03	5.5119e-04	1.8926e-03	3.6883e-03	0:36:55	378
123	2.8954e-03	1.0858e-03	1.1153e-03	5.4388e-04	1.8607e-03	3.6056e-03	0:37:00	377
124	2.8608e-03	1.0712e-03	1.1027e-03	5.3911e-04	1.8302e-03	3.5254e-03	0:37:02	376
125	2.8301e-03	1.0567e-03	1.0905e-03	5.3246e-04	1.8028e-03	3.4526e-03	0:37:03	375
126	2.8094e-03	1.0460e-03	1.0759e-03	5.2866e-04	1.7778e-03	3.3865e-03	0:37:03	374
127	2.7665e-03	1.0316e-03	1.0629e-03	5.1869e-04	1.7543e-03	3.3265e-03	0:37:01	373
128	2.7400e-03	1.0176e-03	1.0516e-03	5.1328e-04	1.7357e-03	3.2765e-03	0:36:58	372
129	2.7246e-03	1.0050e-03	1.0406e-03	5.0946e-04	1.7190e-03	3.2320e-03	0:36:55	371
130	2.6872e-03	9.9179e-04	1.0288e-03	5.0083e-04	1.7040e-03	3.1949e-03	0:36:51	370
131	2.6687e-03	9.7956e-04	1.0160e-03	4.9584e-04	1.6913e-03	3.1679e-03	0:36:47	369
132	2.6399e-03	9.6586e-04	1.0044e-03	4.8974e-04	1.6809e-03	3.1501e-03	0:36:42	368
iter	continuity	x-velocity	y-velocity	z-velocity	k	epsilon	time/iter	
133	2.6097e-03	9.5150e-04	9.9263e-04	4.8513e-04	1.6699e-03	3.1376e-03	0:36:38	367
134	2.5771e-03	9.3808e-04	9.8002e-04	4.8003e-04	1.6582e-03	3.1215e-03	0:36:32	366
135	2.5522e-03	9.2319e-04	9.6761e-04	4.7285e-04	1.6442e-03	3.1015e-03	0:36:27	365
136	2.5200e-03	9.0821e-04	9.5608e-04	4.6715e-04	1.6314e-03	3.0813e-03	0:36:22	364
137	2.4979e-03	8.9446e-04	9.4324e-04	4.6505e-04	1.6212e-03	3.0692e-03	0:35:04	363
138	2.4635e-03	8.8033e-04	9.2956e-04	4.5777e-04	1.6078e-03	3.0527e-03	0:35:13	362
139	2.4444e-03	8.6700e-04	9.1596e-04	4.5602e-04	1.5915e-03	3.0317e-03	0:35:19	361
140	2.3978e-03	8.5126e-04	9.0243e-04	4.4767e-04	1.5698e-03	2.9981e-03	0:35:22	360
141	2.3653e-03	8.3674e-04	8.8960e-04	4.4368e-04	1.5453e-03	2.9582e-03	0:35:24	359
142	2.3406e-03	8.2342e-04	8.7538e-04	4.3968e-04	1.5186e-03	2.9138e-03	0:35:24	358
143	2.3011e-03	8.0968e-04	8.6280e-04	4.3424e-04	1.4907e-03	2.8629e-03	0:34:11	357
iter	continuity	x-velocity	y-velocity	z-velocity	k	epsilon	time/iter	
144	2.2703e-03	7.9697e-04	8.5071e-04	4.3087e-04	1.4639e-03	2.8139e-03	0:34:24	356
145	2.2539e-03	7.8554e-04	8.3764e-04	4.2823e-04	1.4353e-03	2.7514e-03	0:34:32	355
146	2.2174e-03	7.7280e-04	8.2311e-04	4.2091e-04	1.4068e-03	2.6924e-03	0:34:38	354
147	2.1883e-03	7.5951e-04	8.1104e-04	4.1465e-04	1.3758e-03	2.6294e-03	0:34:41	353
148	2.1642e-03	7.4707e-04	7.9967e-04	4.1079e-04	1.3450e-03	2.5668e-03	0:33:32	352
149	2.1398e-03	7.3499e-04	7.8987e-04	4.0606e-04	1.3150e-03	2.5075e-03	0:33:46	351
150	2.1308e-03	7.2658e-04	7.7785e-04	4.0443e-04	1.2874e-03	2.4539e-03	0:33:57	350
151	2.0891e-03	7.1566e-04	7.6547e-04	3.9467e-04	1.2588e-03	2.3973e-03	0:34:03	349
152	2.0684e-03	7.0539e-04	7.5543e-04	3.8900e-04	1.2310e-03	2.3372e-03	0:34:08	348
153	2.0401e-03	6.9614e-04	7.4606e-04	3.8359e-04	1.2061e-03	2.2825e-03	0:34:10	347
154	2.0080e-03	6.8613e-04	7.3774e-04	3.7864e-04	1.1856e-03	2.2366e-03	0:34:10	346
iter	continuity	x-velocity	y-velocity	z-velocity	k	epsilon	time/iter	
155	1.9861e-03	6.8021e-04	7.2814e-04	3.7582e-04	1.1662e-03	2.2021e-03	0:34:10	345
156	1.9546e-03	6.7242e-04	7.1650e-04	3.6964e-04	1.1484e-03	2.1739e-03	0:34:08	344
157	1.9204e-03	6.6230e-04	7.0694e-04	3.6164e-04	1.1296e-03	2.1461e-03	0:34:05	343
158	1.8970e-03	6.5416e-04	6.9856e-04	3.5749e-04	1.1125e-03	2.1263e-03	0:32:53	342

159	1.8884e-03	6.4697e-04	6.8787e-04	3.5359e-04	1.0958e-03	2.1044e-03	0:34:11	341
160	1.8565e-03	6.3938e-04	6.7818e-04	3.4593e-04	1.0796e-03	2.0832e-03	0:32:56	340
161	1.8315e-03	6.3244e-04	6.7003e-04	3.4108e-04	1.0643e-03	2.0633e-03	0:33:03	339
162	1.8088e-03	6.2828e-04	6.5909e-04	3.3874e-04	1.0510e-03	2.0438e-03	0:33:07	338
163	1.7803e-03	6.2041e-04	6.4971e-04	3.3184e-04	1.0369e-03	2.0252e-03	0:33:10	337
164	1.7454e-03	6.1258e-04	6.4124e-04	3.2484e-04	1.0225e-03	2.0029e-03	0:33:10	336
165	1.7280e-03	6.0464e-04	6.3434e-04	3.2051e-04	1.0106e-03	1.9858e-03	0:33:09	335
iter	continuity	x-velocity	y-velocity	z-velocity	k	epsilon	time/iter	
166	1.7164e-03	5.9755e-04	6.2588e-04	3.1611e-04	9.9706e-04	1.9634e-03	0:33:08	334
167	1.6908e-03	5.8971e-04	6.1787e-04	3.1014e-04	9.8477e-04	1.9407e-03	0:33:05	333
168	1.6717e-03	5.8243e-04	6.0934e-04	3.0632e-04	9.7153e-04	1.9163e-03	0:34:08	332
169	1.6524e-03	5.7665e-04	5.9973e-04	3.0232e-04	9.5914e-04	1.8889e-03	0:33:51	331
170	1.6205e-03	5.7003e-04	5.9071e-04	2.9696e-04	9.4605e-04	1.8603e-03	0:33:36	330
171	1.6124e-03	5.6454e-04	5.8159e-04	2.9510e-04	9.3364e-04	1.8320e-03	0:33:22	329
172	1.5734e-03	5.5717e-04	5.7346e-04	2.8830e-04	9.1988e-04	1.8023e-03	0:32:05	328
173	1.5531e-03	5.5071e-04	5.6652e-04	2.8432e-04	9.0599e-04	1.7681e-03	0:32:08	327
174	1.5337e-03	5.4422e-04	5.5990e-04	2.8124e-04	8.9304e-04	1.7341e-03	0:32:09	326
175	1.5258e-03	5.4020e-04	5.5148e-04	2.7940e-04	8.8025e-04	1.7045e-03	0:32:08	325
176	1.4888e-03	5.3207e-04	5.4353e-04	2.7208e-04	8.6546e-04	1.6684e-03	0:32:07	324
iter	continuity	x-velocity	y-velocity	z-velocity	k	epsilon	time/iter	
177	1.4715e-03	5.2494e-04	5.3767e-04	2.6773e-04	8.5056e-04	1.6346e-03	0:32:04	323
178	1.4562e-03	5.1928e-04	5.3138e-04	2.6420e-04	8.3562e-04	1.5973e-03	0:33:05	322
179	1.4363e-03	5.1391e-04	5.2414e-04	2.6021e-04	8.2214e-04	1.5648e-03	0:32:49	321
180	1.4182e-03	5.0798e-04	5.1765e-04	2.5538e-04	8.0757e-04	1.5317e-03	0:32:34	320
181	1.3986e-03	5.0270e-04	5.1109e-04	2.5108e-04	7.9469e-04	1.5045e-03	0:31:17	319
182	1.3830e-03	4.9742e-04	5.0513e-04	2.4740e-04	7.8181e-04	1.4765e-03	0:31:19	318
183	1.3690e-03	4.9375e-04	4.9775e-04	2.4373e-04	7.7018e-04	1.4476e-03	0:31:19	317
184	1.3456e-03	4.8885e-04	4.9084e-04	2.3835e-04	7.5896e-04	1.4266e-03	0:31:17	316
185	1.3310e-03	4.8479e-04	4.8417e-04	2.3494e-04	7.4848e-04	1.4053e-03	0:31:15	315
186	1.3115e-03	4.7925e-04	4.7834e-04	2.2984e-04	7.3951e-04	1.3934e-03	0:31:12	314
187	1.2964e-03	4.7422e-04	4.7281e-04	2.2593e-04	7.3020e-04	1.3738e-03	0:31:09	313
iter	continuity	x-velocity	y-velocity	z-velocity	k	epsilon	time/iter	
188	1.2842e-03	4.6965e-04	4.6726e-04	2.2245e-04	7.2164e-04	1.3588e-03	0:31:04	312
189	1.2654e-03	4.6473e-04	4.6137e-04	2.1763e-04	7.1284e-04	1.3423e-03	0:31:00	311
190	1.2556e-03	4.6116e-04	4.5554e-04	2.1490e-04	7.0673e-04	1.3342e-03	0:30:55	310
191	1.2380e-03	4.5629e-04	4.4987e-04	2.1033e-04	7.0012e-04	1.3297e-03	0:30:50	309
192	1.2248e-03	4.5175e-04	4.4399e-04	2.0690e-04	6.9139e-04	1.3026e-03	0:30:45	308
193	1.2062e-03	4.4668e-04	4.3908e-04	2.0293e-04	6.8552e-04	1.3003e-03	0:30:40	307
194	1.2020e-03	4.4257e-04	4.3389e-04	2.0144e-04	6.7512e-04	1.2715e-03	0:30:34	306
195	1.1841e-03	4.3780e-04	4.2726e-04	1.9685e-04	6.7042e-04	1.2753e-03	0:30:28	305
196	1.1682e-03	4.3289e-04	4.2128e-04	1.9298e-04	6.5913e-04	1.2472e-03	0:30:23	304
197	1.1542e-03	4.2803e-04	4.1602e-04	1.8991e-04	6.5108e-04	1.2296e-03	0:30:17	303
198	1.1375e-03	4.2301e-04	4.1070e-04	1.8687e-04	6.4201e-04	1.2143e-03	0:30:11	302
iter	continuity	x-velocity	y-velocity	z-velocity	k	epsilon	time/iter	
199	1.1264e-03	4.1787e-04	4.0563e-04	1.8439e-04	6.3268e-04	1.1911e-03	0:30:05	301
200	1.1166e-03	4.1270e-04	4.0125e-04	1.8176e-04	6.2402e-04	1.1822e-03	0:30:00	300

```
  201 1.1032e-03 4.0758e-04 3.9594e-04 1.7769e-04 6.1255e-04 1.1558e-03  0:29:54  299
  202 1.0954e-03 4.0214e-04 3.9187e-04 1.7499e-04 6.0201e-04 1.1321e-03  0:29:48  298
  203 1.0864e-03 3.9685e-04 3.8750e-04 1.7298e-04 5.9134e-04 1.1152e-03  0:29:42  297
  204 1.0683e-03 3.9150e-04 3.8248e-04 1.6925e-04 5.8067e-04 1.0932e-03  0:30:35  296
  205 1.0588e-03 3.8748e-04 3.7774e-04 1.6732e-04 5.7098e-04 1.0718e-03  0:30:17  295
  206 1.0500e-03 3.8413e-04 3.7364e-04 1.6666e-04 5.6181e-04 1.0559e-03  0:30:02  294
  207 1.0242e-03 3.7748e-04 3.6808e-04 1.6089e-04 5.4938e-04 1.0319e-03  0:29:48  293
  208 1.0175e-03 3.7205e-04 3.6429e-04 1.5854e-04 5.3923e-04 1.0105e-03  0:29:36  292
  209 1.0047e-03 3.6699e-04 3.6054e-04 1.5594e-04 5.2997e-04 9.9119e-04  0:30:23  291
 iter continuity x-velocity y-velocity z-velocity        k    epsilon     time/iter
!  210 solution is converged
  210 9.9279e-04 3.6258e-04 3.5668e-04 1.5351e-04 5.2145e-04 9.7377e-04  0:30:02  290
```

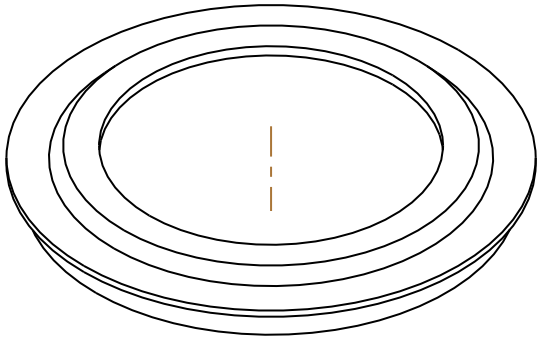

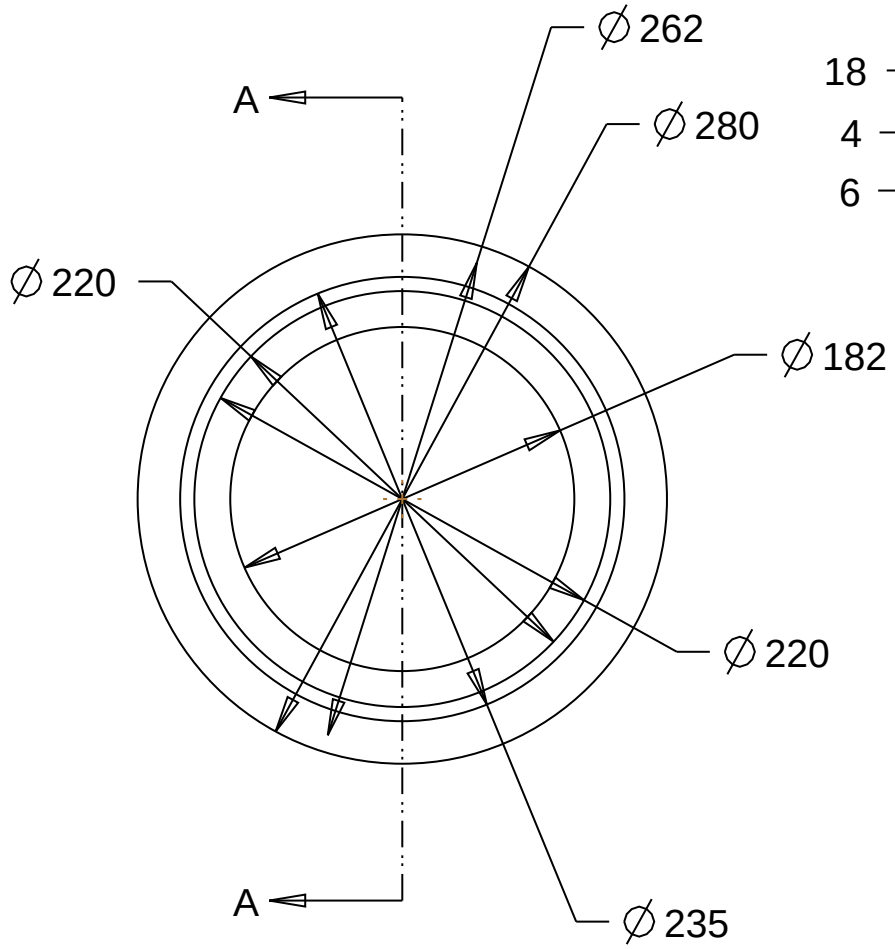

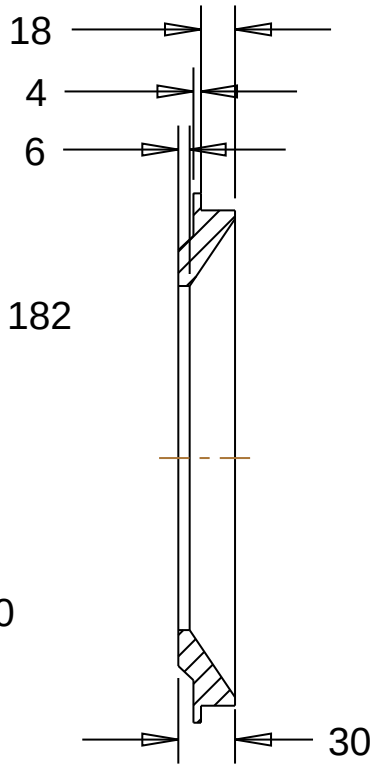

SECTION A-A

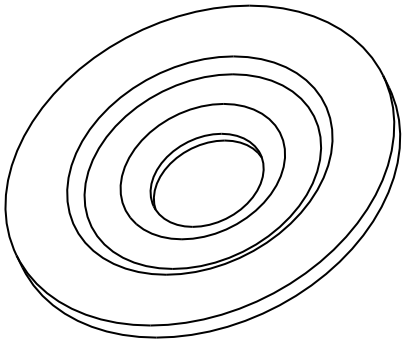

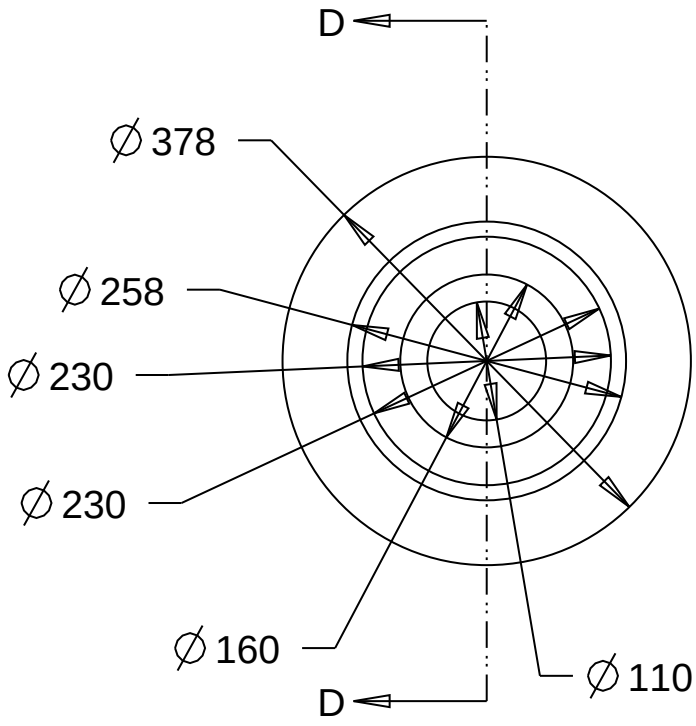

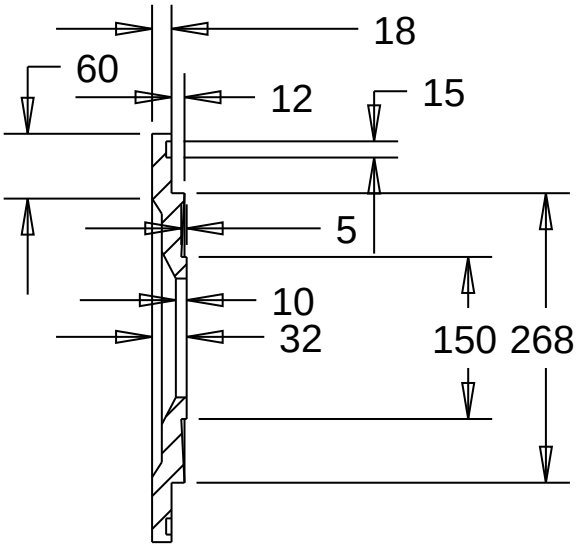

SECTION D-D

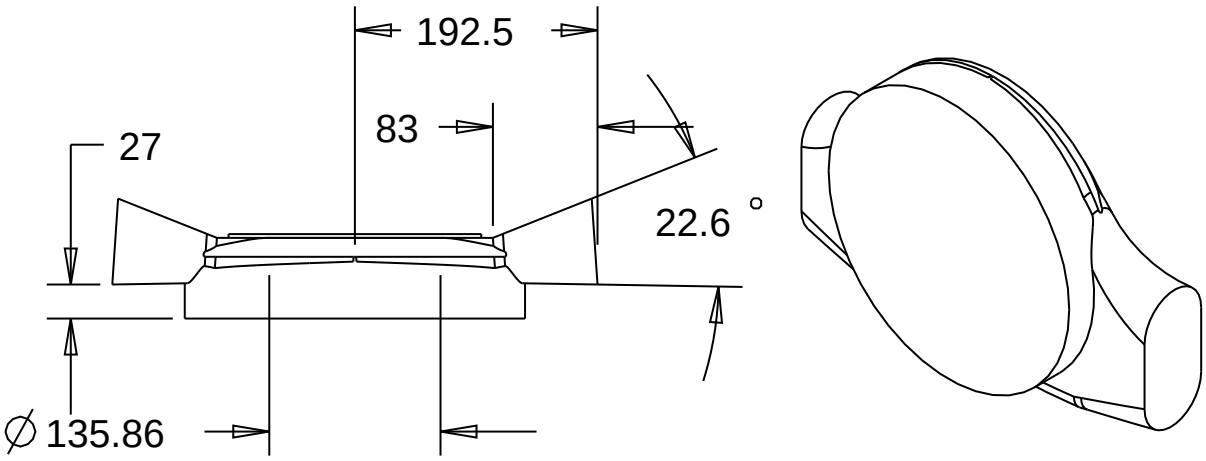
192.5
83
27
22.6 °
∅135.86

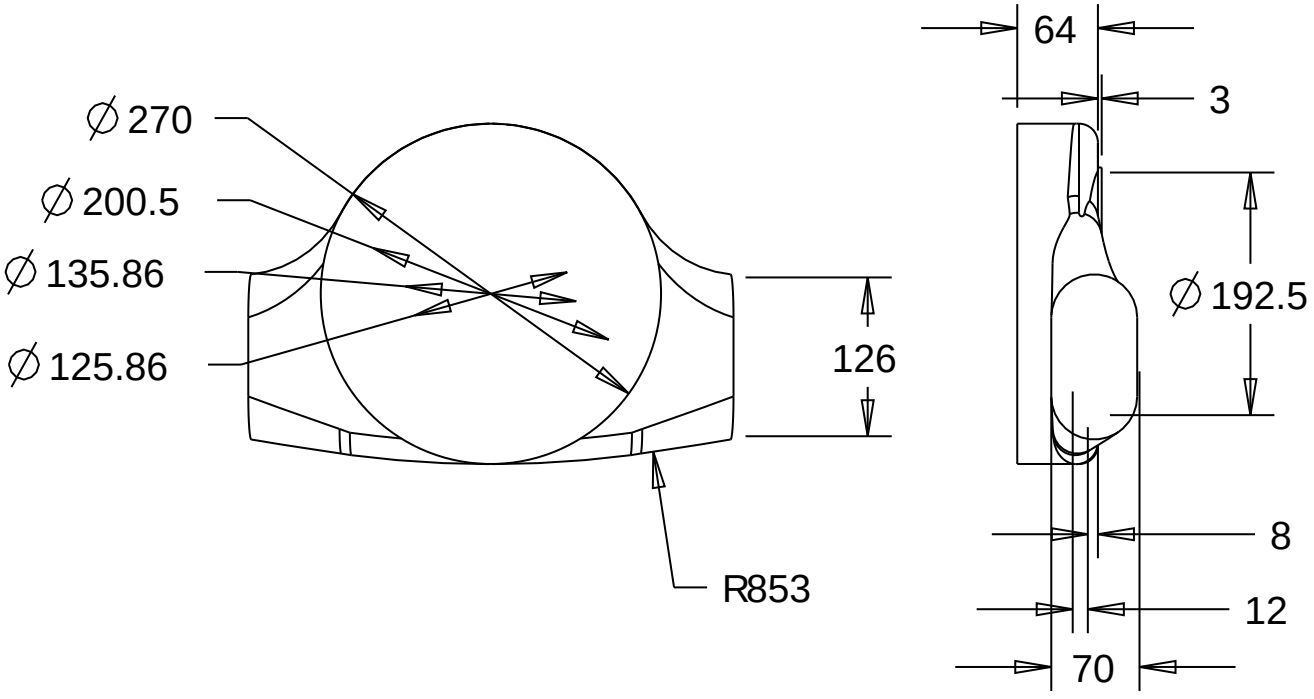
∅270
∅200.5
∅135.86
∅125.86
126
R853
64
3
∅192.5
8
12
70

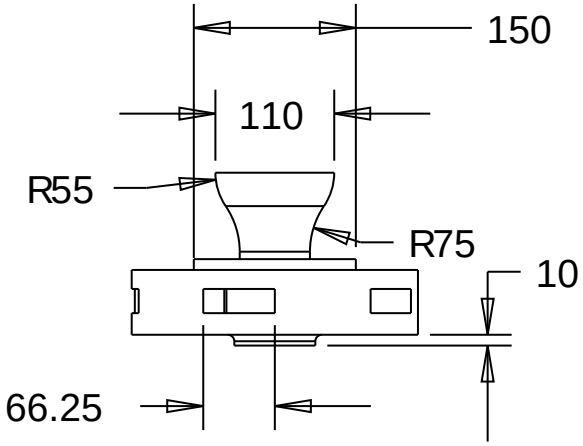
150
110
R55
R75
10
66.25

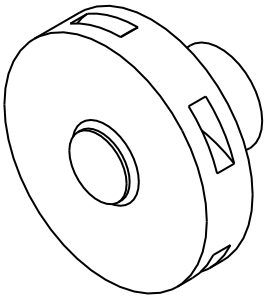

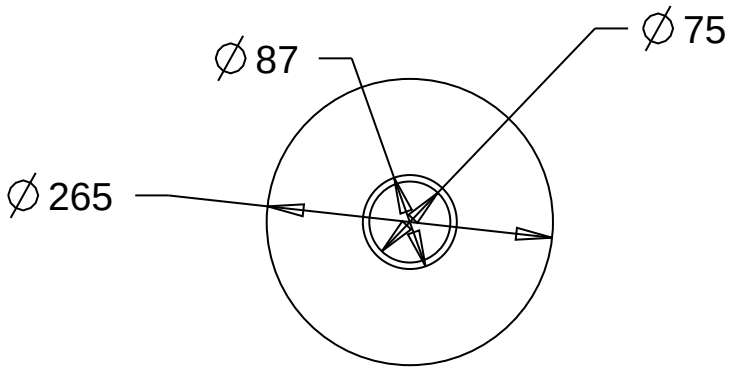
∅87
∅75
∅265

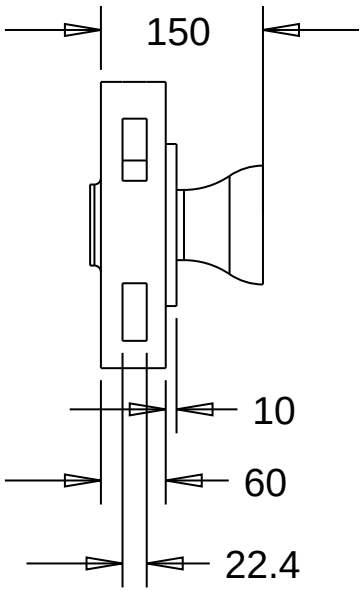
150
10
60
22.4